

ELASTIN AS A KINETIC ELASTOMER:  
An Analysis of Its Conformational,  
Mechanical, and Photoelastic  
Properties.

by

BEN-MEYER BENSON AARON

B.Sc., The University of British Columbia, 1976

A THESIS SUBMITTED IN PARTIAL FULFILMENT OF  
THE REQUIREMENTS FOR A DEGREE OF  
MASTER OF SCIENCE

in

THE FACULTY OF GRADUATE STUDIES

Department of Zoology

We accept this thesis as conforming  
to the required standard

THE UNIVERSITY OF BRITISH COLUMBIA

August 1980

© BEN-MEYER BENSON AARON, 1980

In presenting this thesis in partial fulfilment of the requirements for an advanced degree at the University of British Columbia, I agree that the Library shall make it freely available for reference and study.

I further agree that permission for extensive copying of this thesis for scholarly purposes may be granted by the Head of my Department or by his representatives. It is understood that copying or publication of this thesis for financial gain shall not be allowed without my written permission.

Department of Zoology

The University of British Columbia  
2075 Wesbrook Place  
Vancouver, Canada  
V6T 1W5

Date Sept 11<sup>th</sup> 80

ABSTRACT

The elastic tissue composite is made up of a number of materials that are characterized by different chemical and mechanical properties. The protein elastomer elastin makes up almost 80% of bovine ligamentum nuchae with collagen and the matrix substances making up the other 20%. The analysis of the mechanical properties of the unpurified and purified tissue indicates that elastin is the dominant mechanical component at low strains with collagen contributing significantly at the higher extensions.

The physical properties of single, 5 to 8 $\mu$ m diameter, water-swollen elastin fibres were investigated on a micro-test apparatus attached to a polarizing microscope, and the results were analyzed by using the kinetic theory relationships. The analysis of the mechanical properties at extensions below 100% indicate that elastic modulus,  $G = 4.1 \times 10^5 \text{ Nm}^{-2}$ , the average molecular weight of the chains between cross-links is in the range of 6000 to 7100g/mol, and the stress-optical coefficient,  $C' = 1 \times 10^{-9} \text{ m}^2 \text{ N}^{-1}$  at 24°C. Analysis of the temperature dependence of the stress-optical coefficient indicated that the polarizability of the random link decreases with increasing temperature. The apparent activation energy for this process is in the order of 1.6 kcal/mole. Analysis of the non-Gaussian mechanical and optical properties at extensions above 100% suggest that the chain between cross-links contains approximately 10 'effective' random links, with each link consisting of 7 to 8 amino acid residues.

The explicit assumption of a random network that is made by the kinetic theory was tested by a number of techniques. 400 MHz pmr spectra of the soluble alpha-elastin closely resembled the spectra that were predicted for the random-coil conformation, and the spectra obtained for its amino acid hydrolysate. Polarized microscopy studies showed intact elastin fibres to be devoid of any crystalline structures. Finally, the parameters for the random chains in the elastin network were used to predict the dimensions of other random proteins. The close correlation of these predictions with published values for a series of proteins in solution in 6M GuHCl provided an independent test of the random conformation, validating the use of the kinetic theory relationships to analyze the macroscopic properties of elastin.

TABLE OF CONTENTS

ABSTRACT.....	I
TABLE OF CONTENTS.....	iii
LIST OF TABLES.....	x
LIST OF FIGURES.....	xi
ACKNOWLEDGEMENTS.....	xiv
I. INTRODUCTION. ....	1
II. GENERAL CHARACTERISTICS OF ELASTIC TISSUE. ....	4
A. Introduction .....	4
B. Elastin Development .....	4
(a) Embryology .....	4
(b) Morphogenesis Of Elastin Fibres .....	5
(c) Elastin Turnover .....	7
C. Elastin Chemistry .....	7
(a) Amino Acid Composition .....	7
(b) Elastin Cross-links .....	9
(c) Soluble Elastin .....	10
D. Composition Of Elastic Tissue .....	11
(a) Water Content .....	12
(b) Elastin Content .....	12
(c) Neutral Sugars .....	12
(d) Mucopolysaccharides .....	12
(e) Collagen Content .....	14
E. Organization Of Elastic Tissue .....	14
(a) Methodology .....	14

(b)	Organization Of Ligament Elastin .....	15
(c)	Organization Of Arterial Elastin .....	18
F.	Purification Techniques .....	21
(a)	Amino Acid Compositions .....	21
(b)	Hexosamine And Neutral Sugar Content .....	24
(c)	Evaluation By Scanning Electron Microscopy ....	24
G.	Mechanical Properties Of Elastin Bundles .....	24
(a)	Methods .....	28
(b)	Results .....	28
H.	Mechanical Properties Of Single Elastin Fibres ....	31
I.	Discussion .....	34
(a)	Variation In Elastin Biochemistry .....	34
(b)	The Composite Tissue .....	35
(c)	Evaluation Of Purification Techniques .....	36
III.	CONFORMATION OF ELASTIN: THE CONTROVERSY. ....	38
A.	Introduction .....	38
B.	The Random Network Model .....	38
(a)	Elastin Thermcelasticity .....	41
(b)	Differential Scanning Calorimetry .....	43
(c)	E.M. And X-ray Diffraction Studies .....	43
(d)	N.M.R. Evidence .....	44
C.	Liquid Drop Model .....	45
(a)	Preliminary Evidence .....	45
(b)	Thermodynamic Evidence .....	46
D.	Oiled Coil Model .....	47
E.	Fibrillar Models .....	48
(a)	Electron Microscope Evidence .....	49

(b) Nuclear Magnetic Resonance Evidence .....	50
F. Discussion .....	54
(a) Two-phase Models .....	54
(b) Evidence For Secondary Structures .....	56
(c) Hydrogen Bonded Structures .....	58
(d) Fibrillar Models .....	60
G. Conclusions .....	60
IV. CONFORMATION OF ELASTIN: COACERVATE STRUCTURE. ....	62
A. Introduction .....	62
B. The Phenomenon Of Coacervation .....	62
C. Preparation Of Alpha-Elastin .....	63
(a) Enzyme Hydrolysis .....	64
(b) Removal Of SDS .....	65
(c) Characterization Of The Alpha-elastin .....	65
D. Viscosity And Shape .....	66
(a) The Relevant Equation .....	66
(b) Evaluation Of The Shape Parameter .....	69
(c) Application To Soluble Elastins .....	70
E. Viscosity Studies Of Alpha-Elastin .....	73
(a) Viscosity Measurements .....	73
(b) Calculation Of Partial Specific Volume And Hydration .....	76
(c) Results And Discussion .....	76
F. Nuclear Magnetic Resonance .....	80
(a) Theory .....	80
(b) The Chemical Shift .....	84
(c) Relaxation Processes .....	85

G. N.M.R. Studies Of Alpha-Elastin .....	87
(a) Materials And Method .....	87
(b) Prediction Of Random-coil Spectra .....	91
(c) Results And Discussion .....	92
H. Conclusions .....	105
V. CONFORMATION OF ELASTIN: BIREFRINGENCE PROPERTIES. ...	108
A. Introduction .....	108
B. Phenomenological Explanation Of Double Refraction .	109
(a) Retardation Of Polarized Light .....	110
(b) Quantitating The Retardation .....	115
C. Qualifying The Types Of Birefringence .....	116
(a) Intrinsic Birefringence .....	116
(b) Form Birefringence .....	124
(c) Strain Birefringence .....	125
D. Materials And Methods .....	126
E. Birefringence Properties Of Single Elastin Fibres .	127
(a) Form Birefringence .....	127
(b) Intrinsic Birefringence .....	132
(c) Explanation For The Apparent Birefringence ...	136
F. Discussion .....	146
(a) Previous Studies .....	146
(b) The Fibrillar Models .....	148
G. Conclusions .....	150
VI. CONFORMATION OF ELASTIN: SCANNING ELECTRON	
MICROSCOPY. ....	152
A. Introduction .....	152
B. Methods .....	152

C. Results .....	153
D. Discussion .....	156
VII. ELASTIN AS A KINETIC ELASTOMER. ....	163
A. Introduction .....	163
B. Entropy Elastomers: The Kinetic Theory Of Rubber Elasticity .....	164
(a) Gaussian Chain Statistics And Entropy .....	164
(b) The Elastic Network .....	168
(c) Mechanical Properties Of Kinetic Rubbers .....	169
(d) Photoelasticity .....	171
(e) Non-Gaussian Effects And The Evaluation Of S ..	172
(f) Reduction Cf Elastin Data To The Unswollen Form .....	173
C. Materials And Method .....	174
(a) Purification Of Elastin .....	174
(b) The Experimental Stage .....	175
(c) Preparation Of Experimental Specimen .....	175
(d) Measurement Of Strain .....	178
(e) Measurement Of Force .....	178
(f) Calculation Of Cross-sectional Area .....	179
(g) Measurement Of Birefringence .....	180
(h) ERRORS .....	180
D. Physical Properties Of Single Elastin Fibres .....	181
(a) General Characteristics .....	181
(b) Mechanical Properties And The Derivation Of Mc	181
(c) Photoelasticity .....	185
(d) Temperature Dependence Of The Optical	

Anisotropy .....	188
(e) Non-Gaussian Properties Of The Elastin Network	192
E. Conclusions .....	195
VIII. A PREDICTIVE TEST FOR ELASTIN CONFORMATION .....	197
A. Introduction .....	197
B. Characterization Of Random Proteins .....	197
(a) The Measurable Dimension .....	197
(b) Accounting For The Non-ideality .....	201
C. R.M.S. Values From Viscosity .....	202
(a) Viscosity Of Random Coils .....	202
(b) Correction Of Viscosity Values .....	203
D. Predictions From The Elastin Network .....	204
(a) Calculation Of S .....	204
(b) Calculation Of L .....	206
E. Discussion And Conclusions .....	207
IX. CONCLUSIONS. ....	211
APPENDIX.I: Thermoelasticity .....	216
(A) Thermodynamic Relationships .....	216
(B) The Thermodynamic Experiment .....	217
(C) Thermoelasticity Of Kinetic Elastomers .....	218
APPENDIX.II: PREPARATION OF SOLUBLE ELASTIN BY PHOTOLYSIS. ....	220
A. Introduction .....	220
B. Methodology .....	220
(a) Rationale .....	220
(b) Procedure .....	224
C. Results And Discussion .....	225

(a) Yield .....	225
(b) Characterization Of The Soluble Peptides .....	226
Appendix.III: PREDICTIONS FOR TROPOELASTIN VISCOSITY .....	231
A. The Relevant Equation .....	231
B. Application To Tropoelastin .....	231
Appendix.IV: EVALUATION OF PROTEIN CONFORMATION .....	236
Appendix.V: DETERMINATION OF SOLVENT EFFECTS ON RANDOM COILS .....	242
Appendix.VI: AMINO ACID COMPOSITION AND ELASTIN EVOLUTION .....	245
LITERATURE CITED .....	249

LIST OF TABLES

Table.2.1: Amino Acid Composition Of Elastic Proteins. ...	8
Table.2.2: Chemical Composition Of Elastic Tissue. ....	13
Table.2.3: Amino Acid Composition Of Elastin Preparations. ....	25
Table.4.1: Viscosity Of Alpha-elastin. ....	77
Table.4.2: Spectral Parameters Used For Random-coil Predictions. ....	90
Table.4.3: Peak Assignments For Alpha-elastin At 400 MHz. .....	95
Table.5.1: Form Birefringence Of Single Elastin Fibres. .	128
Table.7.1: Kinetic Theory Parameters For Elastin. ....	186
Table.8.1: Predictions For Random-coil Proteins. ....	205
Table.A.3.1: Prediction For Tropoelastin Viscosity. ....	234
Table.A.6.1: Difference Index For Elastin Composition. ..	246

LIST OF FIGURES

Figure.2.1: Organization Of Ligament Elastin. ....	16
Figure.2.2: Organization Of Arterial Elastin. ....	19
Figure.2.3: The Elastic Tissue Composite. ....	22
Figure.2.4: Evaluation Of Purification Techniques. ....	26
Figure.2.5: Mechanical Properties Of Elastin Bundles. ...	29
Figure.2.6: Mechanical Properties Of Single Elastin Fibres. ....	32
Figure.3.1: Proposals For The Conformation Of Elastin ...	39
Figure.3.2: Beta-turns. ....	51
Figure.4.1: Coacervation Profile Of Alpha-elastin. ....	67
Figure.4.2: Dependence Of The Simha Factor On Axial Ratio. ....	71
Figure.4.3: Dependence Of Elastin Water Content On Temperature. ....	74
Figure.4.4: Viscosity Of Alpha-elastin. ....	78
Figure.4.5: Precession Of A Proton In A Magnetic Field. .	81
Figure.4.6: The Lorentzian Line Shape. ....	88
Figure.4.7: 400 MHz Nmr Spectrum Of Alpha-elastin. ....	93
Figure.4.8: Predicted Nmr Spectra For Alpha-elastin. ....	97
Figure.4.9: Nmr Spectrum Of Alpha-elastin Hydrolysate. ..	100
Figure.4.10: Nmr Spectra Of Albumin. ....	103
Figure.5.1: Propagation Of Polarized Light Through Isotropic Material. ....	111
Figure.5.2: Propagation Of Polarized Light Through Anisotropic Material. ....	113

FIGURE.5.3: The Birefringence Experiment. ....	117
Figure.5.4: The Sign Of The Birefringence. ....	120
Figure.5.5: Form Birefringence. ....	122
Figure.5.6: Form Birefringence Of Elastin Fibres. ....	129
Figure.5.7: Form Birefringence Of Ccollagen. ....	133
Figure.5.8: Expected Relationship For Intrinsic Birefringence. ....	137
Figure.5.9: Expected Birefringence For An Anisotropic Coating. ....	140
Figure.5.10: Birefringence Pattern Of Single Elastin Fibres. ....	144
Figure.6.1: S.E.M. Of Unpurified Ligament Elastin Fibre.	154
Figure.6.2: Surface Texture Of Autoclaved Elastin Fibres. .....	157
Figure.6.3: Fracture Surfaces Of Elastin Fibres. ....	159
Figure.7.1: The Random-coiled Chain .....	166
Figure.7.2: The Experimental Stage. ....	176
Figure.7.3: Physical Properties Of Single Elastin Fibres. .....	183
Figure.7.4: Temperature Dependence Of Photoelasticity. ..	189
Figure.7.5: Non-Gaussian Properties Of The Elastin Network. ....	193
Figure.8.1: The Random Walk. ....	199
Figure.8.2: Predictions For The Dimensions Of Random-coil Protein. ....	208
Figure.9.1: Summary Figure For The Thesis. ....	213
Figure.A.2.1: Photolysis Of Elastin. ....	222

Figure.A.2.2: Molecular Weight Of Photolysis Peptides. ..	228
Figure.A.3.1: Viscosity Of Random-coil Proteins. ....	232
Figure.A.4.1: Radius Of Gyration For Various Shapes. ....	237
Figure.A.4.2: Evaluation Of Protein Conformation. ....	239
Figure.A.5.1: Evaluation Of Solvent Effects On Random Coils. ....	243
Figure.A.6.1: Elastin Evcluticn. ....	247

ACKNOWLEDGEMENTS

This research was made possible by the patience and support of many people. I would especially like to thank Dr. J.M. Gosline who suffered through my everpresent bouts of incompetence and procrastination without losing interest in the directing of this research. I would also like to thank Karen Martin for her help with the preparation of this thesis and for giving me the emotional support over these past years. The occupants of the lab and my other associates, Mark Denny, Tony Harmon, Bob Shadwick, and Kevin Bush have all contributed to this thesis through their many criticisms and discussions, and their input is gratefully acknowledged. Lastly, I would like to thank Dr. P.D. Burns from the Department of Chemistry, without whose co-operation and many hours of experimental work the nmr studies would not have been possible, and Tina Duke from the Department of Computer Science who helped with the documentation of this thesis.

This research was supported by grants from the B.C. Heart Foundation and the Canadian Natural Sciences and Engineering Council to Dr. J.M. Gosline.

This thesis is dedicated to my family: my parents Benson and Seemah Aaron, and my brother Solomon Aaron, whose support and advice provided the catalyst for this work.

## Chapter.I. INTRODUCTION.

We have all experienced instances where having boasted about the knowledge of an objects function have subsequently been embarassed by our ignorance of the 'mode of functioning'. Proteins, which serve a vast number of functions in nature, present the same dilema. As most of us know from watching detergent commercials on television, enzymes break down certain compounds. This tells us about their 'function' but does not in any way inform us about the manner in which it performs. If one is to comment on this aspect of the enzyme's character it becomes necessary to obtain some structural information for the protein in question. The same argument applies to elastin. Although one can claim that elastin is a rubbery protein, the basis of this elasticity, which is the topic of interest, cannot be elucidated without knowledge of the protein's conformational state. Different theories of elasticity assume different conformations at the molecular level for the material in question. Hence, it seems reasonable that one should investigate the molecular conformation of this protein in an attempt to shed some light on the validity of the wide spectrum of theories that claim to explain the basis of elastin elasticity. Hence the major focus of this thesis was to investigate the structure of the elastin protein and, then, to interpret it's physical properties in terms of a theoretical framework for rubber elasticity.

The techniques of conformational analysis used in this investigation were selected on their value as sensitive probes

of structure with the minimum amount of disturbance to the native conformation in terms of experimental techniques. The studies themselves were developed at different levels of organization starting with the investigation of soluble peptide properties and building up to the intact elastic fibre. Nmr and viscosity experiments were used to study the structure of soluble proteins from elastin, with polarized microscopy and scanning electron microscopy providing the tools for the analysis of intact elastin fibres. All of these studies showed elastin to be a random network elastomer, and on the basis of this conclusion I then proceeded to use the theoretical framework provided by the kinetic theory of rubber elasticity to characterize the macroscopic mechanical and photoelastic properties of this protein. Finally, a test for the random network network conformation was conducted by predicting the dimensions of random-coil proteins, and comparing these to published values.

The thesis itself is organized in the following manner. I have started by discussing the properties of the intact tissue composite (chapter II) to show the exact relationship of the elastic fibre to the other components present in the tissue. The following four chapters deal with the question of elastin conformation and involves the presentation of the current controversy (chapter III), the nmr and viscosity investigations (chapter IV), the polarized microscopy studies (chapter V), and the scanning electron microscopy results (chapter VI). The next chapter (chapter VIII) deals with the

evaluation of the elastin network properties in terms of the kinetic theory of rubber elasticity. The predictive test for elastin conformation is presented in chapter IX.

## Chapter.II. GENERAL CHARACTERISTICS OF ELASTIC TISSUE.

### A. Introduction

Given a mechanically functioning material, the macroscopic properties of this tissue will depend on, (a) the chemical composition of the tissue, (b) the mechanical properties of the individual components, (c) the architectural organization of these components, and (d) the effect of the chemical properties of one component on the mechanical properties of itself and the other components.

As will be shown in this chapter the elastin protein forms a major mechanical component of elastic tissue, and it is probably justifiable to discuss the chemistry of this particular protein which, along with its organization, will eventually determine its functional properties. Since elastin is implicated in the pathology of the vascular system, there has been considerable activity in this field, so for the sake of convenience (and lack of breath) I have just outlined the major aspects of its biochemistry. A detailed discussion of the chemistry of elastin has been presented by Sandberg (1976) and Franzblau (1971).

### B. Elastin Development

#### (a) Embryology

All elastin, like collagen and other connective tissue, arises from the third germ layer commonly referred to as

mesoderm. The exact type of mesoderm that gives rise to any particular elastin is dependent on where it occurs (the mesodermal source of arterial elastin is different from that of ligament or skin). This could account for the variability of the composition that is observed between different types of elastic tissue (Kieth et.al. 1979). A review of elastin embryology is given by Hass (1939) and is summarized in the following paragraph.

According to Hass, the vascular system is the first part of the body to be supplied with elastin, and can be demonstrated to be present in four day old chick embryos. In humans the elastin is first found in the third or fourth week. In the embryo, the majority of the elastin is concentrated in the aorta with the exact distribution changing after parturition. After birth, the relative amount of elastin in the artery decreases while the relative amounts in the veins increases. A similar time course can be found for the development of elastin in the lungs, with the development of elastin in the skin lagging by about three months. The alimentary tract is thought to be one of the last organs to receive elastic tissue.

#### (b) Morphogenesis of elastin fibres

Although it has been known for a long time that the elastin fibre is a two component system, i.e. an inner amorphous core with a surrounding fibrillar coat, the exact relationship between the two has only recently been

elucidated. Ross and Bornstein (1969) demonstrated that these components of the elastin fibre are very distinct chemically, the external fibrillar coat being a polar glycoprotein with the amorphous core being an extremely hydrophobic protein. The chemistry of the microfibrillar component has been studied and it has been shown to be composed of fibrils, ranging from 10 to 40 nm in diameter, which could be extracted with agents that reduced di-sulphide bonds (Robert et.al. 1971, Anderson 1976).

In order to assign a functional role to these glycoprotein fibrils it has been proposed that they are involved with the aligning of the elastin protein during its secretion. It has been shown that elastic ligaments in the embryo are almost devoid of elastin in their early stages of development, but have a high amount of glycoprotein present. In the later stages of development the elastin protein can be seen to be interspersed between these microfibrils which, due to their negative charge, may tend to aggregate the elastin (which has a net positive charge) around themselves (Ross et.al. 1977).

Further evidence for this type of a role for the microfibrils has been obtained by Cotta-Pereira et.al. (1977), who histologically demonstrated the presence of two types of developing elastin fibres. Oxytalan fibres, composed mainly of glycoproteins, and elaunin fibres which consisted of microfibrils and amorphous elastin. On the basis of their observations they proposed a oxytalan-- elaunin-- mature

elastic fibre hierarchy for the development of the elastin protein, which is synthesized in vivo by fibroblast and smooth muscle cells (Boucek 1959, and Pathrapamkel et.al. 1977).

### (c) Elastin turnover

The turnover of elastin in normal elastic tissue is characterized by a half-life that is approximately equal to the life span of the animal (Ayer 1969). It has been proposed by some workers that the diseased states represent an alteration in the turnover rate of the elastic tissue, increasing with age and pathology. This increase in turnover is largely due to the presence of degradative processes (Robert 1977).

## C. Elastin Chemistry

### (a) Amino acid composition

In order to characterize the amino acid composition of a protein one has to first decide on the question of what is to be considered as being the 'pure' protein. Fortunately the case for elastin is quite clear cut, in that investigators have been able to treat elastic tissue quite drastically and still arrive at a protein of constant composition which can account for the elasticity of the intact tissue. This residue that remains after treatment is termed elastin, and will be defined as such for the rest of this thesis.

Amino acid analysis of this protein shows elastin to be

Table.2.1: Amino acid composition of elastic proteins.

AMINO ACID COMPOSITION OF  
ELASTIC PROTEINS.\*

	ELASTIN <sup>1</sup>	RESILIN <sup>2</sup>	ABDUCTIN <sup>3</sup>	CONNECTIN <sup>4</sup>	OCTUPUS FIBRES <sup>5</sup>
asx	6.4	102	69.9	92	90.6
thr	8.9	28	7.4	59	64.4
ser	9.9	80	36.4	60	71.8
glx	15	47	19.4	128	121
pro	120	77	7.4	65	54.9
hyp	10.7	--	--	12	--
gly	324	385	620	104	85
ala	232	111	26.5	84	71
cys	4.1	--	--	4	7.4
val	135	28	3.5	60	62
met	--	--	117	23	21
ile	25.5	17	4	52	60
leu	61.1	23	3	70	73.5
tyr	7.1	27	10.7	28	36.2
phe	30	26	51.3	29	42.3
his	0.6	9	0.3	15	21
lys	7.4	5	12.4	61	68.3
arg	5.4	35	9.8	56	45.8

\* in residues/1000.

<sup>1</sup>Ross and Bornstein 1969.

<sup>2</sup>Weis-Fogh 1961.

<sup>3</sup>Kelly and Rice 1967.

<sup>4</sup>Maruyama et.al. 1976.

<sup>5</sup>Shadwick 1980.

one of the most hydrophobic proteins yet discovered, with nearly 60% of the residues being non-polar. As will be presented later, this characteristic, more than any other, has been responsible for the mis-interpretation of the physical properties of this elastomer. Elastin also has an unusually large content of glycine, valine, and proline residues. The amino acid composition of elastin (Ross and Bornstein 1969) and it's comparison to the other known elastomers, Resilin (Anderson 1971), Abductin (Kelly and Rice 1967), Connectin (Maruyama et.al. 1976), and the recently discovered elastomer from octopus arteries (Shadwick 1980) is shown in table 2.1.

#### (b) Elastin cross-links

Since elastin is a protein that has a mechanical function, it has to be cross-linked in order to prevent the polypeptide chains that make up the tissue from 'flowing' under stress. In the case of natural rubber this is accomplished by forming covalent bonds between carbon residues of adjacent polymer chains (Flory 1953). With regard to elastin, the cross-links of this elastomer were first discovered by Thomas et.al. (1963) who showed them to be pyridinium derivatives and named them desmosine and isodesmosine. These structural proposals were confirmed concurrently by nuclear magnetic resonance studies (Bedford and Katritzky 1963).

These same authors (Partridge et.al. 1965) later showed that these compounds cross-linked two polypeptide chains and

proposed a possible route for the formation of these links. It is currently thought that the desmosines and iso-desmosines are formed by the condensation of four lysines, three of which have been oxidized by the enzyme lysyl oxidase (Sandberg 1976). There is also some evidence that residues other than the (iso)desmosines, such as lysinonorleucine, also serve as cross-linking agents in the elastin network (Lent et.al. 1969).

### (c) Soluble elastin

As mentioned before, insoluble elastin results from the cross-linking of soluble elastin precursors into a functional network. Due to this relationship there has been some interest in the characterization of these precursor proteins.

Although a number of methods for the solubilization of elastin are known, such as digestion with oxalic acid (Partridge and Adair 1955), elastase (Hall 1961), urea (Bowen 1953), KOH (Mcczar et.al. 1979). The only method available at the moment for the isolation of an unbranched precursor is the extraction of tropoelastin from lathyrotic animals.

This method is based on the biochemistry of cross-link formation which requires the oxidation of the lysine residues, involved in the formation of (iso)desmosines, by the copper requiring enzyme lysyl oxidase (Franzblau 1971). Inhibition of this enzyme's activity, by raising animals on copper deficient diets or by inducing lathyrism using agents such as B-amino-propionitrile, allows the extraction of soluble proteins from

the elastic tissue of the animal.

The extraction procedure results in a protein which has an amino acid composition that is similar to mature elastin (with the exception of a high lysine content, due to the lack of cross-links) and is termed tropoelastin in analogy to the collagen- tropocollagen scheme (Sandberg 1976). It is currently thought that tropoelastin, which has a molecular weight of 72,000, represents the building block of mature insoluble elastin. There is some speculation that there exists a higher molecular weight species, which would be comparable to procollagen, and recent publications have stated the presence of such a protein, named proelastin, having a molecular weight of 130,000 to 140,000 (Foster et.al. 1976, 1977). This speculation, however, has been put to rest by a recent paper that provides strong evidence that tropoelastin is the primary precursor in elastin biosynthesis (Rosenbloom et.al. 1980).

The precursor-product relationship between tropoelastin and fibrous elastin has been demonstrated recently by the in vitro cross-linking of the soluble proteins to give cross-linked elastin (Narayanan and Page 1976, Smith et.al. 1975). Partial primary sequence data for porcine tropoelastin have also been published in the literature on elastin biochemistry (Sandberg et.al. 1977).

#### D. Composition of Elastic Tissue

### (a) Water content

Unpurified elastin samples from ligament nuchae were blotted on paper towels to remove excess water and weighed at 24°C. The same samples were then dried to constant weight in an oven at 110°C and reweighed. The results indicate that ligament elastin is approximately 72% water by weight. A similar value of 70% has been reported for arterial elastin samples (Harkness et.al. 1957).

### (b) Elastin content

Unpurified ligament elastin samples were dried in an oven to constant weight. The samples were then purified by repeated autoclaving (Partridge et.al. 1955), dried and reweighed. The value of elastin content so obtained was about 80% by dry weight. Values for the elastin content of thoracic arteries occur in the range of 40% elastin (w/dry weight) (Charm et.al. 1974, Harkness et.al. 1957).

### (c) Neutral sugars

Neutral sugar content of unpurified ligament elastin was evaluated using the phenol-sulphuric acid assay of Lo et.al. (1970), using glucose (Sigma) as a standard. A value of 0.3% (w/dry weight of tissue) was obtained.

### (d) Mucopolysaccharides

It is almost impossible to determine the exact mucopolysaccharide content of elastic tissue due to the large

Table.2.2: Chemical composition of elastic tissue.

CHEMICAL COMPOSITION OF ELASTIC TISSUE.

	Ligamentum nuchae	Aorta
Mucopolysaccharides:	2.3%	1.6%
hexosamines	(36%)	(26%)
uronic acids	(41%)	(34%)
sulphate	(15%)	(12%)
Collagen	20%	18%
Elastin	78%	18%
Neutral Sugars	0.3%	?

variability from sample to sample. A general composition is given in table 2.2 for ligament (Meyer et.al. 1956) and arterial tissue (Kirk 1959). In the case of ligament elastin the mucopolysaccharides are seen to make up about 2.3% of the whole tissue (w/dry wt. Tissue). Of this approximately 36% is present in the form of hexosamines, 41% as uronic acids with approximately 15% acid hydrolyzable sulphate.

#### (e) Collagen content

After accounting for the various other components present in ligament tissue, the collagen content works out to be approximately 17.4% as compared to values of 18% reported for arterial samples (Harkness et.al. 1957).

The summary for the chemical composition of arterial and ligament tissue is given in table 2.2 .

### E. Organization of Elastic Tissue

Since the main function of elastic tissue is a mechanical one, it is not surprising that the organization of the elastin fibres in elastic tissue varies with the direction(s) of the strain that are imposed on the tissue in vivo . In keeping with this generally accepted hypothesis, the following is a presentation of the microscopical organization of the two extremes of elastic tissue as demonstrated by ligament nuchae and arterial elastin.

#### (a) Methodology

### Histology:

Samples of unpurified pig aorta were stripped of the adventitial layer and other adhering tissue. Ligament elastin was also cleaned of adhering tissue, and both the arterial samples and the ligament samples were treated with Bouins fixative for 72 hours. They were then rinsed with distilled water, cut into small pieces and embedded in paraffin wax using standard histological techniques. After embedding the tissue was cut into 5 to 7  $\mu$ m sections and stained. The procedure, which was a slight modification of that presented by Clark et al. (1973), consisted of staining sections with orcein followed by a counter-stain of naphthol green B. This protocol results in red elastin fibres with the collagen fibres appearing faint green.

### Scanning electron microscopy:

Instead of using fixatives, the samples were frozen in liquid nitrogen and dried in a vacuum. They were then mounted onto stubs and coated with a fine layer of gold. The examination of the samples was conducted on a Cambridge Instrument Company, Stereoscan microscope (see methods, chapter 6 for more details).

### (b) Organization of ligament elastin

As expected, ligament elastin in the light microscope shows a very distinct alignment in the longitudinal direction, which is the direction of the in vivo strain (figure 2.1a). The 1 $\mu$ m collagen fibres seem to form a very fine network

Figure.2.1: Organization of ligament elastin.

(a) light micrograph of sectioned, unpurified ligament nuchae. The elastin fibres, E, are aligned in the direction of the strain (arrow) with the collagen (C) interspersed between the elastin. The bar represents 30um.

(b) s.e.m. of unpurified ligament showing the collagen.

(c) s.e.m. of unpurified ligament. The arrow indicates a branch point in the elastin network. The solid bar in b, and c represents 10um.

Figure.2.1.



around (between) the elastin fibres which have a diameter of about 6 to 8  $\mu\text{m}$ . There was no histological evidence for the presence of a collagen sheath, or other such collagenous structure, associated with the individual elastin fibres.

Scanning electron microscopy essentially supported the findings of the light microscope study as well as giving a clearer picture of the fine details. It showed a very diffuse network of collagen fibres dispersed in the elastic network (figure 2.1b). There was also some evidence for the branching of the individual elastin fibres (figure 2.1c).

#### (c) Organization of arterial elastin

In contrast to the ligament samples, cross-sections of arterial samples show a very distinct lamellar organization of its constituents (figure 2.2a), with the lamella (which are about 2 $\mu\text{m}$  in thickness) running in the circumferential direction. The elastin in any given lamella seem to be organized unidirectionally, with the adjacent lamellae showing a successive change in this direction (figure 2.2b). The presence of interlamellar fibres is also evident (figure 2.2c). The collagen seemed to occur between the elastin lamellae in a dense fibrillar network. Although it was not possible to determine the direction of the collagen alignment (with respect to the longitudinal direction of the artery) there have been reports that the collagen network actually follows a helical path (Wolinsky and Glagov 1964).

The composite structural organization of ligament and

Figure.2.2: Organization of arterial elastin.

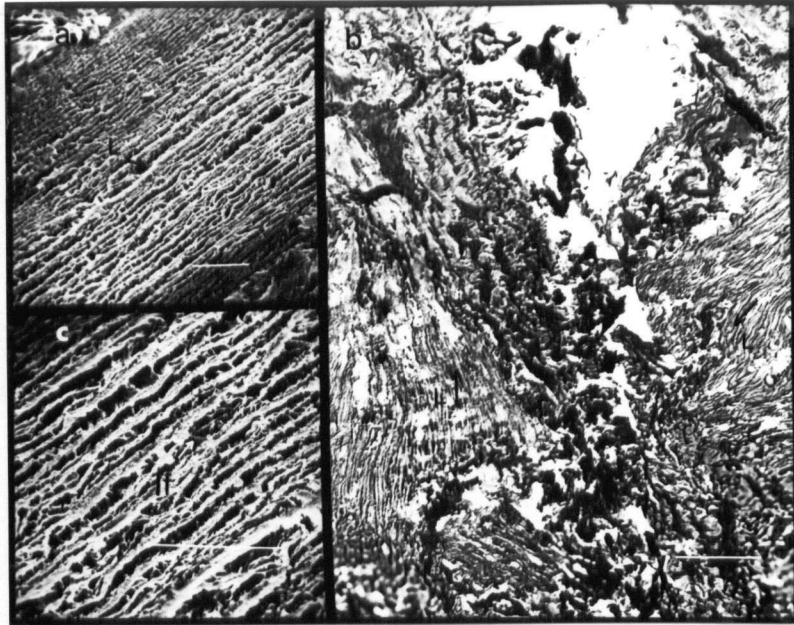
(a) s.e.m. showing the lamellar (L) organization of arterial elastin.

(b) Light micrograph of sectioned arterial media showing the relative organization of adjacent lamellae. The bar represents 20um.

(c) s.e.m. of artery showing the presence of the interlamellar fibres (If).

The solid bars in a, and c represents 10um.

Figure.2.2.



arterial tissue is depicted in figure 2.3. A more complete analysis of the structure of elastic tissue can be found in articles by Cotta-Pereira et.al. (1977), Carnes et.al. (1977) and Kadar (1977).

#### F. Purification Techniques

In order to study the properties of the elastin protein, it is necessary to isolate the protein from the rest of the tissue with which it occurs in vivo. This can be done by the use of a number of purification techniques for which the methodology (Robert and Hornebeck 1976) and the chemical evaluation of the resulting elastin (Partridge 1962, Grant et.al. 1971) has been well documented. In this thesis, which deals primarily with the physical properties of the elastin protein, the alkali extraction procedure (Lansing et.al. 1952) and the repeated autoclaving method of (Partridge et.al. 1955) were used exclusively. The following section is therefore presented as a comparison of these two techniques on a chemical and structural basis.

##### (a) Amino acid compositions

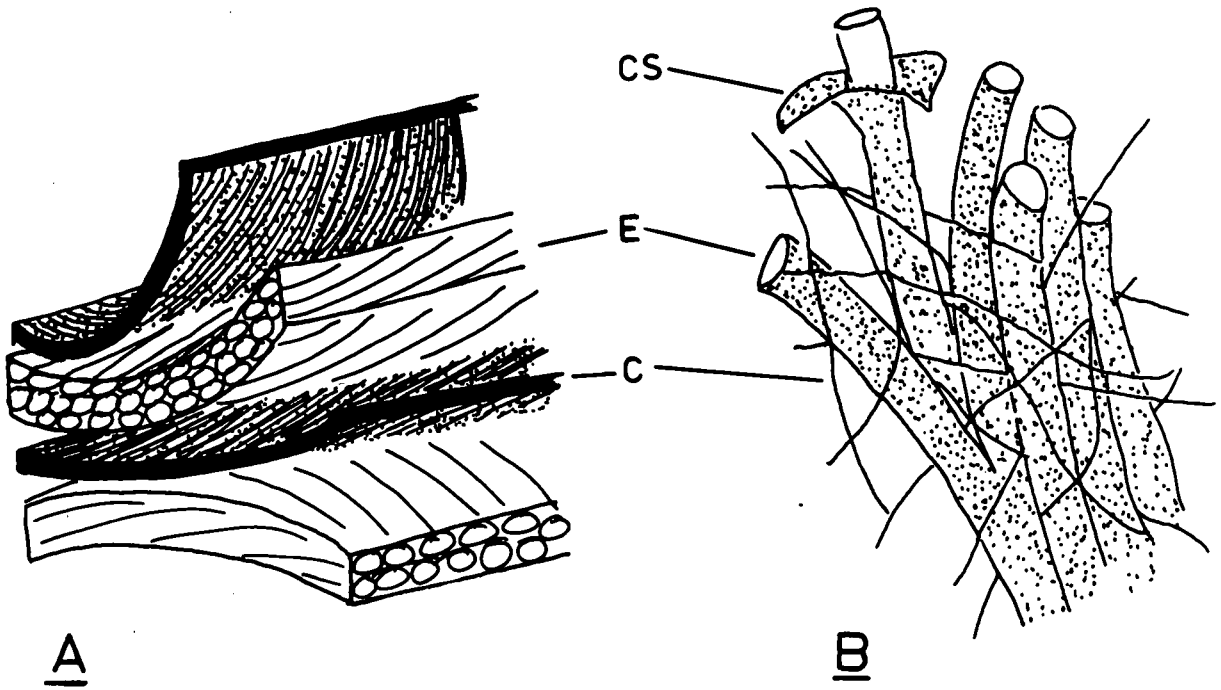
In evaluating the amino acid composition one has to first decide on a standard against which to compare the results of the purification product. This standard is usually taken to be the precursor molecule, tropoelastin. Table 2.3 lists the amino acid composition for tropoelastin, autoclaved elastin and alkali extracted elastin as presented by Grant et.al.

Figure.2.3: The elastic tissue composite.

(A) The arterial media showing the relative organization of the collagen (C) and the elastin (E).

(B) A schematic diagram of ligamentum nuchae showing the organization of the elastin, collagen, and the collagen sheath (CS).

Figure.2.3.



(1971). Both procedures are seen to give comparable elastin preparations with regard to the amino acid composition.

(b) Hexosamine and neutral sugar content

The data obtained by Grant et.al. (1971) indicate that alkali extracted elastin contains about half as much hexosamine as autoclaved samples (both are below 0.04% w/w). The neutral sugars were quantitated with the phenol-sulphuric acid assay of Lo et.al. (1970) using glucose (Sigma) as a standard. The results show that autoclaved elastin had a neutral sugar content of 0.02% (w/w). There were no detectable sugars in alkali purified elastin.

(c) Evaluation by scanning electron microscopy

Samples of autoclaved and alkali purified elastin were frozen in liquid nitrogen and dried in a vacuum. The pieces of tissue were mounted onto stubs, coated with gold and observed in a Stereoscan microscope as described before.

Both purification procedures gave clean preparations as observed in the scanning electron microscope, with no indication of collagen or 'matrix' substances (figure 2.4, a and b). However, there was some indication of alkali attack of the elastin fibres prepared by 0.1N NaOH extraction (figure 2.4c). No such degradation was observed for autoclave purified elastin.

G. Mechanical Properties of Elastin Bundles

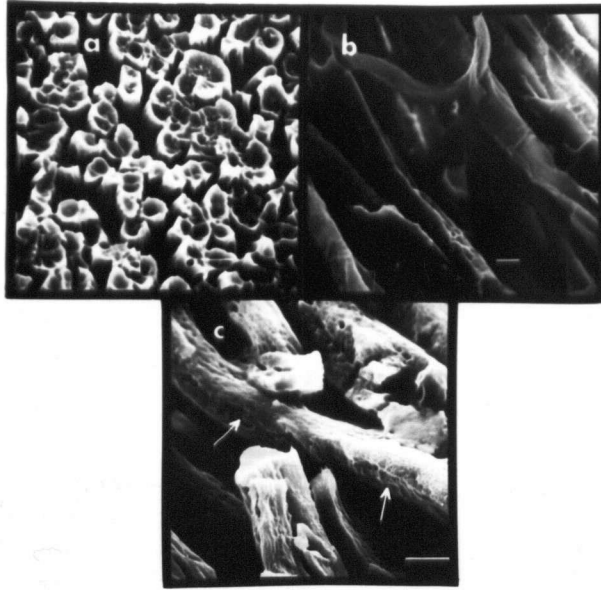
Table.2.3: Amino acid composition of elastin preparations.

AMINO ACID COMPOSITION OF ELASTIN PREPARATIONS.\*

	Tropoelastin	Autoclaved	Alkali
asx	3.3	6.4	5.4
thr	13.2	7.4	5.3
ser	9.2	8.7	6.6
glx	15.8	15.7	11.9
pro	101.1	118.4	96.4
hyp	6.6	8.7	12.9
gly	333.4	310.5	316.2
aia	237	238.6	243.1
cys	--	--	--
val	125.4	143.9	154.3
met	--	--	--
ile	16.1	23.3	24.6
leu	47.5	59.5	63
tyr	14.1	10.7	13
phe	28.3	28.6	32.1
his	--	--	--
lys	45.1	3.1	3.1
arg	4.3	7.7	2.7

\*from Grant et.al. 1971.

Figure.2.4: Evaluation of purification techniques.  
(a) s.e.m. of alkali purified elastin.  
(b) s.e.m. of autoclave purified elastin.  
(c) Higher magnification of alkali purified elastin showing the hydrolytic attack of the elastin fibre.  
The solid bars represent 10um.

Figure.2.4.

### (a) Methods

Samples of ligament elastin were dried and their ends were embedded into threaded steel cups with epoxy glue. They were then hydrated in distilled water over a period of seven days under sterile conditions before testing. The stress-strain properties of the elastin were determined with an Instron tensile testing machine, with the samples (of about 1.5 cm length) being extended at a rate of 1mm/min.

The unstrained cross-sectional area was measured as follows. The length of the sample between the anchoring points was measured with calipers before the start of a test. This was taken to be the value of  $L_0$ , used for the subsequent calculation of the extension ratio and unstrained cross-sectional area. Immediately after the mechanical test, the sample was cut at the anchor points, dried to constant weight and weighed. The volume of the protein was calculated from this weight and a value of 1.33g/cc for the density of the protein. The volume of the hydrated sample was calculated by using a volume fraction of 0.65 for the protein at 24°C (Gosline 1978), which was the temperature at which the tests were conducted. The nominal cross-sectional area could then be calculated by dividing the value for the hydrated volume by  $L_0$ .

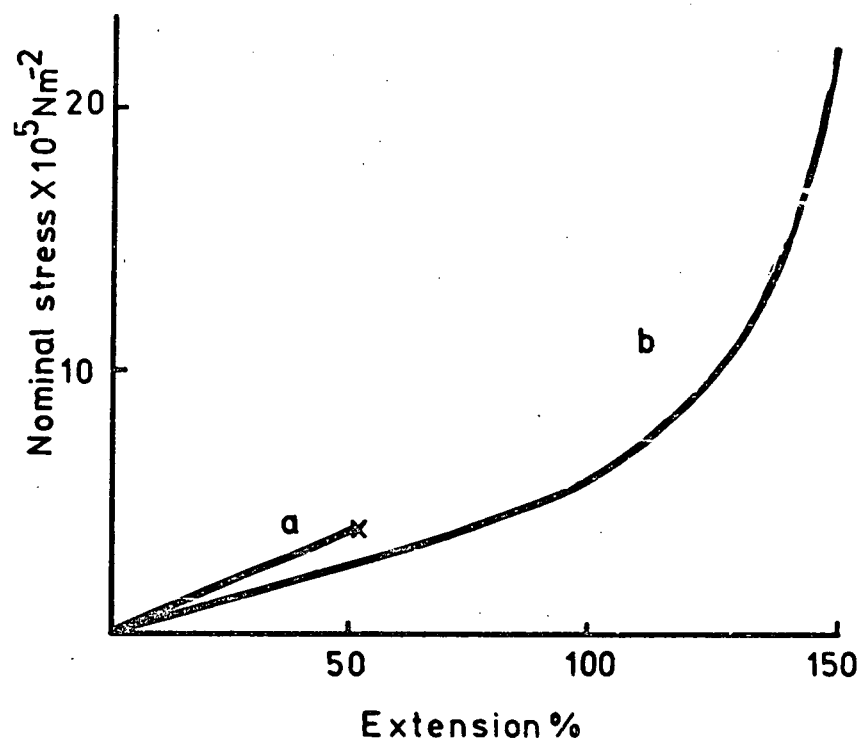
### (b) Results

Figure 2.5 shows the results of the stress-strain

Figure.2.5: Mechanical properties of elastin bundles.

Plots of nominal stress versus strain for:

- (a) autoclaved ligament elastin bundles. (x) represents the failure strain.
- (b) unpurified ligament elastin bundles.

Figure. 2.5.

experiments on unpurified and autoclave purified ligament elastin. The unpurified samples show a biphasic curve with an initial tensile modulus of  $6.87 \times 10^5 \text{ Nm}^{-2}$  and a final modulus of  $3.8 \times 10^6 \text{ Nm}^{-2}$ . These unpurified bundles could be extended by about 150% of their initial length before failure. In contrast to this, autoclaved elastin samples failed at about 50% extension, and upto failure exhibited a single value for the tensile modulus of  $8.6 \times 10^5 \text{ Nm}^{-2}$  which is higher than the modulus of the unpurified bundles in the same region of extension. These values obtained for autoclaved elastin samples are in close agreement with the values attained by Mukerjee et.al. (1976).

Although this result, of a higher modulus for the purified ligament as compared to the unpurified tissue, appears ridiculous at first glance, it can be explained if one assumes that only the elastin component of the unpurified samples is contributing to the mechanical properties for elongations approaching 50% extension. Since the cross-sectional area is calculated for the whole tissue, of which only 80% is elastin, the nominal stress values will be an underestimate due to the overestimate of the 'contributing' cross-sectional by approximately 20%. This is borne out by the absolute magnitude of the two moduli with the ratio of the unpurified modulus/purified modulus being about 0.75 .

#### H. Mechanical Properties of Single Elastin Fibres

The first studies on the mechanical properties of

Figure.2.6: Mechanical properties of single elastin fibres.

Plots of nominal force versus extension for:

- (a) unpurified fibres (Carton et.al. 1962).
- (b) autoclaved fibres.

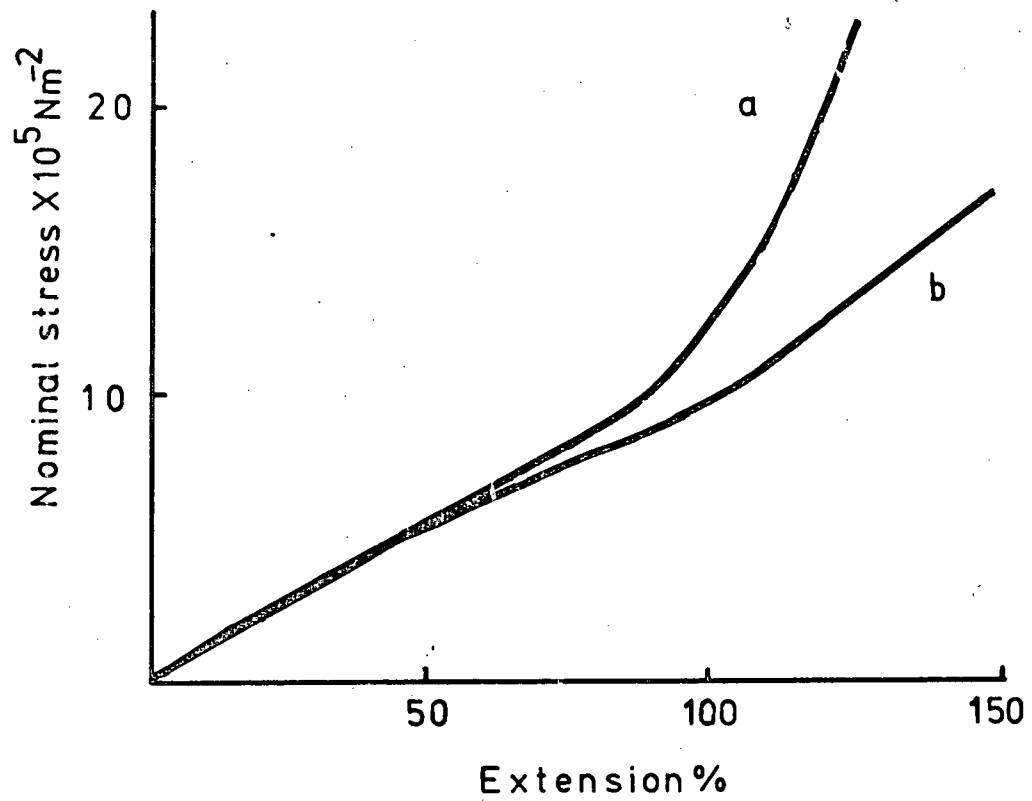


Figure.2.6.

unpurified single elastin fibres were reported by Carton et.al. (1960, 1962). Their results are presented along with the mechanical properties obtained for purified single elastin fibres in this study in figure 2.6 (the methodology is discussed in chapter 7).

The relationship obtained by Carton also exhibited a biphasic stress-strain curve similar to that obtained for unpurified bundles of elastin. In comparison to this, autoclaved elastin fibres show a fairly linear relationship upto approximately 100% extension, beyond which they also tend to deviate upwards, but by an amount that is much smaller than that shown by the unpurified fibres. In contrast to the autoclaved bundles, purified single fibres could be extended to 120-150% extension before failure. The Young's modulus for the initial extension region, of both the unpurified and autoclaved single fibres, had a value of about  $1 \times 10^6 \text{ Nm}^{-2}$ .

## I. Discussion

### (a) Variation in elastin biochemistry

Although there is a general concensus about the composition of elastin, there is also some indication that a few distinct differences exist in the amino acid profiles and/or primary sequence of elastin from different sources. Recently there have been reports on the elastin from auricular cartilage, which have shown this protein to have an unusually large content of polar residues (twice as much as arterial

elastin) with a 20% reduction in the amount of valine residues (Field et.al. 1978).

The sequential variability was pointed out by Kieth et. Al. (1979), who analyzed the valine-proline sequence content of elastin from different tissue. They showed that this particular sequence occurs about 41 times/1000 residues in aortic elastin and only 9 times/1000 residues in auricular elastin. On the basis of these results they favoured the existence of more than one gene for the elastin protein.

This aspect of elastin biochemistry is worrisome since it raises doubts about the use of elastin from ligament nuchae to make generalizations about elastin from other sources e.g., arterial elastin. These differences in the primary sequence would be very crucial, if as suggested by several authors (Urry et.al. 1977a), the val-pro sequence is a major determinant of elastin structure.

#### (b) The composite tissue

Elastic tissue, like most other biological tissue, occurs as a chemical and mechanical composite in vivo. Its organization is seen to vary from tissue to tissue depending on it's exact functional state. In general, it seems evident that the elastin protein is probably the dominant mechanical component at low strains with the collagen contributing the more significant component at higher elongations.

Comparison of single fibre results for purified and unpurified elastin, seems to show that another mechanical

component is intimately associated with the single elastin fibre. There is some speculation that this other component consists of collagen which is present as a sheath around the individual elastin fibres (Finlay and Steven 1973, Serafini-Fracassini et. Al. 1977). This aspect of elastin organization which is based on mechanical properties, could not be supported by the results of the histological and scanning electron microscope studies conducted for this report.

Although the ground substance is unlikely to be a major mechanical component in elastic tissue (it probably contributes a small amount as shown by Banga and Baló 1960), it's chemical properties are probably important in determining the environment within the elastic tissue. Alterations in these environmental properties would inevitably effect the mechanical properties of the elastic component.

Recent studies on the dynamic mechanical properties of elastin (Gosline and French 1979) indicate that the functional properties of the elastin protein are adversely altered by slight degrees of dehydration. In view of this the crucial role, of 'controlling the environment', which is performed by the embedding matrix in vivo cannot be ignored.

### (c) Evaluation of purification techniques

In comparing the feasibility of any given purification procedure one has to first consider the experiment that is to be conducted on the purified sample. It is evident from this study that alkali purification yields a more pure elastin

(chemically closer to tropoelastin) than the autoclaving procedure. On the other hand, scanning electron microscopy showed that, structurally, both preparations gave similar results in gross observation. However, closer examination of the preparations revealed that there was some evidence of hydrolytic attack of the elastin fibre in the samples that had been purified by alkali treatment. In contrast, there was no indication of such unwanted side effects in the autoclaved preparations.

This brings me back to the first statement. If the experiment that one had in mind was biochemical in nature, then it would be advisable to use the cleaner preparation afforded by the alkali technique. Alternately, if the experiment involves the measurement of physical properties, such as stress-strain relationships, it is more feasible to use an autoclaved sample which, though less pure chemically, is probably more appropriate for such purposes since there is no evidence of elastin degradation.

## Chapter. III. CONFORMATION OF ELASTIN: THE CONTROVERSY.

### A. Introduction

Several models for elastin have been proposed over the years. These range from the extreme of the collagen-like triple helix structure, proposed by Ramachandran (1963), to the other extreme of a totally amorphous random network similar to other kinetic elastomers (Hoeve and Flory 1958). The remaining possibilities lie somewhere in between these two extremes, such as the Liquid-drop model of Weis-Fogh and Anderson (1970), the Oiled-coil model of Gray et.al. (1973) and the recently published cross-Beta spiral of Urry (1976a). These models for elastin structure are depicted in figure 3.1. This chapter will be directed towards presenting the various proposals for elastin conformation, and will try to evaluate the evidence on which they are based.

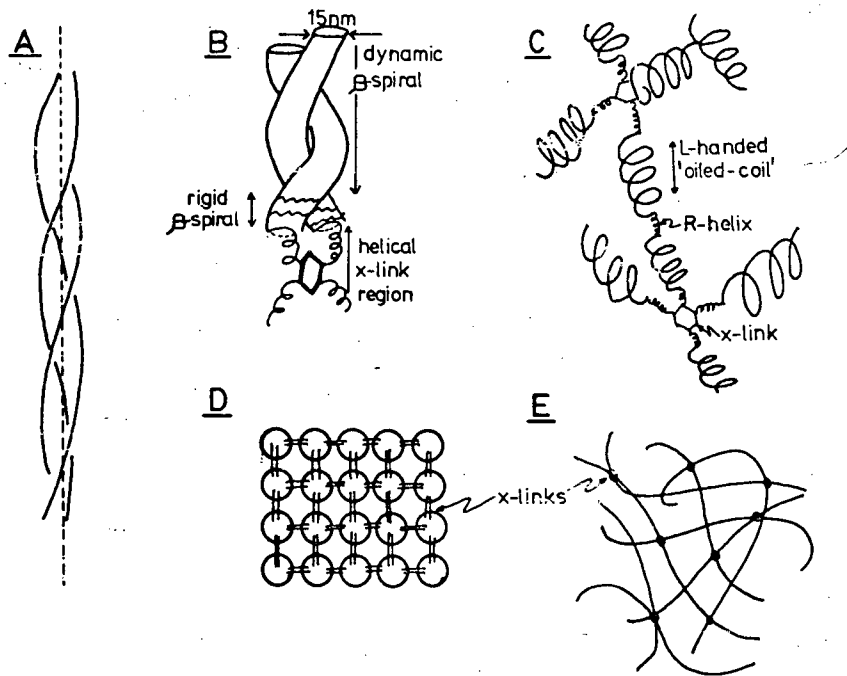
### B. The Random Network Model

The random network model for elastin was essentially an extension from the work of polymer chemists on the properties of hydrocarbon elastomers. Since these materials exhibited mechanical behaviour that could not be accounted for by the standard theories of solid elasticity present at the time, a new theoretical framework, commonly referred to as the Kinetic Theory of Rubber Elasticity, was developed (Guth et.al. 1946). The theory was based on Gaussian statistics requiring a random conformation for the material in question.

Figure.3.1: Proposals for the conformation of elastin

- (A) Collagen-like triple-helix (Ramachandran 1963).
- (B) Beta-spiral structure (Urry 1978b).
- (C) Oiled-coil model (Gray et.al. 1973).
- (D) Liquid-drop model (Weis-Fogh and Anderson 1979).
- (E) Random network conformation (Hoeve and Flory 1958).

Figure. 3.1.



This Kinetic theory was already in existence when people started to study the protein rubbers, and it is not surprising that the initial attempts to characterize the properties of these protein elastomers involved the application of the kinetic theory relationships. This was done for the bivalve hinge ligament Abductin (Alexander 1966) and the insect protein rubber Resilin (Weis-Fogh 1961a). Both were convincingly shown to be entropic elastomers as predicted by the kinetic theory. Since this theory is based on a random network structure, it was logical to then extrapolate to the conformation of these elastomers and state that they were random at the molecular level. The idea of a random conformation for the elastin protein was also based on the analysis of its macroscopic properties according to the kinetic theory of rubber elasticity.

#### (a) Elastin thermoelasticity

The initial work on the thermoelastic properties of elastin, using the constant length experimental technique (appendix 1), indicated that a large energy component was associated with the elastic mechanism which was in contradiction to the notion of an entropy elastomer (Meyer and Ferri 1936, Wohlsch et.al. 1943). It was later shown that these investigators failed to account for the temperature dependent swelling of elastin, which has a large energy component associated with it (Hoeve and Flory 1974).

Hoeve and Flory (1958) had gotten around this

experimental difficulty, of temperature-deswelling, by studying the thermoelasticity of elastin in a mixed diluent system, of 30:70 ethylene-glycol:water, where the volume of elastin was independent of temperature. Their experiments showed that, under these conditions, elastin behaved as a typical kinetic rubber with the energy component being close to zero. This conclusion was later supported by Volpin and Cifferi (1970) who conducted a similar experiment in the temperature range of 50°-70°C, where the volume of elastin is also independent of temperature.

The mixed diluent systems utilized by Hovee and Flory was later criticized by Oplatka et.al., (1960), who pointed out that although this approach circumvented the problem of a temperature dependent volume change it did not test for a composition change i.e. the changes in the distribution of the types of solvent molecules bound as a function of temperature. It was therefore necessary to make some changes in the basic theoretical relationships to explain the thermoelastic behaviour of open systems such as elastin. This was accomplished by Oplatka et.al., (1960), and Bashaw and Smith (1968) for polymer systems of highly swollen rubbers. The specific application of these relationships to the elastin protein was provided by Mistrali et.al., (1971).

Hence with regard to elastin thermoelasticity, at any rate, it seems fairly safe to conclude that the results point to elastin being a typical kinetic elastomer as described by the kinetic theory of rubber elasticity. Since this theory is

based on a random network conformation, it seems reasonable to expect elastin to be random in its conformation as well.

(b) Differential scanning calorimetry

Kakivaya and Hoeve (1975) used the technique of differential scanning calorimetry to study the glass point of elastin. They were able to show that elastin undergoes a second order transition, in a temperature range that depends on its water content. Such second order transitions are typical of the glass transitions that are observed for most amorphous polymers. They did not see any evidence for first order transitions that might be associated with the 'melting' of stable secondary structures. The values for the glass transition temperatures correlated well with the observed mechanical behaviour of elastin which is characterized by a sudden drop in the modulus as it goes from being a rigid glass to an extensible polymer (Gotte et.al. 1965). It was also found that diluents, such as ethylene glycol and water, depressed the glass transition temperature equally, on a volume basis, which argues against the objection of Oplatka (1960) regarding the use of a mixed diluent system for thermodynamic studies of elastin. They also argued that these results were consistent with a random network model, and only a random network model consisting of a single homogeneous phase.

(c) E.M. And X-ray diffraction studies

Early examination of negatively stained elastin fibres, in the electron microscope, showed elastin to be an amorphous protein with no detectable structural features (Cox and Little 1962, Ross and Bornstein 1969, Karrer and Cox 1961). This however was not an unanimous conclusion as various other investigators at that time also reported seeing fibrillar structures within the elastin fibre (Lansing et.al. 1952, Gross 1949). Similar structures have been seen in recent studies, and these observations form the basis for a filamentous model of elastin, that will be discussed later on in this chapter.

The X-ray diffraction studies of elastin conducted at that time were also in support of a random network model for elastin (Astbury 1940, Cox and Little 1962). Both papers reported diffuse diffraction haloes at  $4.6\text{\AA}$  and  $7.8\text{\AA}$  which did not change upon stretching. This type of pattern is typical of amorphous polymers and indicated a lack of crystalline structure. Again the interpretations were not unanimous with some reports of strong diffraction patterns for elastin (Kolpack 1935, Bear 1942 and 1944). All of these results were later shown to be artifacts caused by collagen contamination.

#### (d) N.M.R. Evidence

The rationale for testing the random network model using nuclear magnetic resonance lies in the high sensitivity of this technique in measuring the the mobility of the components

involved. Torchia and Piez (1973) obtained a  $^{13}\text{C}$ -nmr spectrum of ligament elastin and they were able to show that the correlation times, which are taken to be indicators of backbone movements (with the small times representing fast kinetic motion), as obtained from the line widths of the various resonances, had values in the 10 nanosecond range indicating a high mobility for about 80 percent of the backbone carbons (Lyerla and Torchia 1975). The remaining 20 percent were proposed to be involved in the cross-linking region which would be expected to have lower mobilities. These data also support the random network conformation.

### C. Liquid Drop Model

#### (a) Preliminary evidence

The initial idea of a two-phase model for elastin was seeded by Partridge (1967a, 1967b) who hypothesized a corpuscular structure for elastin on the basis of gel filtration experiments conducted on columns packed with elastin fibres. He was able to show that these elastin packed columns could separate molecules on the basis of their molecular weights, and that these separation characteristics were consistent with the matrix (elastin) being a material that contained pores of about  $32\text{A}^\circ$  in diameter, or a system of randomly distributed rods having a length of  $16\text{A}^\circ$ . Partridge also noticed that this system would adsorb alcohols, and that this adsorption of alcohols was directly related to the

hydrocarbon chain length. It therefore seemed reasonable, at the time, to think of elastin as a two-phase system with discrete regions of hydrophobic clusters and interspersed solvent, especially since these structures were supported by electron microscope evidence (Partridge 1968).

A similar type of model was eluded to by Kornfeld-Poullain and Robert (1968) using evidence from alkali degradation studies of elastin. They quantitated the alkali digestion of elastin as a function of solvent hydrophobicity and showed that the addition of alcohols to the reaction mixture greatly facilitated the degradation of elastin. They then proposed a series of steps in the degradation process of elastin which involved the initial dispersion of hydrophobic regions by the organic solvent followed by alkaline attack of the peptide moieties. Although it is not stated explicitly, there is an implicit assumption in this type of degradation process of a two-phase system.

#### (b) Thermodynamic evidence

Using the constant temperature thermoelastic experiment (appendix 1) Weis-Fogh and Anderson (1970) observed a heat during elongation that was many times larger than the work of extension. This was viewed as a result that was inconsistent with the random network model for elastin since, for an entropy based elasticity, the heat released during extension should be equal to the mechanical work done to elongate the sample (see appendix 1). It was also observed that this effect

of 'excess heat' could be reduced by adding long chain hydrocarbon molecules like alcohols. On the basis of these results they proposed a liquid drop model for elastin structure, which consisted of corpuscular units having a hydrophobic core with the hydrophilic groups on the surface. Extension of this network would force parts of the hydrophobic core to the surface and the retractive force was hypothesized to arise from this interfacial energy effect. Further support for this model was obtained from n.m.r. Data (Ellis and Packer 1976) and by Gosline et.al. (1975) who used fluorescence probe analysis to confirm this reversible exposure of hydrophobic groups, from the corpuscular units, to the interspersed hydrophilic solvent during extension.

#### D. Oiled Coil Model

The oiled coil model was proposed by Gray et.al. (1973), and is based on the amino acid sequence data accumulated by these investigators for porcine tropoelastin (Foster et.al. 1973, Sandberg et.al. 1971, 1972). They delineated their data into two categories: (a) residues involved in the cross link region and (b) residues involved in the extensible regions. To the first category were assigned the alanine and lysine rich areas, with the glycine, proline and valine residues being assigned to the flexible regions. It is thought that the alanine residues form alpha-helices which align the lysine residues into a position that favours their cross linking into desmosine and isodesmosine residues.

The overall model envisaged a system having helical cross link regions with the extensible regions forming a broad oiled-coil. It was further proposed that the glycine residues would occupy the exterior of these oiled-coils in a solvent exposed position, with the proline, valine, and other hydrophobic residues buried inside the coils away from the solvent. As is obvious, this type of model is conceptually similar to the liquid drop model of Partridge (1967). The only difference lies in the proposal for the shape of the hydrophobic clusters. The model of Partridge seems to presume these clusters to be globules, whereas the oiled-coil proposes them to be fibrillar. Both of them would behave identically, in the thermodynamic sense, and the calorimetric data obtained by Weis-Fogh and Anderson (1970) was also cited as evidence for the oiled-coil model.

#### E. Fibrillar Models

The tone of the fibrillar models for elastin was set by the intense activity in the collagen field that was prevalent at the time when investigators started to study elastin structure. These workers approached it from a point of view which classified it as being part of the collagen family, but with a very low melting temperature (Astbury 1940). It was taken to an extreme in a publication by Ramachandran and Santhanam (1957) who proposed a collagen-like triple helix for elastin. This idea of wanting to fit elastin into a structural hierarchy, as borrowed from the collagen group, is still

prevalant today and forms the major impetus for the increased interest in the fibrillar models.

(a) Electron microscope evidence

The fibrillar appearance of elastin in the electron microscope was first noted by Gross (1949) who stated that the elastin fibre was a composite of a twisted rope structures of 80A° diameter, which were cemented together via an amorphous matrix. Other studies also reported such fibrillar components in the elastin fibre (Lansing et.al. 1952, Rhodin and Dalhamn 1955).

A flood of papers on elastin ultrastructure have taken up this theme of a fibrillar model for elastin with some success. These investigators have utilized drastic techniques such as sonication and heavy metal staining to visualize ordered arrays of fibrils, 30A° in diameter (Gotte et.al. 1965, Serafini-Fracassini and Tristam 1966). Recent publications of electron microscope studies have also confirmed the existence of sub-structure in the elastin fibre (Quintarelli et.al. 1973, Gotte et.al. 1974, Serafini-Fracassini et.al. 1976, 1978). The last authors have also reported a reflection of 40-50A° periodicity in the X-ray diffraction patterns of ligament elastin that had been stretched by 60%. This along with a recent study (Pasquali-Ronchetti et.al. 1979), utilizing freeze fracture and etching techniques, which show the presence of an extension related alignment of the structural components, present strong evidence for the

fibrillar model.

In general, the electron microscope evidence seems to support a fibrillar model which when taken to an extreme, can be visualized as a twisted rope array of two 15A° filaments that, as a unit, are visualized in the electron microscope as 30A° fibrils running along the long axis of the elastin fibre (Gotte et.al. 1976). There is also some evidence that these 30A° fibrils are clustered together into a higher order of sub-fibre, 150 to 200nm in diameter, as observed in the scanning electron microscope (Hart et.al. 1978).

(b) Nuclear magnetic resonance evidence

It has been pointed out in some recent publications that the primary sequence of tropoelastin, which is thought to be the precursor of the fibrous protein, contains recurring sequences of certain amino acids (Sandberg et.al. 1971, 1972). Based on these primary sequence data Urry and his co-workers have synthesized a number of repeat peptides corresponding to the sequences in tropoelastin, and have attempted to decipher the conformation of the elastin protein by using these synthetic peptides as models. Their efforts have concentrated on three such model peptides:

1. A tetrapeptide (Val-Pro-Gly-Gly)<sub>n</sub>
2. A pentapeptide (Val-Pro-Gly-Val-Gly)<sub>n</sub>
3. A hexapeptide (Ala-Pro-Gly-Val-Gly-Val)<sub>n</sub>

For the sake of simplicity a short discussion of the tetrapeptide studies follows.

Figure.3.2: Beta-turns.

(A) The tetrapeptide (val-pro-gly-gly) showing the results of nmr studies: (●) solvent shielded moieties, (○) solvent exposed moieties (from Urry and Long 1976a).

(B) Beta-turn proposal based on these results. Dashed line indicates the hydrogen bond (from Urry and Long 1977b).

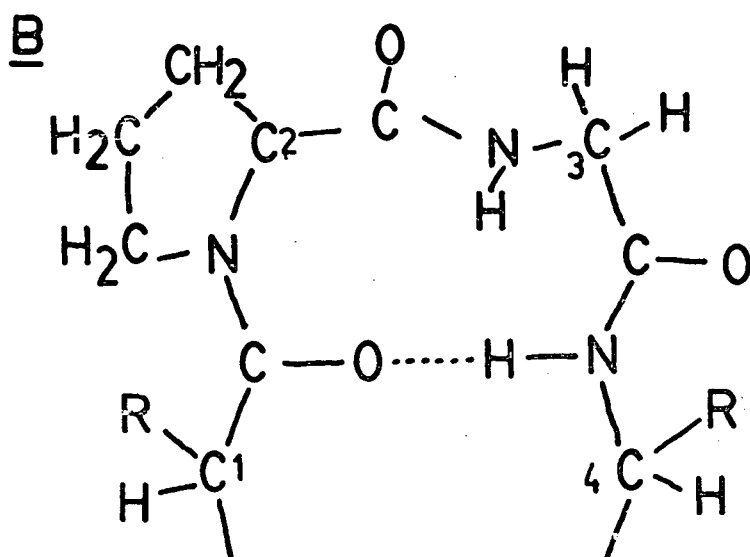
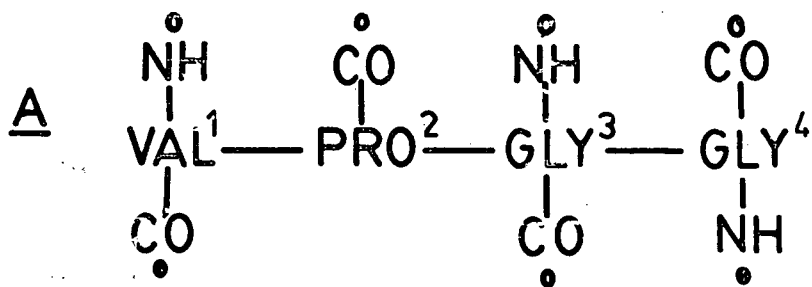
Figure.3.2.

Figure 3.2 (a & b), shows the tetrapeptide and the summary of the proton and carbon nuclear magnetic resonance data obtained from solvent titration techniques (DMSO-Trifluoroethanol), which involves the monitoring of the resonances as a function of solvent composition (Urry and Long 1976a). It was found that some moieties showed a marked solvent dependence of their chemical shifts, while others were relatively unaffected. These unaffected residues were proposed to participate in hydrogen bonds.

In the case of the tetrapeptide, proton resonance data showed the Gly4 NH to be a solvent shielded moiety which was involved in a hydrogen bond with the carbonyl oxygen of the Val1 residue. In comparison to this, the Gly3 and the Val1 NH were found to be solvent exposed, and were not thought to participate in hydrogen bonds. Carbon resonance data also supported these results, showing that the Val1 CO was in fact solvent shielded with the Gly4 CO being solvent exposed (Urry and Long 1976a). On the basis of these findings they have proposed a Beta-turn structure (figure 3.2b) for this tetrapeptide (Urry and Long 1977b).

Studies of the high polymers of this tetrapeptide repeat indicated that, above 50°C, in addition to the Gly4 NH, the Gly8, 12, and 16 NH's also behaved in a solvent shielded manner. Furthermore, the Gly4 CO behaved as though it too was involved in a hydrogen bond. To account for these additional findings a Beta-spiral structure (figure 3.3) was proposed to exist above 50°C (Urry et al. 1977a).

Further support for these Beta-turn structures was obtained through conformational energy calculations (Khaled et.al. 1976) and nuclear overhauser enhancement studies, which showed that the irradiation of the Pro2 CH protons resulted in an enhancement of the Val1 (CH) proton resonances. This indicated the close association between the side chains of these two residues after ring closure (formation of a Beta-turn) (Urry et.al. 1977a).

Similar studies on the poly-pentapeptide (Urry et.al. 1976b) and the poly-hexapeptide (Urry et.al. 1974, 1978a,b) indicated that these polymers were also involved in the Beta-turn as a preferred conformation. A number of additional hydrogen bonds are present in the hexapeptide which make it a more stable (rigid) structure than the other two repeats (Urry 1978a).

Assimilating this nuclear magnetic resonance data with the electron microscope evidence, Urry has proceeded to define a hierarchial model for elastin which is depicted in figure 3.1. This structure consists of dynamic Beta-spirals in the extensible regions with the rigid hexapeptide Beta-spirals occurring in the cross-link regions, facilitating the condensation of the lysine residues into the (iso)desmosines.

## F. Discussion

### (a) Two-phase models

Under this clasification I have grouped the liquid-drop

model (Partridge 1967, Weis-Fogh and Anderson 1970) and the oiled-coil model (Gray et.al. 1973) since both of these propose distinct regions of hydrophobic clusters surrounded by solvent.

The major support for these two-phase models is based on the thermodynamic evidence of Weis-Fogh and Anderson (1970) and it is on this very evidence that it has been refuted. In a communication by Grut and McCrum (1974) it was pointed out that the data obtained by Weis-Fogh and Anderson was predictable from the kinetic theory of rubber elasticity (which supports a random conformation). They argued that the excess heat observed during elongation was a result of the adsorption of water onto the non-polar groups and that the energy term represented the heat of dilution from this process. This also explained the decrease in the energy component with the addition of organic solvents to the diluent (which would have a lower heat of dilution). The point was elaborated further by Dorrington et.al. (1975) who arrived at the same conclusions. This absorption of the water by the elastin network during extension (Hoeve and Flory 1974) could also explain the results of the fluorescence probe analysis (Gosline et.al. 1975) which could, in retrospect, be predicted by the kinetic theory relationships (Mark 1976).

A two-phase model would also be inconsistent with the glass transition temperature studies of Kakivaya and Hoeve (1975). These authors explained that if this glass transition occurred inside these 'hydrophobic globules', then it would be

hard to account for the dependence of the transition temperature on the amount of water that was present outside these globules.

It has also been pointed out in recent studies that the temperature-swelling behaviour of elastin is consistent with the Flory-Rehner model for network swelling which, again, is based on an amorphous, single phase network for the polymer (elastin) in question (Gosline 1977, 1978). Carbon nuclear magnetic resonance studies (Torchia and Piez 1973), have indicated a very rapid back-bone motion for the elastin protein. This is also hard to reconcile with these two phase models for elastin structure, since the protein would be expected to have a reduced mobility inside such compact structures.

#### (b) Evidence for secondary structures

Investigators using different spectroscopic techniques have confirmed that approximately twenty per-cent of the residues in elastin are involved in secondary structures (Torchia and Piez 1973, Lyerla and Torchia 1975, Starcher et.al. 1973, Tamburro et.al. 1977, Mammi et.al. 1970). The controversy that is present at the moment involves the location of these secondary structures: do they occur in the cross-link regions of elastin or are they present in the extensible parts of the polymer chains.

Urry and his co-workers have argued in numerous publications that these ordered regions are an integral part

of the elastin chain in the extensible regions, and as discussed previously, these investigators believe that most of the valine, proline, and glycine residues are involved in Beta-turn structures. On the other hand, a recent study by Fleming et.al. (1980), who also used nuclear magnetic resonance techniques, have shown that almost all of the valine residues in elastin are characterized by rapid movements.

In judging between these two views one has to ask a number of questions: (a) what percentage of the amino acid residues occur as the repeat peptides, which form the basis of Urry's work? (b) can results from other methods be used to differentiate between the two possibilities?

In answer to the first question, only about 20% of the residues occur as repeat peptides in the elastin primary sequence (Foster et.al. 1973). Urry has argued that although this is in fact a reasonable estimate, the structures proposed by him would occur as a major conformation assuming that the repeat peptides could tolerate substitutions and still retain their secondary structure. This assumption, however, is not borne out experimentally since even a relatively conservative substitution (val--pro) results in the disruption of the Beta-turns (Urry et.al. 1977a).

In reference to the second question, it is possible to assimilate thermodynamic data with the nuclear magnetic resonance results to obtain a clearer story. Kakivaya and Hoeve (1975) using the technique of differential scanning calorimetry, failed to observe any first order transitions,

arguing against the presence of Beta-spiral structures, which would be expected to give a sharp peak in the region of the transition (from the spirals to the random coil as induced by high temperatures). Their results would tend to favour the view that elastin is essentially an amorphous protein. It must also be kept in mind that most of the proposals for the Beta-structures are based on studies involving small peptide fragments, which may not be satisfactory models for insoluble elastin.

#### (c) Hydrogen bonded structures

It is evident that the Beta-turn and the Beta-spiral are structures that depend on hydrogen bonding for their stability, and as pointed out before, the thermodynamic data of Kakivaya and Hovee (1975) are inconsistent with these interpretations of elastin structure. There are a number of possibilities that could account for the failure of these investigators to observe a first order transition: (a) the energy change associated with the transition is very small or (b) these structures are extremely stable over the temperature range of the experiment (0°-200°C).

This again creates a dilemma. If the energy for the transition from the Beta-spiral structure to the random coil conformation is very small, then there is no reason to assume that the peptide-peptide hydrogen bonds (needed for Beta-turns) should be favoured over the peptide-solvent interactions. The system is then very close to being an

amorphous, single-phase network with rapid back-bone movements. This view is also consistent with the Beta-spiral structures, if they are present, being very dynamic ones.

On the other hand, if these structures are very stable, then protein-protein interactions can be considered to be favoured over protein-solvent interactions. That this could occur is not surprising since they are known to be present in other fibrous proteins such as collagen, silk, and keratin, which have hydrogen bonded organizations like the alpha-helix and beta-sheet structures. This is where the dilemma arises. Any hydrogen bonded system that would so overly favour peptide-peptide interactions has to, as an inevitable consequence, exhibit relatively stiff mechanical properties as do the above mentioned group of proteins.

Elastin also exhibits such properties, when it is dry. The dry state (or low hydration conditions) can be considered to be analogous to a system where, due to the lack of the plasticising water, the peptide-peptide interactions dominate to a point where the normally rubbery material behaves as a glass. The function of water in systems such as these is to compete with the bonding interactions, essentially 'dissolving' the peptide back-bone and allowing it to be a functional elastic tissue.

In view of the high extensibility and low modulus of elastin, it must be concluded that the hydrogen bonded structures cannot be very stable ones, and it seems reasonable to expect elastin to be an amorphous protein. The possibility

for the stabilization of the Beta-type structures in diseased states is a more plausible idea, which at the moment remains an open question.

#### (d) Fibrillar models

As was pointed out before, the fibrillar model as based on the electron microscope studies, is thought to consist of 3 to 5 nm filaments organized along the long axis of the elastin fibre. Since this type of organization involves the presence of discrete regions of protein and water, all the arguments presented against the oiled-coil model and the liquid drop model also apply here. The only possible way to get around this objection is to propose that the filaments are themselves an isotropic system i.e. that the protein making up the filaments is in a random conformation. This type of structure would be consistent with all the evidence presented in support of the kinetic theory explanations for elastin elasticity. But is this a reasonable statement? At the moment there exists no evidence to support this assumption. On an intuitive basis, it is hard to visualize the 3 to 5nm fibrils as being capable of accomodating random coils of proteins, especially considering the size of individual amino acid residues.

#### G. Conclusions

Examination of the various structural models and the different methods of study seems to indicate that elastin structure can be assimilated most satisfactorily in terms of a

conformation that is very close to the kinetically agitated, random network structure that is demanded by the kinetic theory of rubber elasticity. The following chapters try to further delineate (confuse, disguise) the conflicts presented here, and to test the validity of the random network as a viable description of elastin conformation.

## Chapter.IV. CONFORMATION OF ELASTIN: COACERVATE STRUCTURE.

### A. Introduction

The analysis of the conformational state of the elastin protein is generally confined to the insoluble, fibrous form of this protein. Another approach is to study the conformation of the soluble proteins, and to extrapolate from these to the final product. Although this is an indirect approach to the problem it could provide some interesting results.

### B. The Phenomenon of Coacervation

An operational definition of coacervation was given by Bungenberg de Jong (1949) as:

"If one starts from a sol, that is a solution of colloid in an appropriate solvent, then according to the nature of the colloid, various changes (temperature, pH, addition of a substance) can bring about a reduction of the solubility as a result of which a larger part of the colloid separates out in a new phase. The original one-phase system-the sol thus divides into two phases, one of which is rich in colloid, the other poor. .... Macroscopic or microscopic investigation allows one to distinguish between crystallization when obviously crystalline individuals are formed and coacervation, when amorphous liquid drops are formed, which later coalesce more or less readily into one clear homogeneous colloid-rich liquid layer, called the coacervate layer".

Soluble elastins display this phenomenon of coacervation. Both tropoelastin and alpha-elastin are freely soluble in water at room temperature, but upon raising the temperature to about 37°C, they both show coacervation properties. If left standing for about 20-24 hours, this coacervate becomes insoluble,

presumably due to the entanglement of the protein chains (Wood 1958).

Electron microscope studies of the coacervates of soluble peptides and synthetic peptides of elastin, show a very fibrillar appearance when visualized with negative stains (Volpin et.al. 1976, a, b, c). This raises another controversy. First, are these fibrils a true representation of the coacervate organization, or, are they a result of procedural artifacts? Second, if these fibrils do exist, would they be capable of accomodating random coils of proteins within such a restricted domain?

In attempting to answer these types of questions, it seems that one should choose experimental methods that will allow an examination of the shape and the mobility of the soluble elastin coacervates. In view of this purpose, the present chapter deals with viscosity and nuclear magnetic resonance studies which can, in principle, test for shape and mobility, respectively. The discussion will be limited to the 66,000 m.w. peptide fragment commonly referred to as alpha-elastin, but the arguments presented here are expected to apply to the precursor protein, tropoelastin, as well.

### C. Preparation Of Alpha-Elastin

Instead of using the usual method of producing soluble elastins by oxalic acid digest (Partridge et.al. 1955), the alpha-elastin used in this study was prepared by enzyme hydrolysis of insoluble elastin as outlined by Hall (1976) and

Hall and Czerkawski (1961). The enzyme method of preparation is advantageous since the product is a monomeric peptide as compared to the polydisperse mixture that is otherwise attained through acid digests.

(a) Enzyme hydrolysis

Borate buffer: of pH 8.5 and ionic strength of 0.384 was prepared by mixing 50ml of a mixture of 0.2M  $H_3BO_3$  and 0.2M KCl with 10ml of 0.2M NaOH, and diluting to 250ml. The borate/chloride solution was prepared by dissolving 12.369g  $H_3BO_3$  and 14.911 KCl in 1L of distilled water.

Preparation of elastin: Ligamentum nuchae obtained from mature beef cattle was stripped of free adhering tissue and purified by repeated autoclaving (Partridge et al. 1955). The resultant tissue was finely minced, washed with several litres of boiling distilled water and dried. About 5g of this autoclaved tissue was suspended in 380ml of the borate buffer, 0.5g of SDS was added and the mixture was stirred at 37°C for 1hr. It was then chilled to 4°C and 20ml of borate buffer, which contained 5mg of elastase (Sigma chemical company), was added. The reaction vessel was put into a shaking, water-bath at 37°C and the reaction was allowed to proceed until all the elastin had been dissolved (usually about 5hrs). At the end of this period the solution was brought to a boil to stop the reaction. The entire sample was freeze-dried and stored at -70°C until further use.

### (b) Removal of SDS

The SDS was removed from the peptide by a modification of the ion-pair extraction method proposed by Henderson et.al. (1979). About 100mg of the alpha-elastin powder was dialysed exhaustively against distilled water and freeze-dried. This peptide was redissolved in a solution of triethylamine:acetic acid:water (5ml:5ml:5ml) and stirred at room temperature for 1hr. The mixture was then cooled to 4°C and 85ml of anhydrous acetone was gradually added to the solution. This results in the precipitation of the protein while the SDS salt is extracted in the acetone. The precipitate was redissolved in a 'washing' solution, which consisted of 5ml of water, and 95ml of the acetone was added to precipitate out the protein. This 'washing' was repeated 4 to 5 times and the final product was blown dry in an oven to remove all traces of acetone. N.m.r. Spectroscopy showed this preparation to be totally free of any SDS.

### (c) Characterization of the alpha-elastin

The resultant peptide was a monomeric preparation of 66,000 M.W., as shown by SDS-polyacrylimide gel electrophoresis (Weber and Osborn 1969, Chrambach and Robard 1971). It also displayed the property of coacervation as monitored by the absorbance of the peptide solution at 380nm as a function of temperature (figure 4.1). The amino acid composition was shown to be similar to insoluble elastin by comparing the n.m.r. spectrum of the alpha-elastin

hydrolysate with a spectrum of ligament elastin hydrolysate. The hydrolysates were prepared by acid hydrolysis in vacuo in 6M HCl at 115°C for 24hrs.

#### D. Viscosity and Shape

##### (a) The relevant equation

If one adds a number of solid particles, which are much larger than the solvent molecules, to a solvent of viscosity,  $n$ , one observes an increase in the macroscopic viscosity of the solution due to the distortion of flow patterns, which is induced by the solute particles. The relationship for this effect, assuming that the particles are far enough apart to prevent overlap of the distorted flow lines, was given by Einstein in 1906 as (Tanford 1961):

$$n' = n(1 + v\phi) \dots \dots \dots 4.1$$

where  $n$  and  $n'$  are the viscosities of the solvent and the solution respectively, with  $v$  and  $\phi$  representing the 'geometry' and volume fraction of the solute.

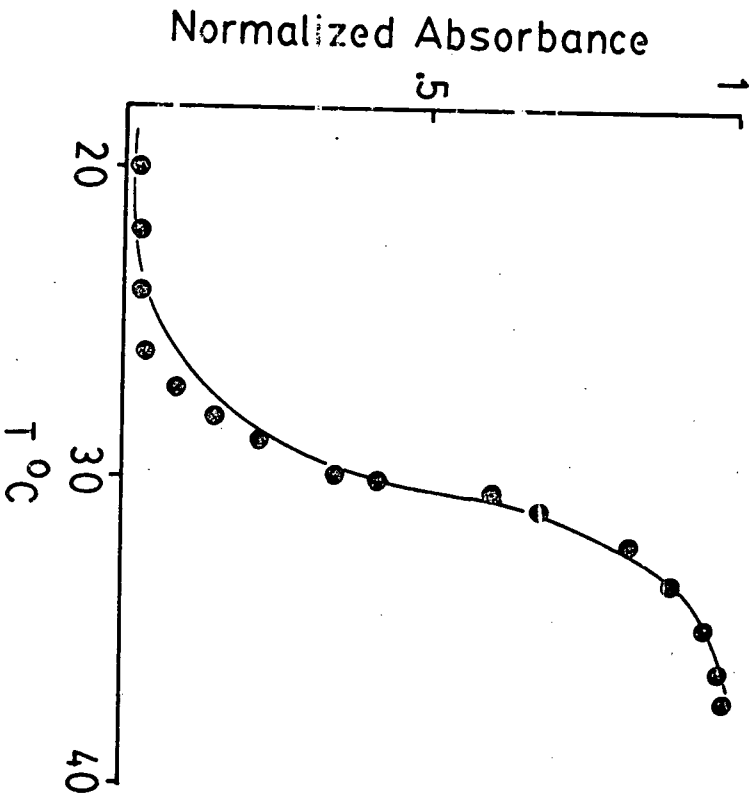
The effect of the solute on the viscosity of the solvent is usually expressed as the specific viscosity,  $n''$ :

$$n'' = (n' - n) / n \dots \dots \dots 4.2$$

The experimental manipulation for non-ideal molecules, to account for the concentration effects, involves the empirical evaluation of the reduced viscosity,  $n''/c$ , as a function of the concentration,  $c$ . The graphical plot of  $n''/c$  versus  $c$ , as  $c \rightarrow 0$ , gives a value termed the intrinsic viscosity  $[\eta]$ :

Figure.4.1: Coacervation profile of alpha-elastin.  
Plot of normalized absorbance at 360nm versus temperature °C, for a solution of alpha-elastin at a concentration of 6.8mg/ml, pH 7. This sample was subsequently used for the nmr experiments.

Figure.4.1.



$$[n] = n''/c, \text{ as } c \rightarrow 0 \dots \dots \dots 4.3$$

Substituting equation 4.3 into equation 4.1 gives:

$$[n] = v\phi/c \dots \dots \dots 4.4$$

since the volume fraction of the solute can be represented by:

$$\phi = N v_h c / \text{molecular weight of the solute} \dots \dots \dots 4.5$$

where  $N$  is Avogadro's number,  $c$  is the concentration in g/ml, and  $v_h$  is the hydrodynamic volume, defined according to Tanford as (1961):

$$v_h = (\text{m.w.}/N) (\bar{v} + \delta \bar{v}^0) \dots \dots \dots 4.6$$

where  $\bar{v}$  is the partial specific volume of the solute molecule,  $\bar{v}^0$  is the partial specific volume of the solvent molecule, and  $\delta$  is the hydration expressed as g solvent/g solute. Combining equations 4.6, 4.5, and 4.4, gives:

$$[n] = v(\bar{v} + \delta \bar{v}^0) \dots \dots \dots 4.7$$

In the case of water,  $\bar{v}^0$  is equal to unity, and equation 4.7 reduces to:

$$[n] = v(\bar{v} + \delta) \dots \dots \dots 4.8$$

#### (b) Evaluation of the shape parameter

The symbol,  $v$ , in equation 4.7 represents the shape of the solute molecule and has been evaluated for ellipsoids of varying axial ratio by Simha (1940). For the specific case of prolate ellipsoids of axial ratio,  $J$ , it takes the form (Tanford 1961):

$$v = J^2/15 (\ln 2J - 3/2) \dots \dots \dots 4.9$$

Since  $v$  can be calculated if the values of  $[n]$ ,  $\bar{v}$ ,  $\delta$ , and  $\bar{v}^0$

are known. This method can be used to empirically evaluate the geometry of the solute molecules. The dependence of  $v_r$  on the shape of the solute molecule, is shown in figure 4.2.

### (c) Application to soluble elastins

If the process of coacervation does not result in a change of shape, to a more anisotropic fibrillar form, then the value of  $v_r$ , as given by the ratio  $(\bar{v} + \delta)/[\eta]$ , should remain constant over the entire temperature range. The exact value of  $v_r$  will probably lie in the range of 12.18 for tropoelastin, as calculated from equation 4.9 and the sedimentation data of Schein et.al. (1977).

On the other hand, if these peptides do in fact form filamentous systems, then the value of  $v_r$  should increase dramatically at the critical temperature at which the transition takes place. The absolute magnitude of  $v_r$ , after the transition, can be predicted for the tropoelastin molecule assuming that the fibrillar form is made up of Beta-spiral structures as suggested by Urry and Long (1977b).

According to Urry (1976a), the Beta-spirals are expected to have a diameter of 15nm with a translation length of 0.44nm/6aa residues. In the case of tropoelastin which has approximately 850 residues (Sandberg 1976), the expected dimensions are 62nm and 1.5nm for the length and diameter respectively. Assuming a prolate ellipsoid as being grossly representative of this shape, the axial ratio of 41.3 amounts to a Simha factor,  $v_r$ , of 39.3 (equation 4.9). A similar

Figure.4.2: Dependence of the Simha factor on axial ratio.

Evaluation of the Simha factor,  $\nu$ , as a function of axial ratio for prolate (a) and oblate (b) ellipsoids, according to equation 4.9.

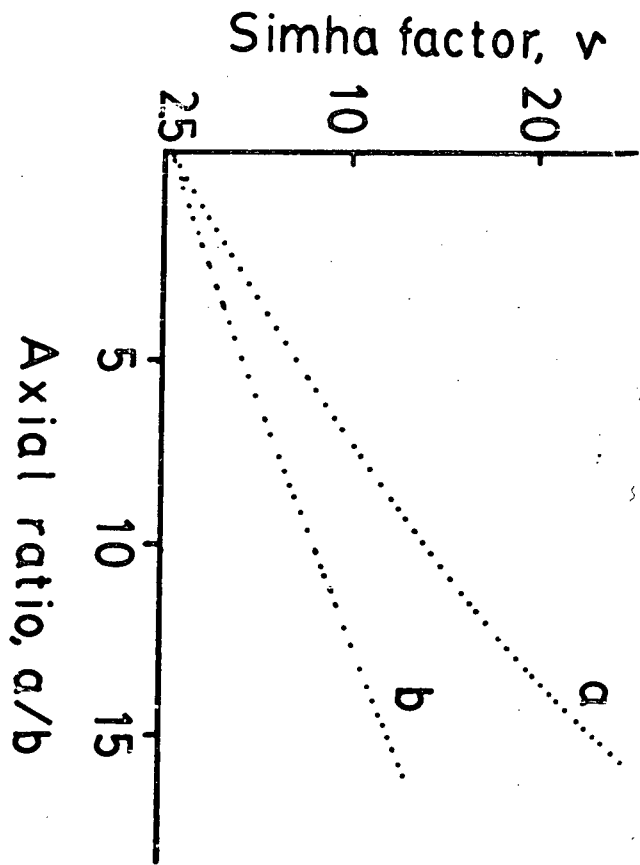


Figure 4.2.

prediction for alpha-elastin cannot be made due to its branched nature, but it is also expected to show a drastic increase in  $\nu$  if it too forms fibrillar structures as reported in the electron microscope studies (Cox et.al. 1973).

### E. Viscosity Studies Of Alpha-Elastin

#### (a) Viscosity measurements

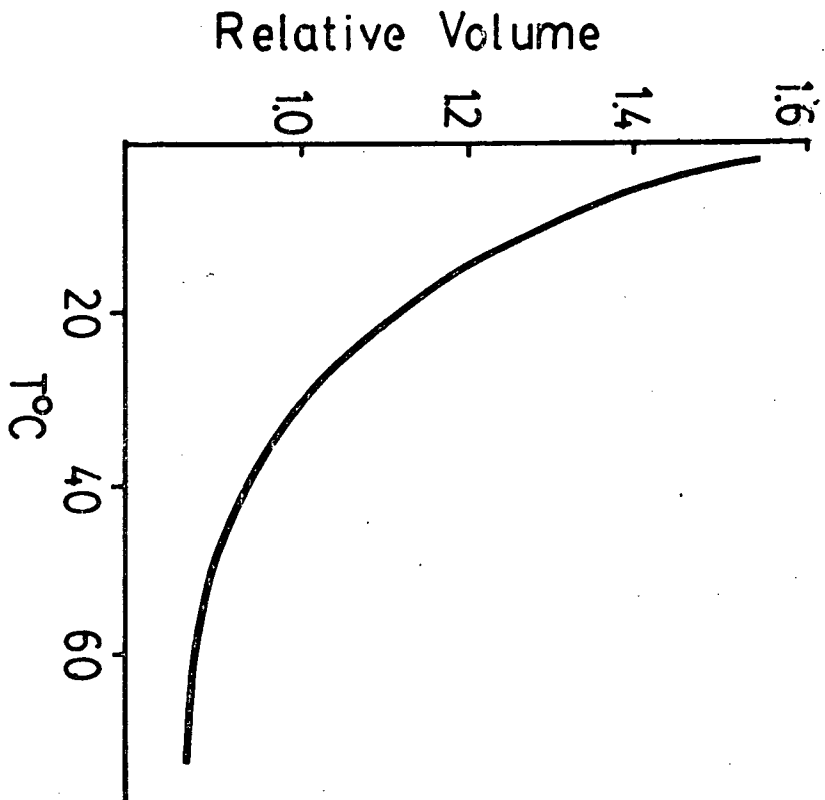
All the viscosity experiments described here were conducted with an Ostwald type capillary viscometer, with transit times for water in excess of 300sec. These long transit times should obviate the need for kinematic corrections. In dealing with an Ostwald type viscometer the viscosity of the solution,  $\eta'$ , is given by:

$$\eta' = B \rho t \dots \dots 4.10$$

where B is an apparatus constant,  $\rho$  is the density and t is the transit time in seconds. The apparatus constant, B, was evaluated at each temperature by calibration with distilled water, using density and viscosity values from standard physical tables.

A standard solution of protein was made up by dissolving about 260mg of purified alpha-elastin in about 250ml of distilled water. This solution was centrifuged at 12,000X for 15min., to remove particulate matter and large aggregates, and the clear supernatant was used for the subsequent viscosity experiments. The exact concentration was measured by taking a 1ml aliquots of the protein solution, drying them in an oven,

Figure.4.3: Dependence of elastin water content on temperature.  
Plot of relative volume (taken to be 1 at 30°C) versus temperature °C for ligament elastin (from Gosline 1978).

Figure 4.3.

and measuring the residue weight. 10ml of the alpha-elastin solution was pipetted into the viscometer and the transit times were measured with an electronic stop-watch ( $\pm 0.1$  sec). The viscosity measurements were repeated on serially diluted solutions of alpha-elastin and the data at each temperature were plotted in the form of  $\eta''/c$  versus  $c$  (see equation 4.3). This allowed the evaluation of the intrinsic viscosity,  $[\eta]$ , for alpha-elastin at each temperature.

#### (b) Calculation of partial specific volume and hydration

The partial specific volume of the alpha-elastin, which was calculated according to the method of Cohn and Edsall (1943) from the amino-acid composition for alpha-elastin given by Starcher et.al. (1973), had a value of 0.739. The hydration of the alpha-elastin, at each temperature, was calculated from the temperature dependence of hydration for insoluble elastin given by Gosline (1978) (figure 4.3). This seems valid since Ceccorulli et.al. (1977) have shown that the two types of elastin exhibit similar temperature dependence for their water contents.

#### (c) Results and discussion

The results of the viscosity studies on alpha-elastin are summarized in table 4.1 and figure 4.4. It is evident that the intrinsic viscosity,  $[\eta]$ , of alpha-elastin remains relatively unchanged with temperature (figure 4.4,a). If anything, there is a slight decrease in  $[\eta]$  with increasing temperature, which

Table 4.1: Viscosity of alpha-elastin.

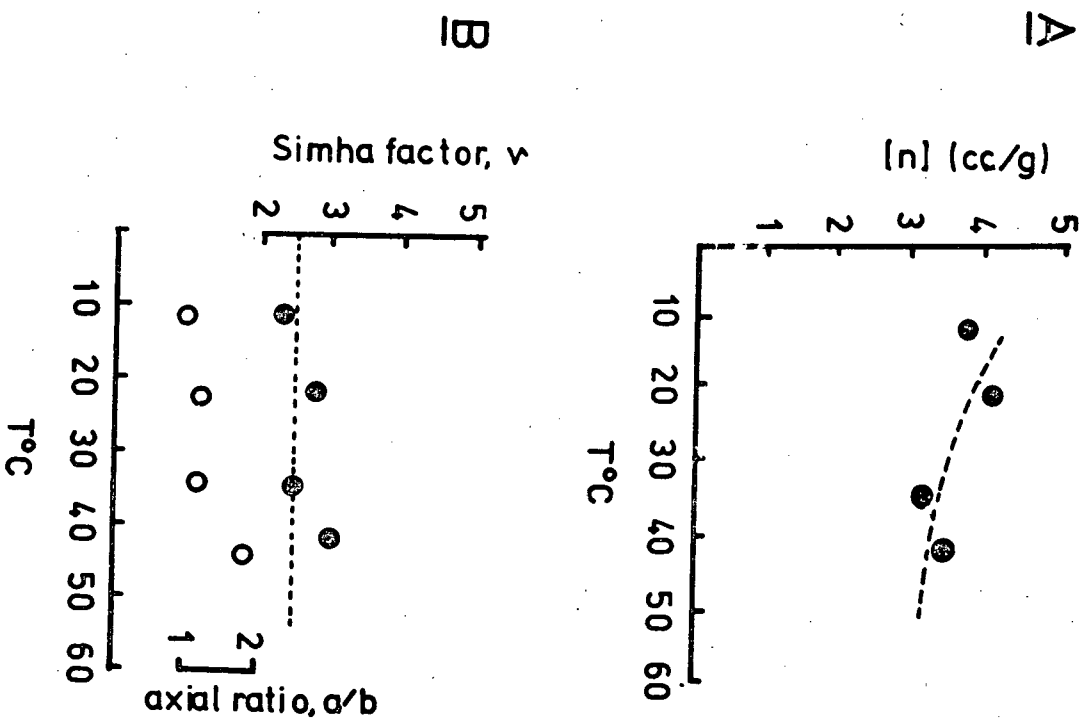
VISCOSITY OF ALPHA-ELASTIN.			
T <sup>0</sup> C	n <sub>sp</sub> /c versus c plots		[ n ]
	slope	correlation coefficient, r	
12	0.67	0.99	3.7
22	1.30	0.84	4.1
36	1.20	0.97	3.1
41	1.40	0.84	3.6

Figure.4.4: Viscosity of alpha-elastin.

(A) Plot of intrinsic viscosity,  $[\eta]$ , versus temperature  $^{\circ}\text{C}$ . The dashed line represents the expected relationship calculated from equation 4.9, assuming no change of shape, and the hydration values from figure 4.3.

(B) Plot of the Simha factor,  $v$ , versus temperature  $^{\circ}\text{C}$  calculated according to equation 4.8 using the needed values from table 4.1 and figure 4.3.

Figure 4.4.



is expected from the decrease in the water content of the peptide (figure 4.3) and equation 4.8 (figure 4.4, a dashed line). Evaluation of the Simha factor,  $v$ , according to equation 4.8 indicates that the alpha-elastin molecule is more or less spherical, and that there is no change with temperature (figure 4.4, b). Incorporating the values of the molecular weight, partial specific volume, and hydration it is possible to calculate the dimensions of the alpha-elastin molecule, assuming a spherical shape, to be in the order 20nm in diameter.

Interestingly, however, a glance at table 4.1 shows that the slopes of the  $n''/c$  versus  $c$  plots tend to increase with increasing temperature. This can be interpreted in the following way. If the particles in solution do not interact with each other, then the slope of the  $n''/c$  versus  $c$  plots should be zero (Tanford 1961, Huggins 1942). The fact that the slopes for the alpha-elastin solutions are positive supports the presence of aggregation processes (Tanford 1961) which, in general, seem to be favoured with increasing temperatures (table 4.1).

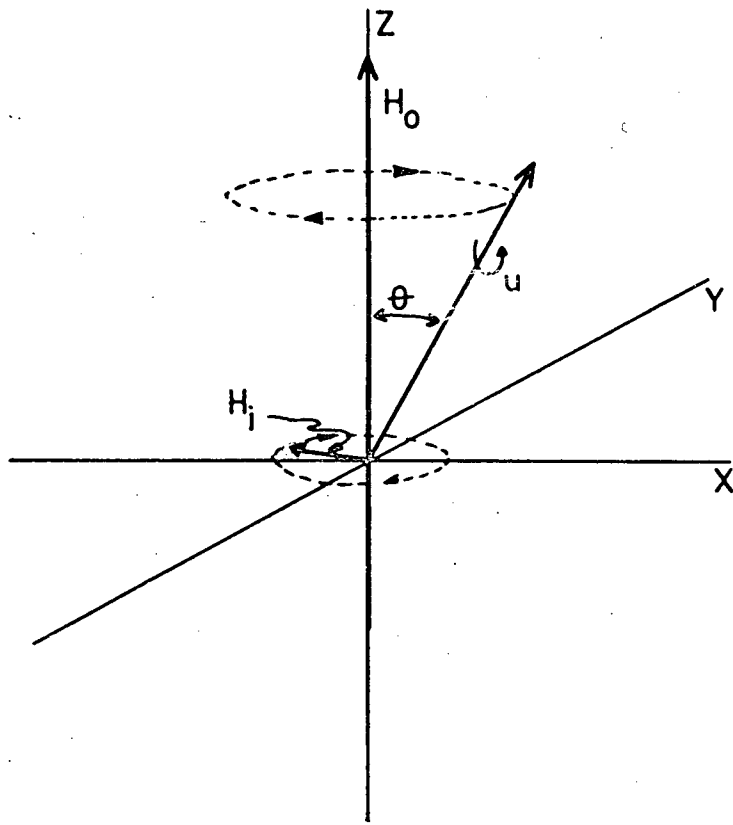
## F. Nuclear Magnetic Resonance

### (a) Theory

The possession of both spin and charge confers on a particle, such as a proton, a magnetic moment. Thus, a spinning proton can be regarded as a bar-magnet along the axis

Figure.4.5: Precession of a proton in a magnetic field.

A proton of magnetic moment,  $\mu$ , is placed in an external magnetic field,  $H_0$ , causing it to precess around the z axis at an angle  $\theta$ .  $H_1$  is the orthogonal magnetic field that is used to determine the frequency of precession.

Figure.4.5.

of spin, and the strength of this magnetic dipole is expressed as the nuclear magnetic moment,  $u$ . If placed in an external magnetic field,  $H_0$ , the interaction of this field with the magnetic moment of the proton will influence it to orientate itself in the direction of the field, but the effect of the spin creates a torque which causes it to precess around the  $z$  axis at a frequency,  $\nu^\circ$ , and angle  $\theta$  (Stothers 1973, figure 4.5). The angular velocity of this precession,  $\omega^\circ$ , is given by:

$$\omega^\circ = \gamma H_0 \dots \dots \dots 4.11$$

where  $\gamma$  is the gyromagnetic ratio defined as:

$$\gamma = 2u_z/h \dots \dots \dots 4.12$$

where  $u_z$  is the projection of the vector  $u$  in the direction of the field  $H_0$ , and  $h$  is Planck's constant. The angle  $\theta$  is determined by the spin number of the nucleus,  $I$ , which for protons has the value of  $1/2$ . The angle of the precession for this spin number is restricted to two orientations, at  $54.9^\circ$  and  $180^\circ - 54.9^\circ$  respectively (Metcalf 1970). The potential energy,  $E$ , of the interaction of the magnetic moment  $u_z$  is given by:

$$E = -u_z H_0 \dots \dots \dots 4.13$$

and the separation between the two energy levels for the proton is:

$$\Delta E = 2u_z H_0 \dots \dots \dots 4.14$$

If a small rotating field  $H_1$  is generated orthogonal to  $H_0$  (figure 4.5),  $u$  would experience the combined effects of both  $H_1$  and  $H_0$ . The nucleus would absorb energy from  $H_1$  if the

angular frequency of  $H_1$  is equal to  $\nu^0$ , changing  $\theta$ . The electromagnetic radiation which will effect such transitions is given by:

$$h\nu^0 = \Delta E = 2u_z H_0 \dots \dots \dots 4.15$$

Since only two values of  $\theta$  are possible the absorption, or emission, of energy quanta causes the nucleus to flip from one orientation to another when  $H_1$  is in 'resonance' with  $\nu^0$  (Metcalf 1970). N.m.r. Spectroscopy is based on the detection of the absorbed energy when the nuclear spins of the system come into resonance (chemical shift) with  $H_1$ .

#### (b) The chemical shift

If all the protons were to undergo magnetic resonance at identical frequencies no conformational information could be derived from this technique. Fortunately, however, the resonance frequency of each proton is sensitive to it's electrical and magnetic environment (Walton and Blackwell 1973). The nuclei can be shielded from the applied magnetic field by the extra-nuclear electrons, hence, the effective magnetic field experienced by the nucleus,  $H_e$ , is not the same as the applied field and can be expressed as (Metcalf 1970):

$$H_e = H_0 (1 - \sigma) \dots \dots \dots 4.16$$

where  $\sigma$  is the shielding factor which is a reflection of the electron distribution around the observed proton.

It is therefore expected that changes in electron distribution around the nuclei, i.e. conformational or

bonding changes, would effect the system because of shielding effects, and one would expect to observe a separate signal, with a characteristic chemical shift for each group of equivalent protons in the molecule. The chemical shifts,  $\delta$ , are measured in a dimensionless number expressed as parts per million (ppm), and is defined as:

$$\delta = (H_S - H_R / H_R) \times 10^6 \dots\dots 4.17$$

where  $H_S$  and  $H_R$  are the resonance fields for the sample and reference compound respectively.

### (c) Relaxation processes

As stated before, protons are re-orientated in an applied magnetic field by the absorption of electromagnetic radiation of the resonance frequency from  $H_1$ . The induced transitions, however, have an equal probability in either direction so that if there were equal populations of nuclei in the two energy levels, there would be no net absorption of energy. In fact, however, there is a small excess of nuclei in the lower energy state which is determined by the energy difference between the two levels (equation 4.13) and the relative populations ( $n'/n$ ) are given by:

$$n'/n = \exp(-\Delta E/RT) \dots\dots 4.18$$

where  $n'$  and  $n$  are the number of protons in the upper and lower levels respectively. The excess of protons is only in the order of 7ppm in a field of 10kG (Metcalf 1970), but this is sufficient to give a net absorption of energy since the number of upward transitions are slightly greater than in the

other direction. These transitions that determine the lifetime of the excited nuclei are termed relaxation processes.

Spin-lattice relaxation (longitudinal relaxation),  $T_1$ , results in the dissipation of the absorbed energy as thermal energy to the other nuclei and electrons in the sample, collectively referred to as the lattice. This process acts directly to maintain an excess of nuclei in the lower energy state.

$T_2$ , the other process of relaxation, limits the lifetime of an excited nucleus by a mutual exchange of orientation with a neighbouring nucleus of the same kind. This is termed spin-spin relaxation (transverse relaxation). This process results in the re-distribution of absorbed energy and does not contribute to the maintenance of the excess nuclei in the lower state. Both of these relaxation processes determine the spectral line-widths.

Both relaxation processes are influenced by molecular motion. For example, the rapid thermal motions in liquids leads to large spin-lattice relaxation times (Metcalfe 1970). The effective field experienced by the nuclei is also averaged out by the rapid isotropic movements, which results in narrow line-widths and large values for  $T_2$ . The reason for this is that the ability of two nuclei to exchange their spins depends directly on how long their motions remain in phase with each other. This time during which relative orientation persists is called the correlation time,  $\tau_c$ , and is the parameter that characterizes the molecular motions. Thus nuclei that exhibit

fast, isotropic motions will be characterized small correlation times and narrow line-widths. The analysis of the n.m.r. spectra can therefore be used to deduce protein mobility.

### G. N.M.R. Studies Of Alpha-Elastin

In comparison to the viscosity experiment whose main result is an evaluation of a molecule's shape, a nuclear magnetic resonance experiment allows the evaluation of the molecules mobility (Dwek 1973). Furthermore, since any n.m.r. spectrum is a composite of the sum of it's component chemical shifts and line-widths, it should be possible to predict n.m.r. spectra if the composition and the mobility (conformation) of the constituent molecules is known. Alternately, if the composition is known one can assume a conformation, and predict a spectrum based on such an assumption, which is then tested by obtaining experimental values.

#### (a) Materials and method

The purified alpha-elastin was dissolved in D<sub>2</sub>O at a concentration of approximately 6mg/ml. Proton nmr spectra were obtained on a Bruker WD-400 FT-NMR spectrometer at the University of British Columbia, Department of Chemistry with the kind co-operation of Dr. A.G. Marshall and Dr. P.D. Burns. Runs were made at 10°C intervals over a temperature range of 15°C to 75°C, which spans the region of alpha-elastin

Figure.4.6: The Lorentzian line shape.

The Lorentzian line, as determined by equation 4.19, where  $1/t$  is the half-width at half-height.  $\omega^0$  is the resonant precession frequency of the nucleus.

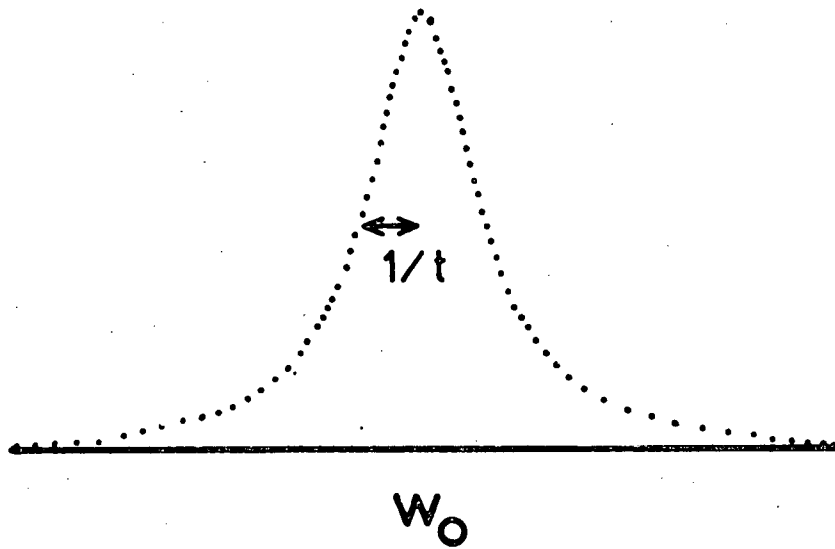
Figure.4.6.

Table.4.2: Spectral parameters used for random-coil predictions.

PARAMETERS FOR THE PREDICTION OF RANDOM-COIL  
SPECTRA AT 400MHz, FROM DSS.

	CHEMICAL PPM	SHIFT Hz	LINE-WIDTH Hz	NUMBER OF a.a	NUMBER OF PROTONS IN:	
					Elastin <sup>1</sup>	Albumin <sup>2</sup>
ala CH <sub>3</sub>	1.34	534	25	3	783	138
arg α-CH <sub>2</sub>	1.75	700	35	2	10	46
γ-CH <sub>2</sub>	1.67	667	32	2	10	46
δ-CH <sub>2</sub>	3.11	1240	21	2	10	46
asn α-CH <sub>2</sub>	2.69	1074	28	2	--	20
asp α-CH <sub>2</sub>	2.73	1092	28	2	9	76
gln α-CH <sub>2</sub>	1.95	780	30	2	43	32
γ-CH <sub>2</sub>	2.43	971	43	2	43	32
glu α-CH <sub>2</sub>	1.95	780	30	2	--	118
γ-CH <sub>2</sub>	2.35	942	35	2	--	118
gly α-CH <sub>2</sub>	3.92	1569	18	2	610	30
his C2-H	8.54	3414	18	1	--	17
C4-H	7.09	2836	18	1	--	17
α-CH <sub>2</sub>	3.05	1222	23	2	--	34
ile α-CH <sub>2</sub>	1.59	634	39	2	34	28
γ-CH <sub>2</sub>	1.59	634	39	2	34	28
(CH <sub>3</sub> ) <sub>2</sub>	0.81	322	30	6	103	84
leu α-CH <sub>2</sub>	1.59	634	39	2	107	122
γ-CH <sub>2</sub>	1.59	634	39	1	54	61
(CH <sub>3</sub> ) <sub>2</sub>	0.84	322	30	6	322	366
lys α-CH <sub>2</sub>	1.70	680	40	2	11	118
γ-CH <sub>2</sub>	1.39	554	30	2	11	118
δ-CH <sub>2</sub>	1.62	647	30	2	11	118
ε-CH <sub>2</sub>	2.92	1167	25	2	11	118
met α-CH <sub>2</sub>	2.17	870	24	2	--	8
γ-CH <sub>2</sub>	2.60	1040	31	2	--	8
δ-CH <sub>3</sub>	2.02	807	36	3	--	12
phe α(CH <sub>2</sub> ) <sub>2</sub>	7.20	2880	19	5	147	130
α-CH <sub>2</sub>	2.93	1172	10	2	59	52
pro NCH <sub>2</sub>	3.56	1423	59	2	234	56
α-CH <sub>2</sub>	1.92	769	36	2	234	56
γ-CH <sub>2</sub>	2.00	796	36	2	234	56
ser α-CH <sub>2</sub>	3.81	1520	36	2	22	56
thr CH <sub>3</sub>	1.14	454	21	3	46	102
α-CH	4.13	1652	10	1	15	34
tyr α(CH <sub>2</sub> ) <sub>2</sub>	7.03	2811	14	.5	10	10
	7.00	2798	15	1.5	30	29
	6.70	2678	15	1.5	30	29
	6.66	2654	14	.5	10	10
β-CH <sub>2</sub>	2.90	1160	17	2	41	38
val α-CH <sub>2</sub>	2.20	878	40	2	232	72
(CH <sub>3</sub> ) <sub>2</sub>	0.87	347	32	6	696	216

<sup>1</sup>amino acid composition from Starcher *et al.* 1973.

<sup>2</sup>amino acid composition from Dayhoff 1976.

coacervation (see figure 4.1). Typical spectral parameters were: 16k f.i.d data set, 1.4 sec. acquisition time with a 4.6 sec. delay between successive acquisitions to avoid resonance saturation. A spectral width of 6000 Hz was used with quadrature detection and phase alteration sequence and exponential apcdization equivalent to 2 Hz line broadening, to enhance the signal to noise ratio. All assignments were made from the residual H<sub>2</sub>O peak taken to be at 4.68ppm from DSS at 25°C.

(b) Prediction of random-coil spectra

In approaching this problem I have opted for an empirical route which utilizes various parameters that have been obtained for proteins which are known to be in the random coil conformation. The shape of the curves was fitted to the equation for a Lorentzian line, which takes the form (Marshall 1979, and figure 4.6):

$$A(\omega) = t / (1 + (\omega^\circ - \omega)^2 t^2) \dots \dots 4.19$$

Where A(ω) represents the absorption at the frequency ω, ω<sup>°</sup> is the resonance frequency (i.e. the chemical shift of a residue) and t describes the line-width such that:

$$1/t = 1/2 (\text{width at half-height}) \dots \dots 4.20$$

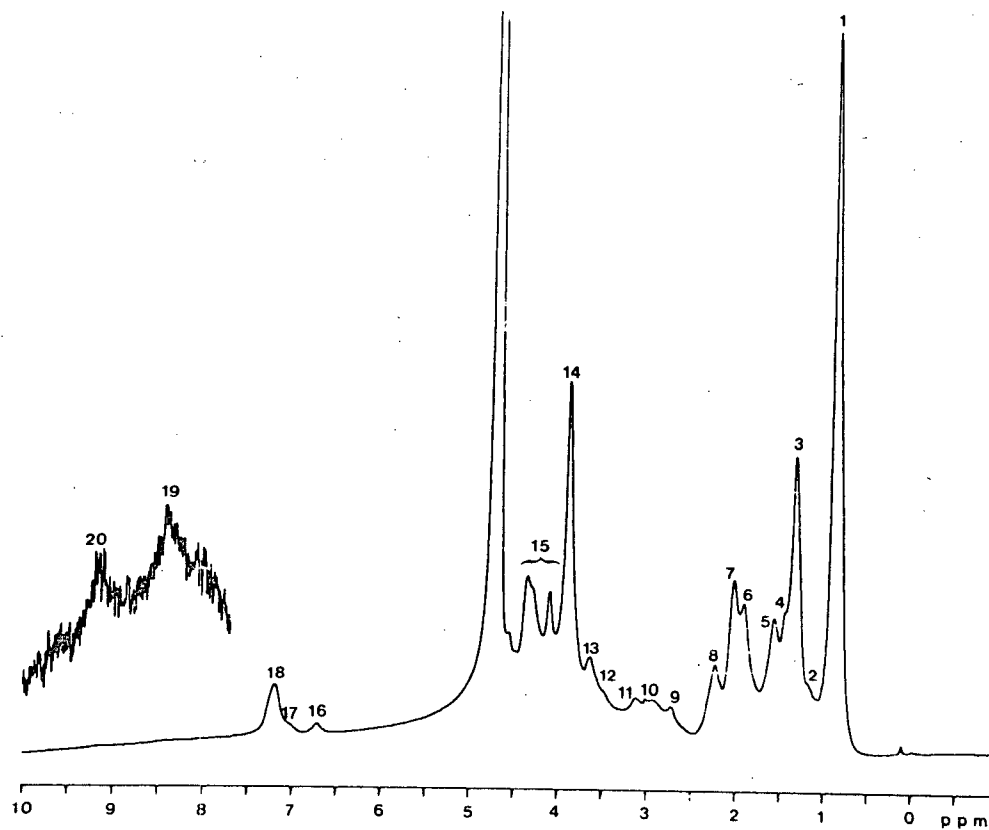
The values used for the predictions involve the amino acid composition, the chemical shift data, and line-width parameters from Bradbury and Rattle (1972) (see table 4.2). The predicted spectra were calculated according to equation 4.19 on a Digital Equipment pdp11 computer, using a Fortran

program.

### (c) Results and discussion

Figure 4.7 shows the 400MHz proton spectra for alpha-elastin in D<sub>2</sub>O at 25°C. The assignments (see legend table 4.3) were made on the basis of the predicted spectra (figure 4.8a) and other published spectra (Egmond et.al. 1979, Cozzone et.al. 1980). Examination of figures 4.7 and 4.8 shows that the main absorption peaks in the n.m.r. spectrum correspond to the valine, alanine, and glycine residues. This aspect of the result is valuable because the distribution of these amino acids is very distinct, in that the alanine residues occur almost exclusively in the cross-link regions, whereas the glycine and valines are restricted to the extensible parts of the elastin chains (Gray et.al. 1973, Anwar 1977). These residues can therefore serve as probes for the conformation in the different regions of the elastin network. The general similarity between the predicted spectra (assuming a random-coil conformation) and the experimentally observed results supports the presence of a random conformation for alpha-elastin. However, there are also some very distinct differences in the two spectra which must be explained satisfactorily before the above statement can be accepted with confidence. The differences in the two spectra seem to be restricted to three types of residues: the alanine residues (1.3ppm), the glycine residues (3.9ppm) and the aromatics (broad envelope at 3ppm and the peaks between 6.7 and 7.2ppm).

Figure.4.7: 400 MHz nmr spectrum of alpha-elastin.  
Pmr spectrum of alpha-elstin in  $D_2O$  at a concentration of 6.8 mg/ml, ph 6.8, at 25°C (see table 4.3 for peak assignments). The large peak at 4.68ppm is from the residual  $H_2O$ .

Figure. 4.7.

90  
Table.4.3: Peak assignments for alpha-elastin at 400 MHz.

PEAK ASSIGNMENTS FOR ALPHA-ELASTIN.

1. ile, leu, val :  $(\text{CH}_3)_2$
2. thr :  $\text{CH}_3$   
lys :  $\gamma\text{-CH}_2$
3. ala :  $\text{CH}_3$
4. ile, leu :  $\beta\text{-CH}_2, \gamma\text{-CH}_2$
5. arg :  $\beta\text{-CH}_2, \gamma\text{-CH}_2$   
lys :  $\beta\text{-CH}_2, \delta\text{-CH}_2$
6. pro :  $\beta\text{-CH}_2, \gamma\text{-CH}_2$   
glu :  $\beta\text{-CH}_2$
7. val :  $\beta\text{-CH}_2$
8. glu :  $\gamma\text{-CH}_2$
9. asp :  $\beta\text{-CH}_2$
10. phe :  $\beta\text{-CH}_2$   
lys :  $\epsilon\text{-CH}_2$   
tyr :  $\beta\text{-CH}_2$
11. arg :  $\delta\text{-CH}_2$
12. pro :  $\text{N-CH}_2$
13. ser :  $\beta\text{-CH}_2$
14. gly :  $\alpha\text{-CH}_2$
15. envelope of alpha-carbons, the peak at 4.1 ppm is from ala.
16. tyr ring : H 3, 5
17. tyr ring : H 2, 6
18. phe :  $\omega(\text{CH}_2)_2$
19. iso-desmosine
20. iso-desmosine and desmosine

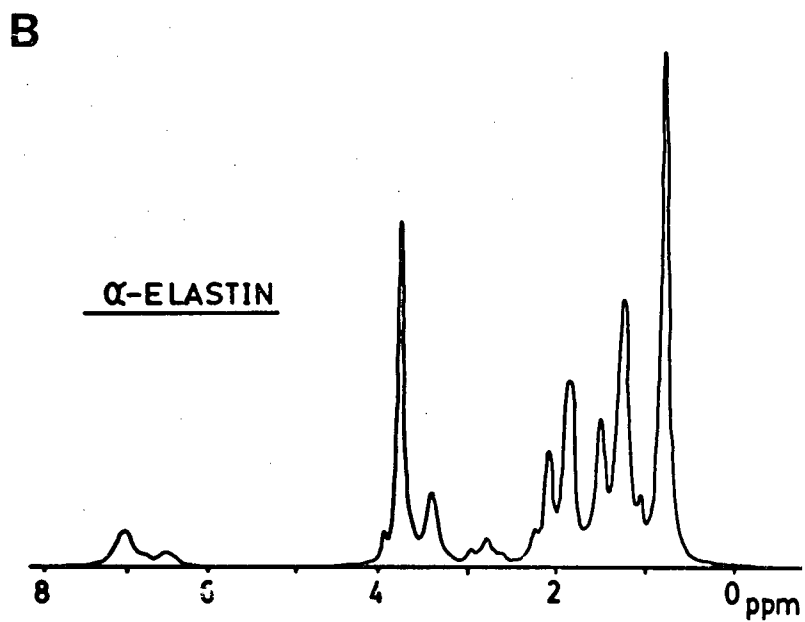
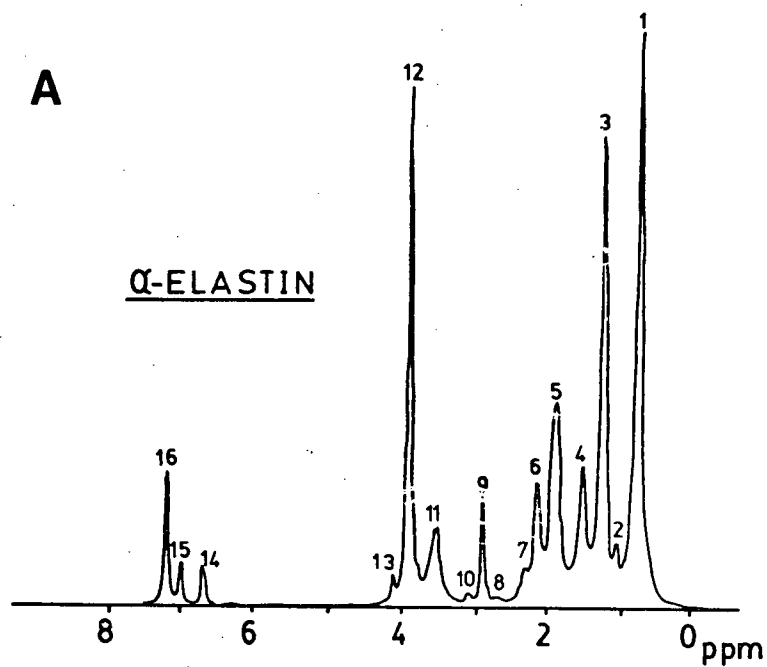
Interestingly, all the deviations seem to be of one type, i.e. the observed line-widths are broader than the predicted ones.

As mentioned before, the alanine residues in the elastin network are localized in the cross-link regions. The results of sequence studies indicate that these alanines are grouped in sequential runs of 4-5 residues, and there is some evidence that these alanines form a  $\alpha$ -helix (Foster et.al. 1976). The presence of helical structures would be expected to result in restriction of the molecular motions in the cross-link regions, as reflected in the broadening of the spectral lines. Since the aromatics are also concentrated around the cross-link regions a similar explanation, as the one forwarded for the alanine residues, can be invoked for the line broadening of these residues as well. But what about the glycines? There are two alternatives that can explain the broadening of this peak. It is possible that the glycines are involved in secondary structures which could result in line broadening due to restricted motions. This is probably not the case since the glycine residues occur with the valines in the elastin sequence (Sandberg et.al. 1977) and this later group does not shown any presence of secondary structures, as visualized in the narrow line-widths (figure 4.7). Alternately, the observed glycine peak could be a composite of a broad distribution of narrow resonances arising from a number of different glycine populations. This is a reasonable statement since the glycine protons are directly bonded to the alpha-carbon of the residue and would therefore be markedly

Figure.4.8: Predicted nmr spectra for alpha-elastin.

(A) Predicted random-coil spectra for alpha-elastin using the spectral parameters from table 4.2, and the amino acid composition from Starcher et.al. 1973.

(B) The same spectrum with the phe, tyr, and ala residues broadened to 50 Hz to simulate their participation in secondary structures. The gly peak has been broadened to 30 Hz.

Figure.4.8.

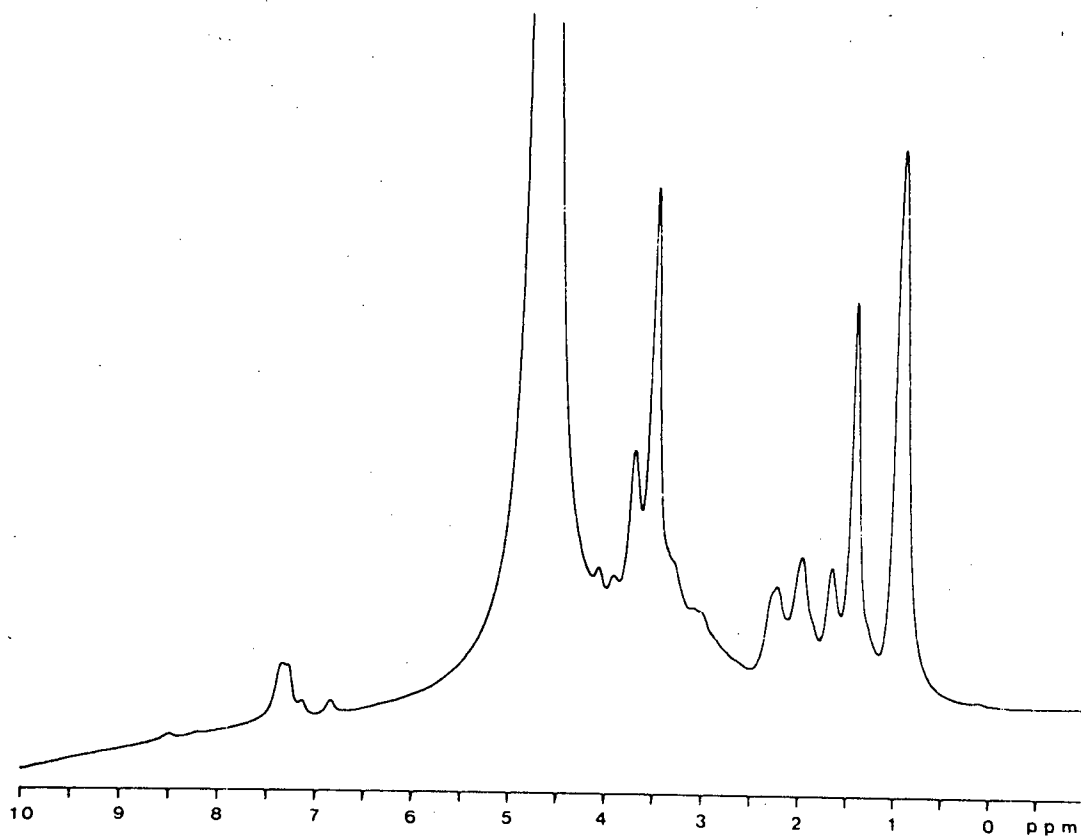
affected by the type of residue that occurred around it in the amino acid sequence. Hence different primary sequences, with regard to the glycine residue, would be expected to result in different chemical shifts for the glycine protons, and since there is no reason to believe that any one type of amino acid always occurs with a glycine in the primary sequence, this explanation for the line broadening of the glycine peak seems acceptable. When the explanations for the differences between the random-coil spectrum (figure 4.8a) and the observed spectra (figure 4.7) are incorporated into the predictive process, one observes a closer agreement between theory and experiment (figure 4.8b and legend).

Figure 4.9 shows the spectrum obtained for a solution of hydrolyzed alpha-elastin where the peaks have been broadened to 30hz. As expected the alpha-protons (3 to 4.5ppm) are affected the most by the hydrolysis of the peptide bonds. The upfield region of this spectrum, for the free amino acids, is seen to be identical with the spectra obtained for intact alpha-elastin (figure 4.7). This again supports the presence of a random-coil conformation for this elastin peptide.

The possibility exists, however, that the fast motions of the protons deduced from the narrow line-widths, is a result of a rapid tumbling of the whole alpha-elastin molecule in solution rather than being a reflection of a kinetically free protein chains. To ensure against this artifact a proton spectra was obtained for bovine serum albumin (Sigma Chemical Company). Albumin has a similar molecular weight and intrinsic

Figure.4.9: Nmr spectrum of alpha-elastin  
hydrclysate.

400 MHz spectrum of alpha-elastin hydrolyzed in  
vacuo in 6M HCl at 115°C for 24hrs. The spectrum has  
been broadened to 30 Hz.

Figure. 4.9.

viscosity (Tanford 1961) as alpha-elastin (see viscosity section of this chapter) and, hence, should display similar frictional properties and tumbling properties in solution. In contrast to elastin, however, albumin has been shown to contain stable secondary structures which are mostly alpha-helical in nature (Timasheff et.al. 1967) and this should be reflected in the n.m.r. spectrum. Figure 4.10,a, shows the 400MHz spectrum obtained for albumin in D<sub>2</sub>O at 25°C. The mass of broad resonance envelopes, as compared to the predicted spectrum for the random-coil conformation (figure 4.10,b), is consistent with the results of C.D. studies of this protein (Timasheff et.al. 1967), more importantly, this demonstrates that the tumbling motion of this molecule does not mask the presence of secondary structures. Broadening all the resonances used in the prediction of the spectra (amino acid composition from Dayhoff 1976) to 100hz results in a better approximation of the observed results (figure 4.10,c).

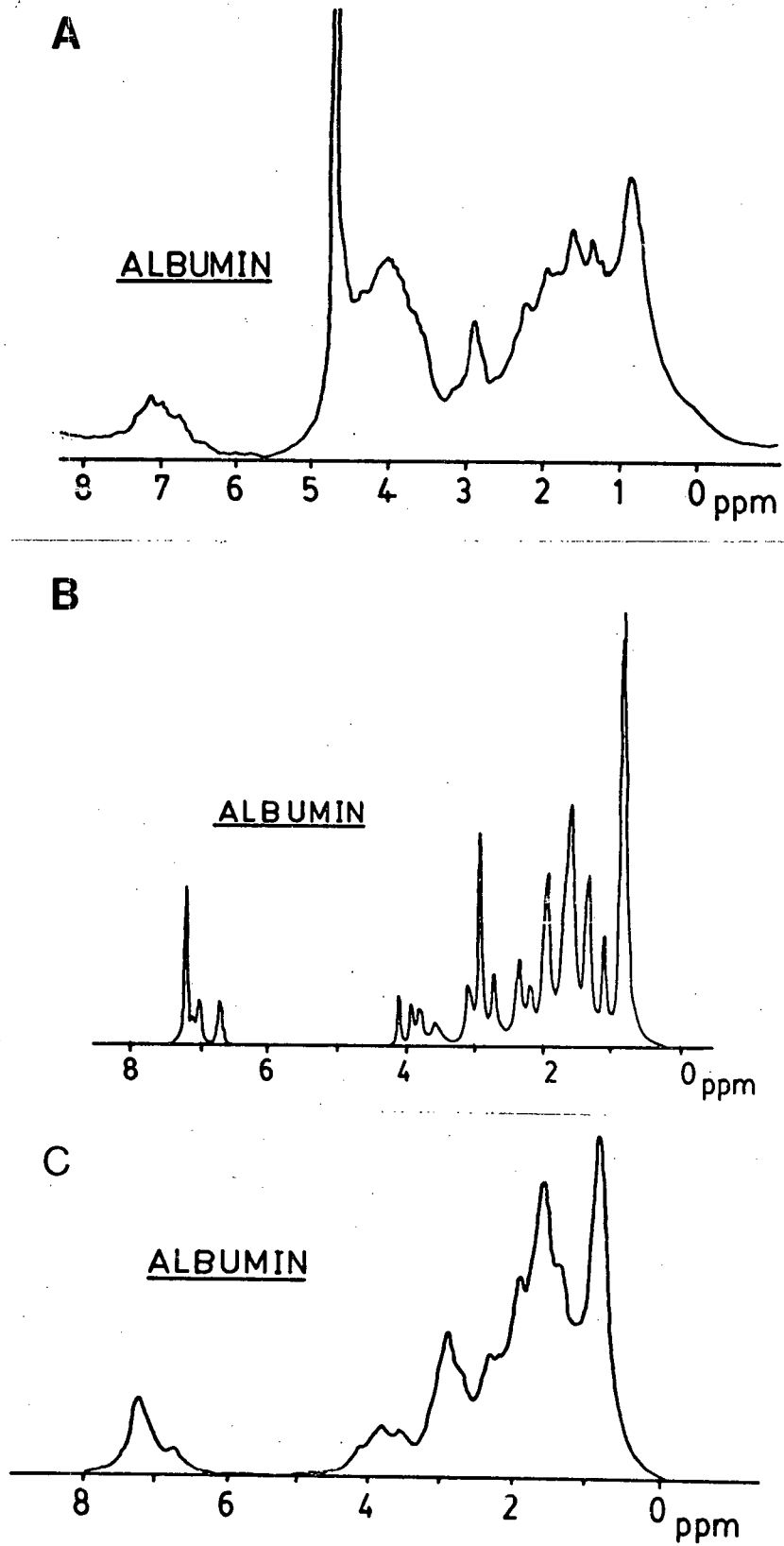
On the basis of the results presented here it seems reasonable to state that the conclusion of a random conformation for the alpha-elastin molecule based on the n.m.r. analysis is not a result of experimental artifact but, rather, it is a true reflection of this proteins conformational state. Furthermore, since there was no observable temperature dependence of the spectra, it seems that the coacervate of alpha-elastin is also characterized by a random conformation.

Figure.4.10: Nmr spectra of albumin.

(A) 400 MHz spectrum of bovine serum albumin at 25°C.

(B) Predicted random-coil spectra for albumin using spectral parameters from table 4.2 and amino acid composition from Dayhoff 1976.

(C) Same as spectrum B, but with all the resonances broadened to 100 Hz to simulate the presence of stable secondary structures.

Figure.4.10.

## H. Conclusions

Because of the difficulties involved in working with insoluble materials such as fibrous elastin, a number of researchers have chosen to look at the structural properties of the soluble elastins: alpha-elastin (Partridge et.al. 1955), and the precursor protein, tropoelastin (Partridge and Whiting 1979).

Since elastin has a very high hydrophobic amino acid content, and since there is an increase in hydrophobic interactions with temperature (Tanford 1973), the soluble elastins exhibit the phenomenon of coacervation at high temperatures (37°C). This coacervation, which is characterized by a phase separation of the solution into a protein dense phase and an equilibrium solution, is thought to be a crucial step for concentrating and cross-linking the precursor molecules into the fibrous tissue (Urry 1978c).

Several workers have shown that both tropoelastin and alpha-elastin exhibit a fibrillar structure in the coacervate state. (Cox et.al. 1973, 1974, Cleary and Cliff 1978), with similar periodicities as the ones observed for insoluble elastin preparations (Gotte et.al. 1976). Urry and his co-workers have also supported this view by demonstrating the presence of these fibrils in the coacervates of the synthetic repeat peptides (Rapaka and Urry 1978, Volpin et.al. 1976a, b, c).

Although the concentrating effect, of coacervation, is very obvious, the 'aligning' aspect implies an ordered

(fibrillar) structure for these soluble elastins in the coacervate states. Taken a step further, the presence of the filaments argues against an entropic elasticity for the elastin protein, and this forms the basis of the controversy currently surrounding the structure of elastin coacervates. This controversy is further fueled by the conflicting evidence obtained by the various workers who are addressing this question.

The n.m.r. data is contradictory in that studies reported by Urry and Long (1977b), for the synthetic peptides, indicate an increase in order with temperature, whereas, Lyerla et.al. (1975) report the converse for fibrous elastin. The analysis of the viscosity studies presented in this chapter indicates that the process of alpha-elastin coacervation is dominated by aggregation processes with no evidence for the formation of parallel isotropic filaments which are seen in the transmission electron microscope. This interpretation of the results is in excellent agreement with the the  $^{13}\text{C}$ -n.m.r. results of Lyerla et.al. (1975), quasi-elastic light scattering experiments (Jamieson et.al. 1972, 1976) and sedimentation data (Schein et.al. 1977), which also support a random conformation for the soluble elastin coacervates.

That there are some secondary structures in the elastin is clearly demonstrated by a number of studies (Starcher et.al. 1973, Tamburro et.al. 1977, Foster et.al. 1976). The unresolved question deals with whether these areas of

secondary structures are localized in the cross-link area or whether they are characteristic of the extensible regions. Since the analysis of the elastin as a kinetic rubber assumes that there are no stable secondary structures, it is important that this conflict be resolved. The results of the proton n.m.r. results presented in this chapter suggest that the secondary structures in the elastin network are restricted to the cross-link regions, and that the majority of the residues are characterized by random, isotropic motions.

Chapter.V. CONFORMATION OF ELASTIN: BIREFRINGENCE PROPERTIES.A. Introduction

As pointed out earlier, several recent electron microscope studies of negatively stained fibrous elastin and coacervates of soluble elastin, reveal a highly ordered, anisotropic structure consisting of 3 to 5nm filaments that are presumed to run parallel to the long axis of the elastin fibre (Quintarelli et.al. 1973, Serafini-Fracassini et.al. 1976 and 1978, Gotte et.al. 1974, Cox et.al. 1974, Cleary and Cliff 1978). The mechanical properties of elastin, however, can be accurately explained by the Kinetic Theory of Rubber Elasticity (Hoeve and Flory 1958, Dorrington et.al. 1975 and 1977, Gosline 1978, Volpin and Cifferri 1970, Aaron and Gosline 1980), and this theory is based on an isotropic, random network structure that is very different from the anisotropic, filamentous systems seen in the electron microscope.

Given these two possible types of structures for elastin, one should be able to distinguish between them by observing the birefringence of single elastin fibres in the polarizing microscope. This approach was chosen because the technique does not require any physical disturbance of the protein, thus reducing the chance of any procedural artifacts. Further, the technique is very versatile, allowing the evaluation of structure at two levels of organization: (a) at the molecular level as reflected by the intrinsic birefringence, and (b) at

the sub-microscopic level ( i.e. , at the level of the 3 to 5nm filaments) as indicated by the form birefringence.

If elastin is isotropic in its organization, then this should be reflected as a lack of birefringence when observed between crossed polarizers. On the other hand, if elastin is in fact filamentous, as implied by the electron microscope evidence, then this should be manifested as an observable form birefringence. Similar studies on collagen (Pfeiffer 1943) and Chitin (Diehl and Iterson 1935) attest to the reliability of this type of analysis. This chapter deals with the birefringence properties of single elastin fibres and it's analysis in terms of the implications for elastin conformation.

#### B. Phenomenological explanation of double refraction

The basis for the phenomenon of birefringence, and it's use as an indicator of molecular conformation, eventually rests on the interaction between the electric properties of particles and the wave nature of light. Hence if one can explain and account for the observed interaction between the two mediums, then, by comparing the nature of the incident light to the resulting radiation, one can make some deductions as to the spatial arrangement of the interacting particles. It seems fitting then, that something should be said about the processes of molecular interactions that give rise to the phenomenon of double refraction.

(a) Retardation of polarized light

The retardation of polarized light is based on the concept that chemical bonds will interact with that component of linearly polarized light whose electric vector is parallel to the bond direction, 'retarding' its transmission velocity. This axis is referred to as the slow axis of transmission. Upon emerging from the birefringent object the retarded vector will add up with the non-retarded vector (which propagated along the fast axis of transmission) to give elliptically polarized light, a component of which is passed by the analyzer (Wilkes 1971).

Consider a beam of linearly polarized light with its electric vector  $V$  as shown in figure 5.1A, and its direction of propagation along the  $y$  axis (*i.e.* out of the plane of the paper). This electric vector can be represented as a resultant of the vector lying in the  $xy$  plane (figure 5.1B), and the vector lying normal to it in the  $zy$  plane (figure 5.1C). If this plane polarized light was to pass through a non-birefringent object, the resulting light would be identical to that depicted in figure 5.1A. Since there is no component parallel to the analyzer axis (which is at  $90^\circ$  relative to the polarizer), none of it will be transmitted by the analyzer. Hence the specimen will appear dark when viewed through the analyzer.

However, for a positively birefringent, cylindrical object, orientated along the  $z$  axis, the plane polarized light in the  $zy$  plane will be parallel to the slow axis of

Figure.5.1: Propagation of polarized light through isotropic material.

(A) Looking down the axis of propagation, showing the relative positions of the polarizer (pol) and the analyzer (an).

(B) The electric vector in the xy plane.

(C) The electric vector in the zy plane.

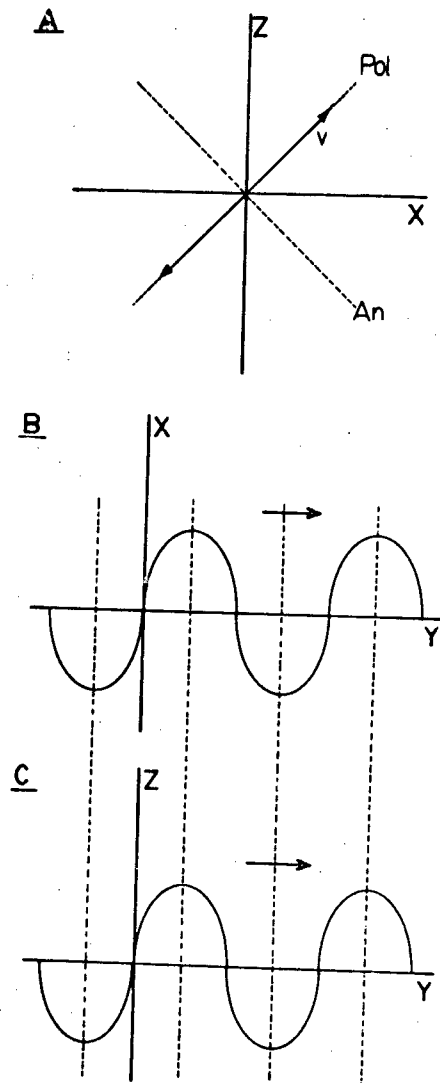
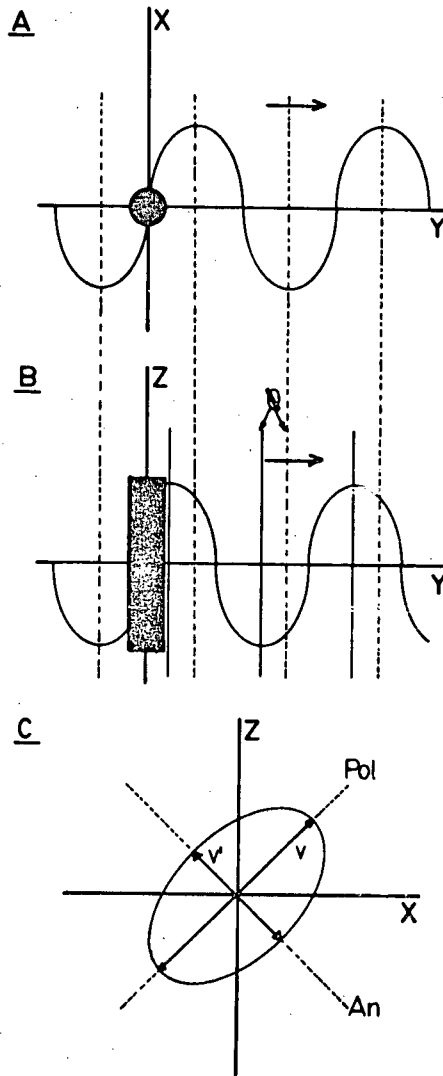
Figure. 5.1.

Figure.5.2: Propagation of polarized light through anisotropic material.

(A) The electric vector in the xy plane, normal to the slow axis.

(B) The electric vector in the zy plane is parallel to the slow axis and is retarded by an amount  $\theta$  relative to the vector in the xy plane.

(C) The resultant light is elliptically polarized with a component ( $V'$ ) that is transmitted by the analyzer (an).

Figure.5.2.

transmission (figure 5.2B), resulting in the retardation of its transmission velocity. On the other hand, the vector in the xy plane will be normal to this slow axis of transmission and will therefore remain unaltered (figure 5.2A). Upon emerging from the birefringent object the retarded vector, which propagated along the slow axis, will be out of phase by an amount  $\delta$  with the unaltered one. As stated before, these two vectors will add up to give elliptically polarized light which has a component  $V'$  parallel to the transmission axis of the analyzer (figure 5.2C). For any given retardation, the maximum transmission at the analyzer (at  $90^\circ$  to the polarizer) will occur at a specimen orientation of  $45^\circ$  with respect to the polarizer (Bennett 1950).

#### (b) Quantitating the retardation

The retardation of the electric vector propagating along the slow axis of transmission can be quantitated by inserting a calibrated compensator between the birefringent object and the analyser. This compensator, as the name implies, functions by reversing the effects of the birefringent specimen. It changes the elliptically polarized emergent light back to linearly polarized light, with its electric vector parallel to that of the polarizer. Since the analyzer will not pass any component that is at  $90^\circ$  to its transmission axis, the experimental manipulation involves rotating the compensator to extinction (of the bright specimen), at which point the 'reverse' retardation of the compensator is equal to the

initial retardation of the specimen. The absolute value of the retardation can then be tabulated by utilizing the appropriate equations for any given compensator and wavelength of light. This value of retardation is divided by the optical path length,  $d$ , usually equated to the thickness of the specimen, to yield a value for the birefringence, which is unitless.

Figure 5.3 is a summary figure showing the relative positions of the various components used in the study of the birefringence properties of materials. A more detailed account of the theory and methodology involved in polarized light microscopy can be found in articles by Bennett (1950), Frey-Wyssling (1953) and Wilkes (1971).

### C. Qualifying The Types of Birefringence

#### (a) Intrinsic birefringence

The concept of intrinsic or crystalline birefringence, which is thought to be the reflection of the organization at the molecular level, is best introduced by considering an isotropic material. In such a material the chemical bonds are distributed equally over all angles, relative to the incident linearly polarized light. As a result of this homogeneous distribution of bond angles there is no selective retardation of the component electric vectors, and the emergent plane polarized light will have its electric vector parallel to that of the incident beam. Hence the isotropic material will appear dark when viewed between crossed-polars.

Figure.5.3: The birefringence experiment.

Pol: polarizer.

S: specimen.

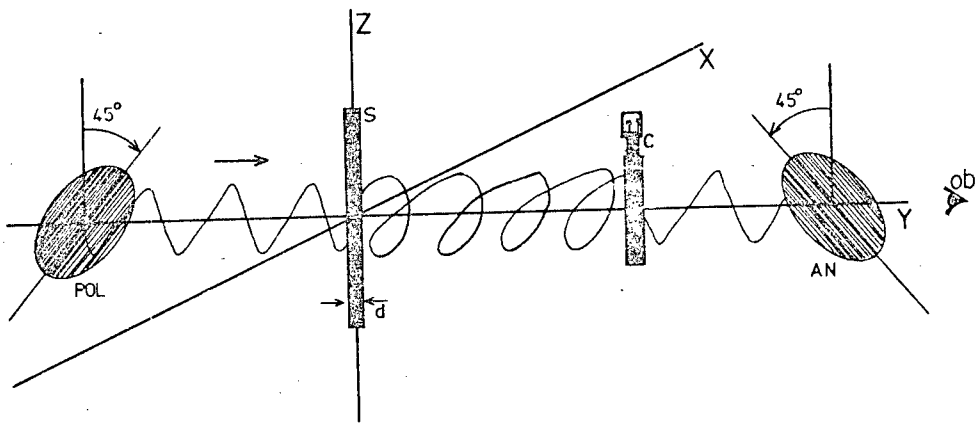
D: path length.

C: compensator.

An: analyzer.

Ob: observer.

The arrow shows the direction of propagation.

Figure.5.3.

This system however, cannot differentiate between an isotropy that is a result of the random thermal motion of anisotropic segments (such as the kinetic elastomers) and the isotropy that arises from a homogeneous distribution of rigid segments (such as glass). Fortunately, this aspect of the molecular characterization can be elucidated on the basis of the mechanical properties of the materials under study. Kinetic elastomers are characterized by a Young's modulus in the order of  $10^6$  Newtons/m<sup>2</sup>, whereas glassy substances usually have modulus values that are about three to four orders of magnitude higher than the rubbery materials.

Now consider a material whose molecular structure shows a predominant directionality of its units. Such a preferred orientation of bond angles, with reference to the incident light, will result in the transformation of the linearly polarized light to elliptically polarized light, and the object will appear bright when examined between crossed polars.

The amount of retardation as a function of the path length, is an indicator of the extent of molecular organization. The sign of the birefringence, which refers to the direction of the slow axis of transmission, has been conventionally defined as being positive when the slow axis is parallel to a 'given dimensional feature' such as the long axis of a cylindrical object. Conversely, if the object has its fast axis parallel to the 'given dimensional feature', it is said to be negatively birefringent (figure 5.4).

Figure.5.4: The sign of the birefringence.

(A) Negatively birefringent specimen: fast axis parallel to the 'dimensional feature'.

(B) Positively birefringent material: slow axis parallel to the 'dimensional feature'.

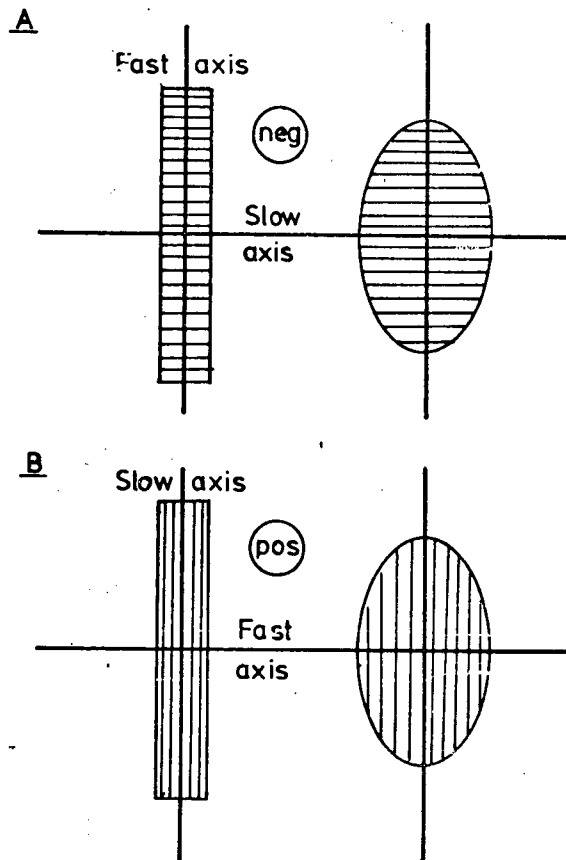
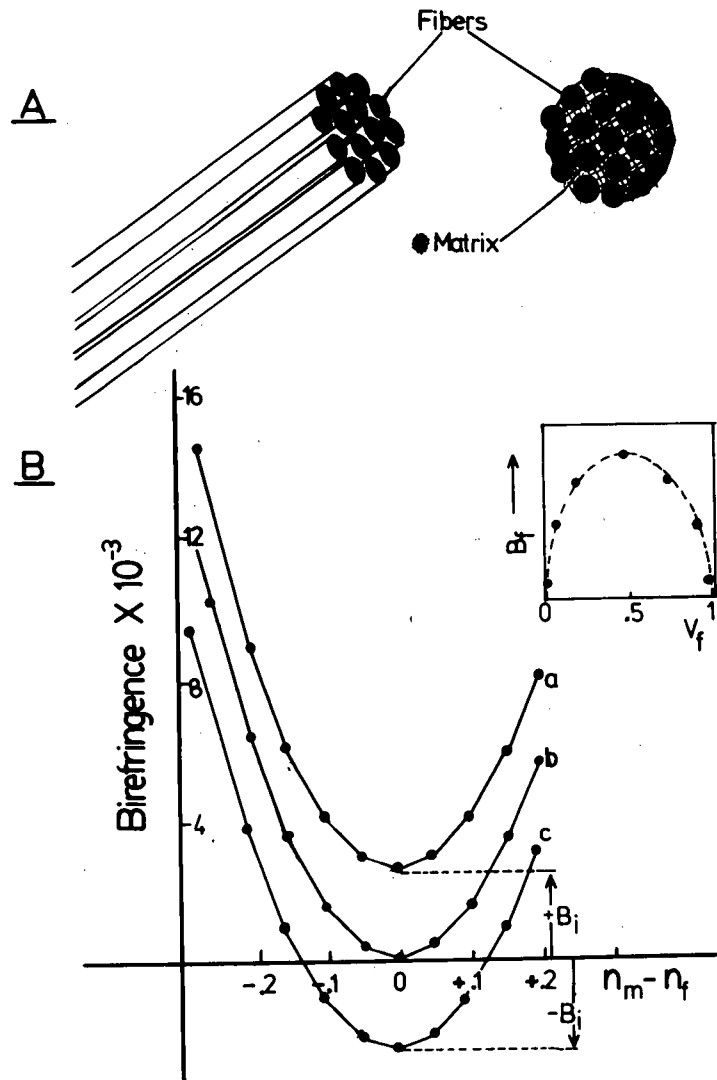
Figure. 5.4.

Figure.5.5: Form birefringence.

(A) A composite of fibres with refractive index  $n_f$ , in a matrix of refractive index  $n_m$ .

(B) Evaluation of the form birefringence according to equation 5.2: (a) for fibres with positive birefringence (b) for isotropic fibres (c) for negatively birefringent fibres. The inset shows the relative dependence of the form birefringence on the volume fraction of the fibres,  $V_f$ .

Figure 5.5.



(b) Form birefringence

Unlike intrinsic birefringence which arises from an anisotropy at the molecular level, form birefringence arises from an anisotropy of a scale that is larger than the dimensions of molecules but smaller than the wavelength of light. The limit to their 'smallness' is set by the requirement that the structural units should be big enough to possess true phase boundaries (Frey-Wyssling 1953).

Consider the structural composite shown in figure 5.5A. This represents a system of parallel, isotropic fibres of refractive index  $n_f$ , surrounded by an isotropic medium of refractive index  $n_m$ . A structure such as this will exhibit form birefringence arising from the preferred orientation of asymmetric bodies in a medium of differing refractive index (Bennett 1950).

The first theoretical relationship for such composites was presented by Weiner in 1912, and it has formed the basis of most of the form birefringence studies to date. For a system of rods, the theoretical expression has the form (Bear et.al. 1937):

$$n_{\parallel}^2 - n_{\perp}^2 = (n_f^2 - n_m^2)^2 f(1-f) / n_f^2(1-f) + n_m^2(1+f) \dots \dots \dots 5.1$$

where  $n_{\parallel}$  and  $n_{\perp}$  represent the refractive index of the system parallel to and normal to the dominant axis of the specimen respectively, with  $f$  representing the volume fraction of the fibres. Another relationship for a similar type of system, based on a modification of the Weiner equation, has been

proposed by Bear et.al. (1937).

If  $n_f$  and  $n_m$  are nearly equal, the above relationship can be simplified to an experimentally more useful one of the form (Stokes 1963):

$$n_{||} - n_{\perp} = (n_f - n_m)^2 f (1-f) / \bar{n} \dots \dots 5.2$$

A graphical representation of this equation is shown in figure 5.5B, curve b. Since the two types of birefringence (form and intrinsic) are thought to be additive, the total birefringence of a system can be characterized as shown in figure 5.5B, curve a, for rods of positive birefringence, and curve c, for rods having negative intrinsic birefringence. In all cases, the form birefringence goes to zero when  $n_f = n_m$ , and the birefringence of the system equals the intrinsic birefringence of the fibres. It also follows from equation 5.2 that for any given refractive index difference the maximum form birefringence occurs at a volume fraction of fibres,  $f$ , equal to 0.5 (figure 5.5 inset).

### (c) Strain birefringence

When an isotropic non-birefringent object is subjected to a strain along one of its axis, it will exhibit a birefringence which is commonly labelled accidental or strain birefringence. The imposed strain has the effect of inducing a preferred directionality on the distribution of the bond angles, in the originally isotropic material, which is subsequently reflected as an optical anisotropy.

The molecular changes responsible for the observed strain

birefringence depends on the type of material in question. The optical anisotropy that results when crystalline solids are strained, arises from the deformation of electron orbits in the material, which in turn is a consequence of the altered inter-atomic distances (Frey-Wyssling 1953). When considering the strain birefringence of rubbery polymers however, a different theoretical basis has to be invoked. Rather than arising from the displacement of electrons, the strain birefringence of these materials is thought to result from the alignment of the 'random links' that make up the kinetically free chains of the polymer network. The optical properties of the links themselves remain unaffected.

The theoretical equations for the strain birefringence of rubbery polymers will be more appropriately discussed in chapter 7. For the moment it suffices to simply state the qualitative differences between the two types of strain birefringence.

#### D. Materials and Methods

Single, 6 to 8  $\mu\text{m}$ , elastin fibres from untreated bovine ligamentum nuchae and from ligament that had been purified by repeated autoclaving (Partridge et. Al. 1955) were isolated with fine forceps on a dissecting microscope. The fibres were viewed between crossed polars on a Wild M-21 polarizing microscope, and the retardations were determined at 546nm using a Zeiss 1/30 wavelength rotary compensator. Illumination was provided by a 100 watt quartz lamp which was used in

conjunction with an interference filter to give the monochromatic green light. Birefringence was calculated by dividing the retardation at the center of the fibre by the fibre diameter.

The form birefringence curves were obtained from measurements on single elastin fibres and rat tail tendon collagen fibres that had been swollen in liquids of known refractive index. These are listed in table 5.1.

The temperature controlled stage was built in the lab to fit the Wild microscope. It consisted of an aluminium piece that had been channelled out to allow an internal closed circulation of water. The outlets from the stage were connected to a thermostated circulating water bath. The temperature at the sample was monitored with GB32 thermistor bead that had been calibrated with a mercury thermometer. Unless otherwise stated, all experiments were conducted at 24°C.

## E. Birefringence Properties of Single Elastin Fibres

### (a) Form birefringence

Single elastin fibres were either swollen in liquids of known refractive index (water, ethylene glycol, glycerol) or air dried and immersed in organic solvents of different refractive index. In all cases the elastin fibres (purified and unpurified), gave a constant low birefringence value of about  $2 \times 10^{-4}$  (table 5.1, figure 5.6 curve a). There was no

Table.5.1: Form birefringence of single elastin fibres.

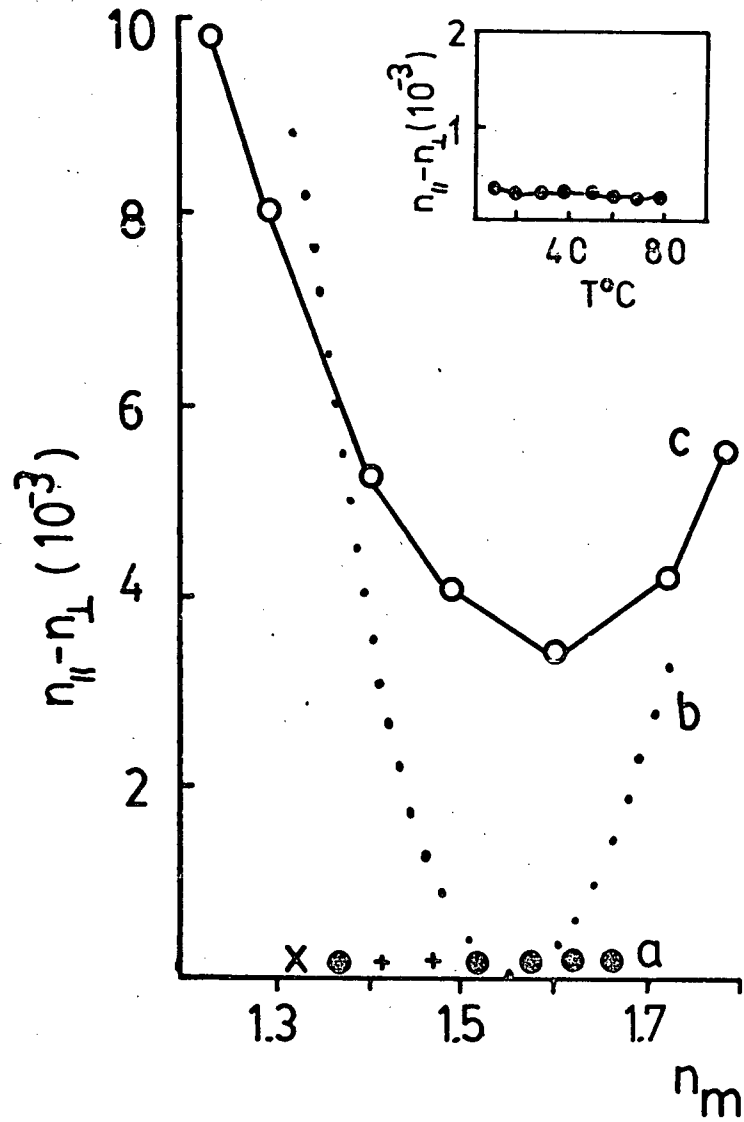
FORM BIREFRINGENCE RESULTS FOR ELASTIN.

	refractive index of solution	birefringence ( $10^{-4}$ )
water	1.33	2.5
acetone	1.37	3.0
ethelene glycol	1.43	1.6
chloroform	1.44	3.2
glycerol	1.48	1.4
benzene	1.49	3.3
benzene : bromonapthelene		
4:1	1.54	3.4
3:2	1.57	3.1
2:3	1.60	2.8
1:4	1.63	2.6
bromonapthelene	1.66	2.8

Figure.5.6: Form birefringence of elastin fibres.

(a) For single elastin fibres in (x) water  $n=1.33$   
(+) ethylene glycol  $n=1.43$  and glycerol  $n=1.48$ , (●)  
for organic solvent of different refractive index.  
(b) Theoretical birefringence calculated for  
isotropic fibres according to equation 5.2.  
(c) Results obtained for single elastin fibres by  
Serafini-Fracassini et.al. 1976.  
The inset shows the temperature dependence for the  
birefringence of single elastin fibres.

Figure 5.6.



indication of form birefringence, which is usually visualized as a U-shaped curve for the graph of birefringence versus refractive index of imbibing liquid. This U-shaped curve is characteristic of fibrous proteins with filamentous substructure, such as collagen, which shows a very distinct form birefringence curve (figure 5.7 curve a), and reported results for silk, chitin, and keratin (Frey-Wyssling 1948, 1953).

If elastin was in fact filamentous, as suggested by the electron microscope studies (Serafini-Fracassini et.al. 1976), then one should expect a result that closely follows the theoretical prediction afforded by equation 5.2, as shown in figure 5.6 curve b. This theoretical curve was calculated by assuming the filaments (if present) to be isotropic, and using a value of 1.55 for the refractive index of the elastin protein. The volume fraction,  $f$ , was taken to have a value of 0.65 (Gosline 1978). It should be mentioned that elastin swollen in water, ethylene glycol, and glycerol retains its elastic properties, hence the experimental results obtained under these conditions are considered to be a more accurate reflection of elastin's functional conformation, as compared to the data points which were obtained for dry elastin fibres in the different organic liquids. Nevertheless, it is encouraging, and probably relevant, that both sets of data showed identical results.

Lastly, it should be pointed out that the results obtained in these experiments are inconsistent with the

reports of positive form birefringence curves (Serafini-Fracassini et.al. 1976), figure 5.6 curve c, and a later report of a negative form birefringence curve (Bairati and Gotte 1977) for single elastin fibres. A possible explanation for these conflicting results will be presented in the discussion section of this chapter.

### (b) Intrinsic birefringence

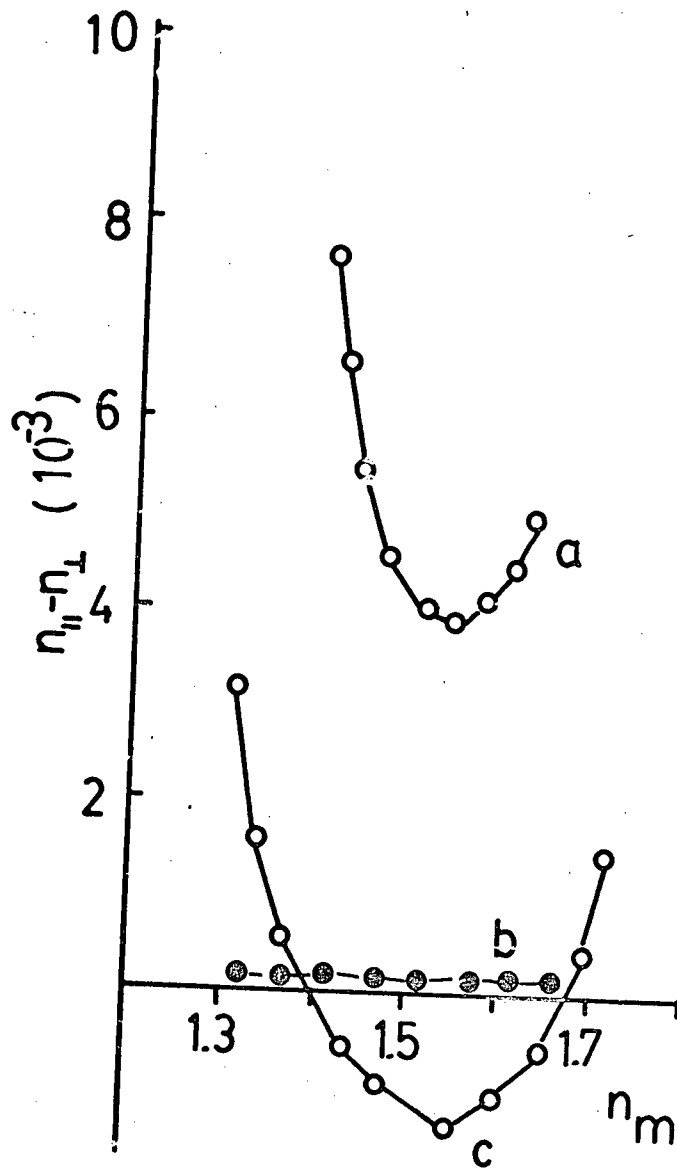
Since there is no indication of form birefringence, it is reasonable to assume that the constant value of  $2 \times 10^{-4}$  represents the intrinsic component of the birefringence. This value is seen to be temperature independent for elastin fibres in water (figure 5.6 inset), and is extremely small as compared to other known crystalline proteins (Schmitt 1950). It is therefore tempting to conclude that elastin is an amorphous protein.

One might argue however, that this low value for the intrinsic birefringence is actually an artifact. Since the total birefringence of a system is a sum of the intrinsic and form birefringence, it is possible that these two types of birefringence counteract each other when they are of equal magnitude and have opposite signs, to yield a zero (or nearly so) total birefringence. This is demonstrated in figure 5.7, where the birefringence of dried collagen fibres and tannic acid fixed collagen fibres (Pfeiffer 1943) is plotted as function of the refractive index of the immersion medium.

Collagen fibres, which are known to be anisotropic at the

Figure.5.7: Form birefringence of collagen.

- (a) unpurified collagen fibres.
- (b) elastin fibres.
- (c) Tannic acid fixed collagen fibres (Pfeiffer 1943).

Figure. 5.7.

molecular and the sub-microscopic levels, show both positive form and positive intrinsic birefringence (figure 5.7 curve a). Tannic acid reverses the sign of the intrinsic birefringence, and as a result of this, tannic acid fixed collagen appear isotropic (show zero total birefringence) at  $n_m$  equal to 1.40 and 1.67 (figure 5.7 curve c). That the lack of birefringence in single elastin fibres does not occur as a result of this phenomenon is supported by the following.

In order for the theoretical form birefringence curve to intersect the observed data point for elastin in water, one has to either (a) assign an unusually large negative (or positive) intrinsic birefringence to elastin, or (b) assume a refractive index for the protein that is much smaller than the value of 1.55 used in this study. Both of these possibilities are unreasonable. A high intrinsic birefringence would indicate a very crystalline structure and this is not supported by the X-ray diffraction reports (Astbury 1940). The second choice, that of a low refractive index, would be an exception to the known refractive indices for a wide variety of proteins, with values that lie between 1.50 and 1.55.

Most importantly however, the possibility of an artifact is precluded by the fact that, as presented in the last section, elastin fibres show a very low, constant birefringence over a broad range of refractive index liquids (figure 5.6). This is taken to mean that there is no form birefringence component associated with the observed value of  $2 \times 10^{-4}$ , which is taken to be the value of the apparent

intrinsic birefringence. The timely interjection of the word 'apparent' is discussed in the following section.

(c) Explanation for the apparent birefringence

Although the magnitude of the residual birefringence is extremely small, it might be interesting to speculate about the source of this 'intrinsic' birefringence. In doing so one is faced with three possibilities:

1. The birefringence is an inherent property of the fibre.
2. That the birefringence is a result of an anisotropic residue around the fibre.
3. That it is due to the refractive index difference at the interface of the swollen protein and the surrounding water.

Inherent birefringence:

Since the retardation is proportional to the path length through the fibre, then, if the birefringence was inherent to the fibre one would expect it to be greatest at the center of the fibre where the path length is at its maximum value. For a circular cross-section one can predict the relative retardations across the fibre of radius,  $r$ , in terms of the path length,  $p$ , according to:

$$p=2(\cos\theta r) \dots\dots 5.3$$

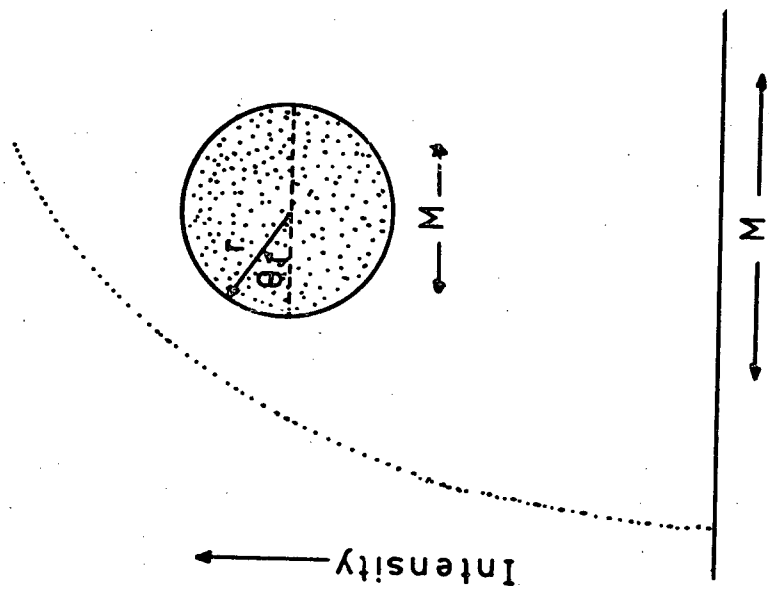
This relationship is depicted in figure 5.8.

Birefringent coating:

In the case of the unpurified fibres it is possible that there exists a sheath of birefringent material (such as the

Figure.5.8: Expected relationship for intrinsic birefringence.

Graphical representation of the relative intensity versus distance across fibre calculated according to equation 5.3. M is the middle of the fibre.

Figure.5.8.

glycoprotein micro-fibrils) around the central amorphous core of the fibre. Similarly, in the case of the autoclaved elastin one might expect that a residue could be left covering the fibres, which if crystalline, would give rise to an observable birefringence. Again assuming a circular cross-section for the elastin fibre, it should be possible to predict the relative retardations through the analysis of the path length across the fibre.

Consider a beam of polarized light propagating through a cylinder of radius  $r'$ , containing within it a cylinder of radius  $r''$ , with both having common centers (figure 5.9A). The total path length,  $p$ , transversed by the ray at a distance,  $x$ , away from the center is given by:

$$p=2(r'^2-x^2)^{1/2}.....5.4$$

The component,  $p'$ , of this total path length which lies inside the inner cylinder of radius,  $r''$ , at a distance,  $x$ , away from the center, is given by:

$$p'=2(r''^2-x^2)^{1/2}.....5.5$$

Since only the coating matrix is birefringent, the effective path length,  $p''$ , which is the path length contributing to the retardation, at a distance,  $x$ , away from the center, for  $x < r''$ , is given by:

$$p''=p-p'.....5.6$$

For values of  $x > r''$ ,  $p'$  goes to zero, and the above equation reduces to:

$$p''=p.....5.7$$

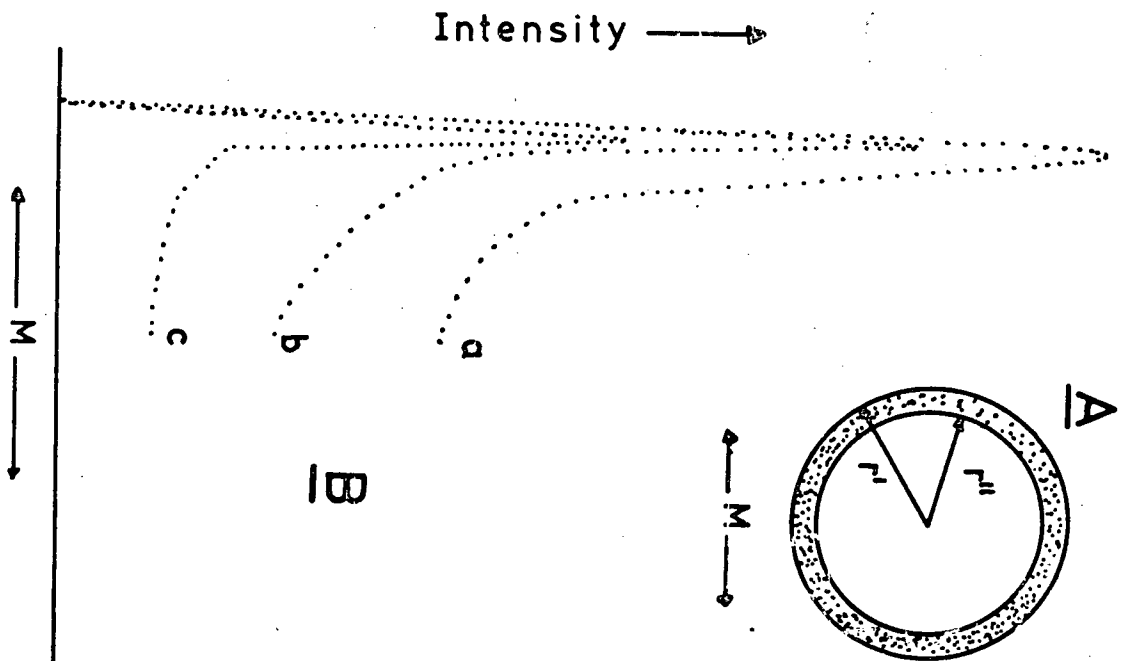
These equations were evaluated for various ratios of  $r':r''$ ,

Figure.5.9: Expected birefringence for an anisotropic coating.

(A) Isotropic material of radius  $r''$  surrounded by a birefringent coating of radius  $r'$ . M represents the middle of the fibre.

(B) Graphical representation of the relative intensity versus distance across fibre calculated according to equations 5.6 and 5.7, for different ratios of  $r''/r'$ : (a) 0.75 (b) 0.90 (c) 0.95.

Figure. 5.9.



and the results are shown in figure 5.9B. This analysis of the system predicts that the birefringence should be greatest at the edges, falling to a finite value towards the middle.

Interfacial effects:

In this case, the source of the birefringence is thought to be the interface at the border of the protein fibre and the surrounding water. The hydrated protein would be expected to have a refractive index somewhere between that of pure water and pure protein, probably around 1.5. The exact value for the refractive index of the hydrated protein is inconsequential as long as it is different from the value of the surrounding liquid (which it obviously is). Although it was not possible to derive a theoretical relationship for a system such as this, it was possible to make some predictions based on empirical observations.

Towards this purpose, observations were made on the birefringence patterns at oil-water interfaces. In all cases it was possible to observe a very evident birefringence zone at the interface. Unfortunately however, it was not possible to extract any useful information from these observations since the interfaces were essentially two dimensional. Totally by chance, in the case of a few of these experiments, a number of air bubbles were trapped in the oil. Since these air bubbles represent a three dimensional system, and show a distinct birefringence, an effort was made to study the pattern of this structure. The results showed that the

birefringence was greatest at the edges , falling off towards the center of the bubble.

In analogy to this, one might expect that the elastin fibre surrounded by water should behave in a similar manner. Furthermore, within the resolution of the experimental methods, it seems that the birefringence should resemble the theoretical prediction for a system which consists of an amorphous core surrounded by an anisotropic sheath, as described in figure 5.9.

Figure 5.10A shows the birefringence pattern observed for an elastin fibre in water. It is clear that the retardation, as indicated by the intensity, is greatest at the edges of the fibre. This conclusively rules out the possibility that the 'apparent' birefringence is an inherent property of the elastin protein.

In dealing with last two choices, it would be possible to distinguish between them, if one could manipulate the experiment by changing the refractive index of the surrounding liquid without altering the hydrated protein. If the birefringence is caused by the presence of an anisotropic sheath, then it should remain unchanged. On the other hand, if the birefringence is a result of interfacial effects, then it should be considerably reduced as the system approaches uniformity (as the refractive index of the surrounding liquid approaches that of the protein).

For practical purposes, it is possible to achieve this by hydrating the elastin fibre in the vapour phase over a dilute

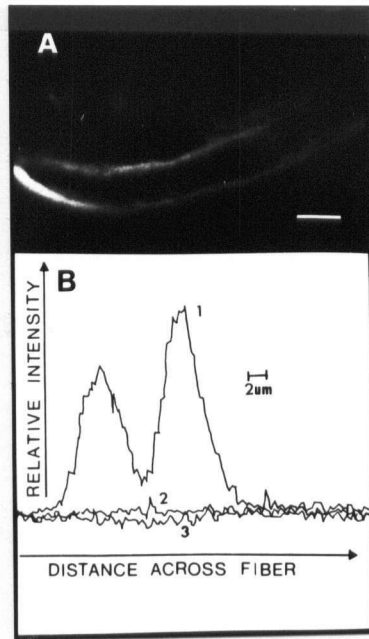
Figure.5.10: Birefringence pattern of single elastin fibres.

(A) The birefringence pattern of single elastin fibres  $n=1.55$ , in water  $n=1.33$ , between crossed polars. The birefringence is seen to be highest at the edges. The bar represents  $10\mu\text{m}$ .

(B) Densitometer tracings for negatives of single elastin fibres in:

- (1) water,  $n=1.33$ .
- (2) immersion oil  $n=1.52$ .
- (3) control tracing of blank field.

Figure.5.10.



salt solution, and then covering the fibre with immersion oil which will not interact with the hydrated protein, but has a value of refractive index (1.52) that is close to that of the swollen fibre. Elastin fibres treated in this manner were mounted between crossed polars and photographed. The negatives were then scanned on a Joyce-Loebel scanning densitometer.

Figure 5.10B, curve 1, is a densitometer tracing for an elastin fibre in water, confirming the previous observation of the higher intensities at the edges of the fibre. Curve 2, shows a tracing of the same fibre after reduction of the refractive index difference at the interface, as described above. It is observed that the retardations are reduced drastically, and is indistinguishable from the control tracing of a blank field (curve 3). Hence it seems safe to state that the 'apparent' residual birefringence is a result of the refractive index difference at the fibre-water interface, and that the actual value for the birefringence of elastin is very close to zero, as expected for a random protein.

## F. Discussion

### (a) Previous studies

There are a number of studies present in the literature that deal with the birefringence properties of elastin and the interpretation of these properties in terms of the molecular structure of this protein (Schmidt 1939, Dempsey 1952, Romhanyi 1958, Gotte 1965, Bairati and Gotte 1977, Serafini-

Fracassini et.al. 1976, Fischer 1979). Most of these studies are in agreement with reference to the low birefringence of elastin (with the exception of Serafini-Fracassin et.al. 1976), reporting values around  $2 \times 10^{-4}$  as obtained in this study. All of these other studies have assumed this low birefringence to be an inherent property of the elastin fibre, and on the basis of this assumption have proceeded to 'visualize' the structure utilizing the phenol reaction (Romhanyi 1958) and the permanganate-bisulfite-toluidine blue reaction (Fischer 1979). Using the results from these manipulations they favoured the anisotropic, ordered structural models for elastin. It should be pointed out that the above studies were conducted on unpurified elastin which could result in artifacts from the chemical interactions of components other than the elastin protein, which also occur in elastic tissue. In order to prevent the occurrence of these artifacts this study has concentrated on the analysis of purified elastin fibres in water, a condition that most closely resembles the in vivo rubbery state.

As mentioned before the results obtained in this study, with regard to the form birefringence, are in conflict with those reported by Serafini-Fracassini et.al. (1976) and Bairati and Gotte (1977). This study failed to reveal any form birefringence for elastin, whereas Serafini-Fracassini and his co-workers obtained a very distinctive curve as well as a high intrinsic birefringence of  $1 \times 10^{-2}$ , which they interpreted as being in favour of the fibrillar models. In trying to explain

this conflict a clue is afforded by glancing at the form birefringence curve obtained by these authors (figure 5.6 curve c) and comparing it with the results obtained in this study for the form birefringence of collagen (figure 5.7 curve a). The resemblance is quite marked and one might speculate that these investigators were actually dealing with a collagen fibre.

This objection is not too far fetched considering the fact that these authors used collagenase to purify their protein, and that this technique has been shown to result in high levels of collagen contamination in the purified tissue (Kadar 1977). Furthermore, both Bairati and Gotte (1977) and Serafinin-Fracassini (1976), used experimental preparations that contained more than one elastin fibre. On the basis of this it could be argued that these authors were reporting artifacts, caused by the interfacial effects, which would be very large for conglomerations of fibres.

#### (b) The fibrillar models

In trying to interpret the birefringence results in the context of the fibrillar models for elastin one is faced with two possibilities:

1. Elastin is made up of an array of parallel filaments aligned in the direction of the long axis, and that these filaments are themselves isotropic, possibly accomodating random coils of protein.
2. That elastin is filamentous in it's organization,

as mentioned above, and in addition to this these filaments contain secondary structures such as the Beta-turns.

In the first case, that of isotropic filaments, one would expect elastin to exhibit a marked form birefringence which would reduce to zero when the refractive index of the immersion medium equalled that of the protein filaments. In the second case, one would also expect a marked form birefringence arising from the well defined spatial arrangement of the filaments along the long axis of the fibre. But in addition, to this form birefringence, one should see an intrinsic birefringence associated with the crystalline structure of the filaments themselves. In the specific case of the occurrence of the Beta-turns in the filaments (Urry 1978c), one would predict a negative intrinsic birefringence since the peptide back-bone involved in this type of structure would be running normal to the long axis of the filaments.

As is quite evident from the previous section, single elastin fibres do not show any form birefringence nor do they seem to have any intrinsic birefringence. These results argue against the presence of any filamentous organization, or the occurrence of stable secondary structures in the elastin protein. Furthermore, the fact that elastin does not display any temperature dependence of its birefringence also argues against any drastic, temperature, induced change of its conformation to a more ordered state as suggested by some workers (Urry 1976a). Finally, since the synthetic fibres of

elastin (Urry and Long 1977b) are known to be highly birefringent (Long 1979) one might be justified in questioning the use of these materials as models for elastin structure.

### G. Conclusions

In view of the evidence presented in this chapter, it is probably justifiable to conclude that elastin possesses a random network structure which is typical of other known kinetic elastomers. However, the technique of polarized light microscopy can only deal with the 'average conformation', and is not able to distinguish between the homogeneous distribution of static units and the random kinetic movements of mobile anisotropic units. Hence it cannot argue against the presence of secondary structures as long as these are thought of as being dynamic (in rapid movements). One can probably disregard the presence of static, crystalline structure on the basis of the pliant mechanical properties of elastin, which are inconsistent with glassy structures, and the nmr analysis presented in chapter 4.

The filamentous organization visualized in the electron microscope may well be the result of drying elastin in the presence of the heavy-metal salts used for negative staining. It is also plausible that the samples of elastin prepared for electron microscope studies were inadvertently extended to high elongations by the receding water during the drying process. This could result in the alignment of the polypeptide chains along the axis of the fibre, which as a result of the

'static' view afforded by the electron microscope technique, would be a mis-interpretation of the normally agitated, kinetically free structure, as being a highly organized filamentous system that is irrelevant to the in vivo rubbery condition.

This point is supported by electron microscope studies, which, using the freeze-etching techniques to avoid the gradual drying down of the tissue, could only demonstrate filamentous structure in samples that had been extended 150 to 200% of their initial length (Pasquali-Ronchetti et.al. 1979).

It is also my opinion that the 200nm sub-fibres which have been observed in the scanning electron microscope (Hart et.al. 1978) are large enough to accomodate an isotropic random network structure, and are not in conflict with the idea of elastin being a typical kinetic elastomer. This aspect of elastin organization is examined in the next chapter.

Chapter.VI. CONFORMATION OF ELASTIN: SCANNING ELECTRON  
MICROSCOPY.

A. Introduction

In the previous chapter I have examined the sub-microscopic and the molecular structure of the elastin protein. Having done so it seems appropriate at this time to evaluate the organization of elastin at a level of order that approaches the range of scanning electron microscope techniques, which should allow an examination of the 200nm sub-fibres if they are in fact present. This is a feasible proposition since the procedures utilized in this study make use of quick freezing techniques in the presence of a solvent (water) that closely resembles the *in vivo* environment. These procedural aspects should protect against organizational artifacts. The disadvantage lies in the fact that the technique of scanning electron microscopy only allows a visualization of the surface texture, which can easily lead to mis-interpretation of the images.

B. Methods

Elastin, from unpurified ligament, alkali extracted ligament, and autoclaved ligament, was cut with a sharp razor into cubes (largest dimension less than 1mm) and left in distilled water at 40°C overnight.

The preparation for scanning electron microscopy was done by dropping the hydrated pieces of tissue into a butanol bath

that was cooled in liquid nitrogen. Some of the samples were fractured while frozen. All samples were dehydrated in a freeze dryer (operating at  $-50^{\circ}\text{C}$ ) and mounted onto stubs with conducting silver paint. These stubs were subsequently coated, in vacuo, with a thin layer of gold approximately  $100\text{\AA}$  in thickness.

The specimens were viewed in a Cambridge Instrument Company, Stereoscan microscope, at a filament accelerating voltage of 50kv. The images were recorded on Polaroid 655 film, and the negatives were preserved by treatment with sodium sulphite for one hour.

### C. Results

Preparations of unpurified ligament elastin showed some indication of a 'fibrillar' arrangement when viewed in the longitudinal direction (figure 6.1). These structures, which had diameters of 80 to 100nm, could represent the collagen sheath that is thought to occur around the individual elastin fibre (Finlay and Steven 1973). The fracture surfaces of these fibres, however, failed to support such an organization, indicating that it is probably a feature that is confined to the periphery of the elastin fibres.

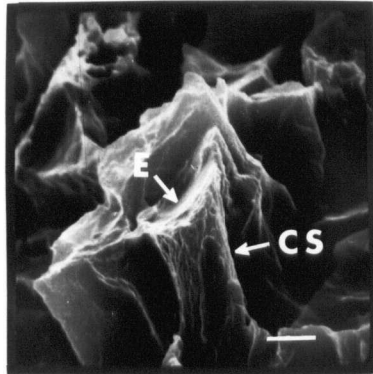
Autoclaving the elastin fibres resulted in the removal of the 'surface coating' revealing what appears to be a clear indication of sub-structure (figure 6.2), that is visualized at the surface as a granular appearance with ridges thrown in for good measure. But again, cross-sectional views of the same

Figure.6.1: S.E.M. Of unpurified ligament elastin fibre.

(E) Elastin.

(CS) Collagen sheath.

The bar represents 10um.

Figure.6.1.

preparations failed to show any sub-structure.

Alkali extracted specimens showed a very distinct surface structure, with 40nm fibres that were spaced approximately 200nm apart, similar to those observed for arterial elastin by Carnes et.al. (1977) (figure 6.3a). Higher magnification of the fracture surfaces showed a very smooth appearance, without any indication of internal structure (figure 6.3b).

#### D. Discussion

Almost all of the studies reported in the literature, dealing with the scanning electron microscopy of elastin, have supported the 200nm sub-fibre arrangement for the elastin protein. In objection to this point of view, it should be stated that most of these investigators have looked at the appearance of the fibres in the longitudinal direction. As is shown by this study, this approach to the problem can be misleading since it cannot distinguish between surface features and inherent organization. The few papers that have dealt with the cross-sectional view of the elastin fibres (Minns and Stevens 1974) are in agreement with the findings of this study that there is no indication of sub-structure. It is interesting to note that these sub-fibres have never been observed in the transmission electron microscope. The following are a few more aspects of the results which also argue against the presence of these 200nm sub-fibres.

Since the fracture of a substance results from the propagation of a crack through the material, and since the

Figure.6.2: Surface texture of autoclaved elastin fibres.

There is some indication of substructure as reflected in the surface texture of these fibres. The bar represents 2 $\mu$ m.

Figure.6.2.

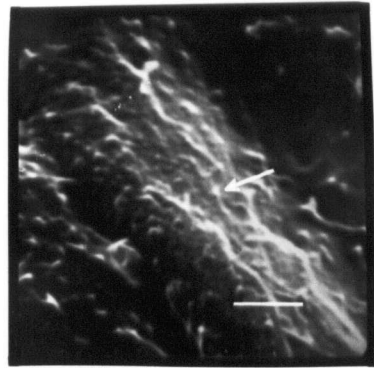
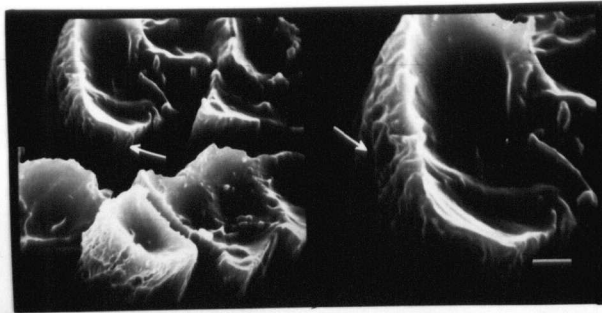


Figure.6.3: Fracture surfaces of elastin fibres.  
Alkali purified fibres showing the 200nm spaces on the elastin fibres. The fracture surfaces, however, are smooth and do not indicate the presence of 200nm sub-fibres. The bar represents 2um.

Figure.6.3.

path of crack propagation follows a route that requires the least expenditure of energy, one would expect the fracture properties of a homogeneous substance, such as glass, to be noticeably different from a composite material, such as fibre-glass which is made up of glass fibres embedded in an epoxy matrix.

Applying this analogy to the fracture properties of elastin, one would expect a 'homogeneous' elastin fibre (at  $-90^{\circ}\text{C}$ ) to fracture in a smooth manner similar to glassy materials. If, however, these sub-fibres do exist the material could be represented as a composite consisting of the elastin protein (200nm) embedded in a cementing matrix. The fracture of this material (at  $-90^{\circ}\text{C}$ ) should give results similar to the fracture of fibre-glass materials, with some of the cracks propagating between these 200nm sub-fibres resulting in a 'splayed' appearance of the fracture surface.

As mentioned before, the fracture surfaces of the elastin fibres were always smooth, with no evidence for the presence of 'splayed' fibrils. It is possible though, that the embedding matrix material has mechanical properties that are identical to the protein fibres as well as being structurally continuous with these sub-fibres. In which case, the material would fracture in a homogeneous manner.

This leaves me with one last point: how to explain the presence of these 200nm surface texture.

The reports that have observed these sub-fibres often state that they are only seen after the purification of the

protein (Hart et.al. 1978). On the basis of this comment it is interesting to speculate that the 200nm structures are an artifact caused by the removal of the glycoprotein fibrils during purification, and actually represent the spaces that would result from their removal. This explanation is plausible because the glycoproteins do in fact occur in 100 to 200nm bundles around the elastin fibre, as seen in the transmission electron microscope (Farenbach et.al. 1966).

Having presented the arguments against the presence of the sub-fibres, I would like to put the controversy into it's proper perspective by stating that it is quite irrelevant. If they are in fact real attributes of the elastin fibre, they would still not be in contradiction to the idea of elastin being a typical kinetic elastomer, since their size is large enough to accomodate random coils of protein. Their presence however, would alter the interpretations of the failure properties of elastic tissue since they would be an introduction of another architectural factor in the network composite.

Chapter.VII. ELASTIN AS A KINETIC ELASTOMER.A. Introduction

In the previous chapters I have attempted to rigourously examine the conformational state of the elastin protein. The reason for that exercise (in futility?) was to validate the use of the kinetic theory of rubber elasticity as an adequate basis for the elastomeric properties of this protein. This chapter, then, deals expressly with the evaluation of elastin as a typical kinetic elastomer, assuming that all the conditions of the kinetic theory are met.

But why do these tests on single elastin fibres? Aside from irrelevant existential and philosophical arguments, there are a number of practical reasons for suffering through the single fibre studies. The analysis of the elastomeric properties of elastin upto now, has been based on experiments using bundles of elastin fibres. Although this is without question the more convenient form of experiment, it's disadvantage lies in the fact that using a sample with sub-structure will make it difficult to distinguish the properties of the 'architecture' from the properties of the material. This study was undertaken with the purpose of getting around the architectural interference by studying the physical properties of single, 6 to 8 $\mu$ m, elastin fibres. This allowed an interpretation of the properties at the molecular level, which was attempted by using the various kinetic theory relationships. Hence the major product of this study was the

evaluation of the various kinetic theory parameters, as they apply to the elastin protein.

Furthermore, since the fibres in the elastin bundles are not continuous, purified bundles of elastin fail at low strain (about 50% extension). As will be shown in this chapter, elastin is still in the 'Gaussian' region of its macroscopic properties, at 50% extension, and therefore, bundle studies do not allow one to examine the additional information that is realized by the analysis of the non-Gaussian properties of the polymer network. It is these properties that need to be evaluated, if one is to extrapolate from the elastin system to other proteins in the random conformation.

Lastly, the photo-elastic experiments demand that the experimental setup utilize single fibres, since bundles of fibres have a large form birefringence, due to the interfacial effects, that masks the properties of the single fibres, making the evaluation of the bundle properties impossible.

## B. Entropy Elastomers: The Kinetic Theory of Rubber Elasticity

### (a) Gaussian chain statistics and entropy

In trying to understand the statistical mechanics of random coiled molecules it is convenient to represent one end of the chain,  $a$ , to be fixed at the origin, and to characterize the 'random walk' to the other end,  $b$ , via the quantity termed the end-to-end distance  $r$ , (figure 7.1). The probability density function, of finding  $b$  in the vicinity of

point  $P$  within the volume element  $[dx, dy, dz]$  (which can also be represented as the probability density function of  $r$  values) forms the basis of the kinetic theory relationships.

The derivation of these probabilities depends on the evaluation of the number of conformations that allow the placing of the chain end,  $b$ , within a given volume element. If one assumes that all conformations are equally probable, then the density function is described by (Treloar 1975):

$$p[x, y, z] = (b^3 / \pi^{3/2}) \exp(-b^2 r^2) \dots \dots \dots 7.1$$

where  $p[x, y, z]$  represents the probability of finding the chain end  $b$  a distance,  $r$  ( $r^2 = x^2 + y^2 + z^2$ ), away from end,  $a$ . The term  $b$  is defined by:

$$b^2 = (3/2) sl^2 \dots \dots \dots 7.2$$

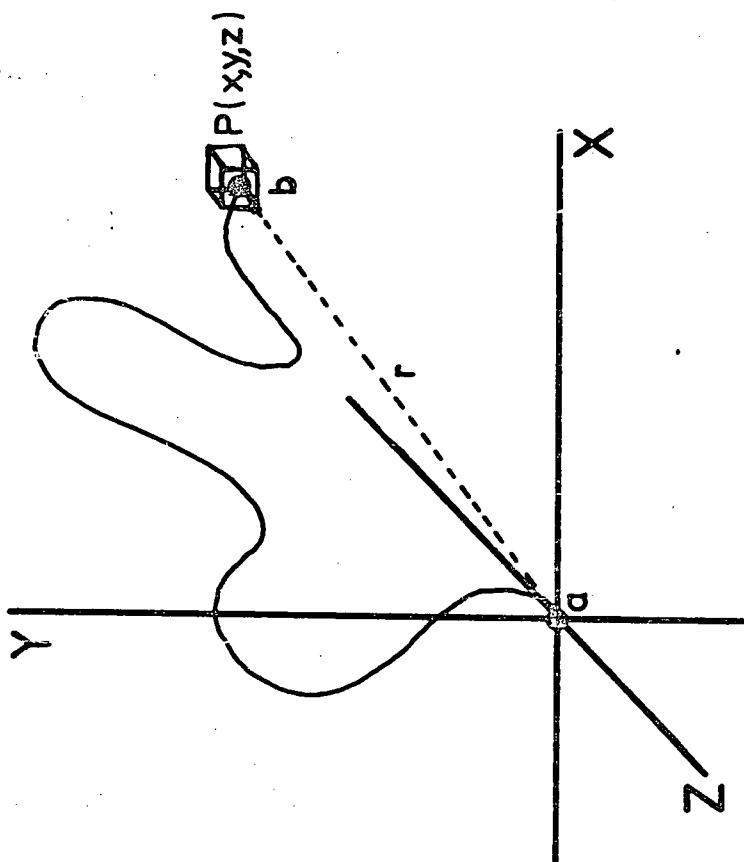
where  $s$  is the number of random links in the chain and  $l$  is the length of each random link. The important result of equation 7.1, is that the function has a maximum at  $r=0$ , which is similar to saying that most of the conformations are consistent with the end,  $b$ , being at the origin (no pun intended). Since the entropy of the chain is proportional to the logarithm of the number of conformations available to the system (Treloar 1975) the entropy is also seen to be at a maximum when  $r=0$ .

For a chain whose points are separated by a distance,  $r$ , the entropy of the chain,  $S$ , is given by (Treloar 1975):

$$S = c - kb^2 r^2 \dots \dots \dots 7.3$$

where  $c$  is an arbitrary constant, and  $k$  is the Boltzmann constant. As is evident from equation 7.3, the imposition of

Figure.7.1: The random-coiled chain  
The random chain with end a at the origin and end b at a point  $P(x,y,z)$  within a volume element  $\{dx,dy,dz\}$ .

Figure. 7.1.

strain on this system will increase  $r$ , resulting in a decrease of the configurational entropy of the system. This decrease, in entropy, forms the basis for the retractive force of kinetic elastomers. The internal energy term remains constant and does not contribute to the elastic properties.

#### (b) The elastic network

Any molecular interpretation of a rubber polymer, based on the kinetic theory of rubber elasticity, assumes a network made up of a three dimensional array of idealized random chains. The chains are cross-linked at various points (this is necessary if the network is to maintain it's structural and mechanical integrity when strained) and one can therefore characterize the chain between cross-links as having an average molecular weight  $M_c$ , and consisting of  $s$  number of random links each of length  $l$ . In the case of real molecules, however, ideal random links cannot occur since bond movements are restricted by valence angles, potential barriers, and steric hindrances. One therefore has to invoke the concept of a 'functional' random link. This link will consist of a number of bonds, which as a unit, appear to satisfy the statistical requirements of the 'ideal' random link.

As stated before, imposing a strain on this network will decrease the configurational entropy, giving rise to the retractive force. The basic assumptions of the kinetic theory, which are discussed in detail by Treolar (1975) and Flory (1953), are as follows:

1. The network contains  $N$  chains per unit volume.

These chains, which were defined above, are held in a network by a few stable cross-links.

2. The mean square end-to-end distance for the whole assembly of chains in the unstrained state is the same as for a corresponding set of free chains.

3. Deformation does not lead to a change in volume.

4. The components of length of each chain change in the same ratio as the corresponding dimensions of the bulk rubber.

5. The entropy of the network is the sum of the entropies of the individual chains.

### (c) Mechanical properties of kinetic rubbers

Assuming an ideal Gaussian system, the kinetic theory makes it possible to characterize the tensional elastic force, resulting from the strain induced free energy change (equal to the entropy change for an ideal rubber), by the following equations (Treolar 1975):

$$f = NkT(\lambda - \lambda^{-2}) \dots\dots 7.4$$

and,

$$\sigma = NkT(\lambda^2 - \lambda^{-1}) \dots\dots 7.5$$

where  $f$  is the nominal stress (force/unit unstrained cross sectional area),  $\sigma$  is the true stress (force/unit strained cross sectional area),  $k$  is the Boltzmann constant ( $1.38 \times 10^{-16}$  erg  $K^{-1}$ ),  $T$  is the absolute temperature,  $N$  is the number of random chains per unit volume of the material, and  $\lambda$  is the extension ratio expressed in units of the unstrained length.

In the case of swollen rubbers, a state that is relevant to the protein elastomers, a volume fraction term is incorporated to give:

$$f = NkTv_2^{1/3}(\lambda - \lambda^{-2}) \dots\dots 7.6$$

and,

$$\sigma = NkTv_2^{1/3} (\lambda^2 - \lambda^{-1}) \dots\dots 7.7$$

where  $v_2$  is the unswollen volume/swollen volume.  $f$  and  $\sigma$  refer to the force per unit swollen unstrained cross-sectional area, and force per unit swollen strained cross-sectional area respectively.

All four of these equations define a term that characterizes the stiffness of the material being tested, called the elastic modulus,  $G$ , according to:

$$G = NkT \dots\dots 7.8$$

Since  $G$  is proportional to the number of chains,  $N$  (based on assumption 5), and since  $N$  is itself related to the cross-linking density, which for the case of one cross-link attaching four chains is approximately equal to:

$$N = 2(\#c) \dots\dots 7.9$$

where  $\#c$  is the number of cross-links per unit volume. It seems intuitively possible to obtain a measure of the molecular weight between cross-links (which for a given composition is inversely proportional to the number of cross-links,  $M = (1/2)\#c$ ), from the value of the elastic modulus  $G$ . This is realized in the following relationship:

$$G = Nkt = \rho RT/Mc \dots\dots 7.10$$

where  $\rho$  is the polymer density,  $R$  is the universal gas constant ( $0.082 \times 10^{-3} \text{ m}^3 \text{ atm mol}^{-1} \text{ K}^{-1}$ ), and  $Mc$  is the molecular weight between cross-links.

Water swollen elastin, being a hydrophobic protein in equilibrium with a hydrophilic solvent, presents some

problems when one tries to interpret it's properties using the above relationships since it's equilibrium degree of swelling, contrary to the assumption of the kinetic theory, changes as a function of both temperature and elongation (Gosline 1978, Hovee and Flory 1976). Oplatka et.al. (1960) and Bashaw and Smith (1968) extended the kinetic theory to account for these compositional changes that take place in open systems, with Mistrali et.al. (1971) providing the preliminary support for it's application to elastin. These relationships, although they are mentioned here, were not tested rigourously since the physical measurements were not accurate enough to allow a critical appraisal of such refined distinctions.

#### (d) Photoelasticity

The kinetic theory also affords a relationship for the strain-birefringence behaviour of rubbery polymers swollen in an optically neutral solvent (Treolar 1975):

$$n_{11} - n_{12} = (\bar{n}^2 + 2)^2 2\pi N (\alpha_1 - \alpha_2) v_2^{1/3} (\lambda^2 - \lambda^{-1}) / \bar{n} 45 \dots \dots 7.11$$

where  $\alpha_1$  and  $\alpha_2$  are the polarizabilities of the random link parallel to it's length and normal to it, respectively,  $\bar{n}$  is the average refractive index of the protein, and N is defined as before.

The assumption is made by this theory that the optical anisotropy of the polymer when it is strained arises from an alignment of the random links, whose inherent polarizability remains unchanged, in the direction of the strain. The birefringence is not thought to represent an anisotropy

arising from the displacement of electron orbitals (due to the alteration of the interatomic distances), as is the case with crystalline or glassy polymers.

The relationship for the stress-birefringence can be derived from the above equation by substituting in equation 7.7, which describes the relationship between the true stress and the extension, into equation 7.11 to give:

$$n_{\parallel} - n_{\perp} = \sigma (\bar{n}^2 + 2) \frac{2\pi (\alpha_1 - \alpha_2)}{\bar{n} 45kT} = \sigma C' \dots \dots 7.12$$

Since  $(\alpha_1 - \alpha_2)$  and  $\bar{n}$  are presumed to remain constant, it is possible to incorporate all the parameters into an overall constant,  $C'$ , which is termed the stress-optical coefficient. This coefficient depends only on the mean refractive index of the polymer and the polarizability of the random link, and it should be inversely proportional to the temperature. The value of  $(\alpha_1 - \alpha_2)$ , which represents the anisotropy of the random link, is theoretically independent of strain, swelling, stress, and temperature. Hence its constancy over a number of parameters could be used as an indicator of the peptide backbone stability.

#### (e) Non-Gaussian effects and the evaluation of s

Since the non-Gaussian effects observed for the mechanical and photoelastic properties of the elastic network is the result of the finite length of the chain between cross-links, and hence a finite number of random links,  $s$ . It seems intuitively obvious that one should be able to work 'backwards' and evaluate the value 's' by analysis of these

non-Gaussian properties.

The Gaussian relationships mentioned upto now, assume that the end-to-end distance,  $r$ , is small compared to the fully extended length of the chains ( $r/sl \ll 1$ ). This assumption restricts their application to small strains, and necessitates the use of the more accurate non-Gaussian relationships at higher levels of extension. For the case of the mechanical data, the relationship takes the form of a series expansion of which the first five terms are (Treolar 1975):

$$f = Nkt (\lambda - \lambda^{-2}) [ 1 + (3/25s) (3\lambda^2 + 4/\lambda) + (297/6125s^2) (5\lambda^4 + 8\lambda + 8/\lambda^2) + (12312/2205000s^3) (35\lambda^6 + 60\lambda^3 + 72 + 64/\lambda^3) + (126117/693(673750)s^4 (630\lambda^8 + 1120\lambda^5 + 1440\lambda^2 + (1536/\lambda) + 1280/\lambda^4) + \dots ] \dots \dots 7.13$$

For the stress-optical data, the non-Gaussian relationship takes the form (Treolar 1975):

$$n_{11} - n_{11} = (n^2 + 2) \frac{24\pi}{3n} (p_1 - p_2) \dots \dots 7.14$$

where  $(p_1 - p_2)$  is defined according to:

$$(p_1 - p_2) = N(\alpha_1 - \alpha_2) [ (1/5)\lambda^2 - (1/\lambda) + (1/150s) (6\lambda^4 + 2\lambda - 8/\lambda^2) + (1/350s^2) (10\lambda^6 + 6\lambda^3 - 16/\lambda^3) \dots \dots 7.15$$

Comparison of the experimentally obtained curves (for the mechanical and photoelastic properties) with these relationships should allow an evaluation of  $s$ .

#### (f) Reduction of elastin data to the unswollen form

Since the protein elastomers such as Resilin, Abductin, and Elastin, exhibit their elastomeric behaviour only when

they are swollen by a diluent (such as water), it might seem a little irrelevant to attempt the reduction of the data obtained for the swollen form to an 'unswollen' state. This is necessary, however, if one is to make a valid comparison between the theoretical relationships for the non-Gaussian systems mentioned in the last section (which are derived for the unswollen network) and the elastin data.

The data for elastin was reduced according to the relationships provided by Flory (1953):

$$f^0 = f^s / v_2^{2/3} \dots \dots \dots 7.16$$

$$\lambda^0 = \lambda^s / v_2^{1/3} \dots \dots \dots 7.17$$

$$\sigma^0 = \sigma^s / v_2^{2/3} \dots \dots \dots 7.18$$

$$(n_{||} - n_{\perp})^0 = (n_{||} - n_{\perp}) / v_2^{2/3} \dots \dots \dots 7.19$$

where the superscripts <sup>0</sup> and <sup>s</sup> refer to the 'unswollen' and swollen forms of the designated terms, which are defined as before.

### C. Materials and Method

#### (a) Purification of elastin

Bovine ligamentum nuchae of mature beef cattle was obtained from a local slaughter house and purified by repeated autoclaving in distilled water according to the method of Partridge et.al. (1955). Briefly, this procedure involves 'cooking' the elastin in an autoclave operating at fifteen pounds per square inch for a period of an hour. This removes the associated proteinaceous material, such as the collagen

and the matrix substances, leaving behind the insoluble elastin protein. The procedure is repeated 6 to 8 times, with fresh changes of distilled water, to ensure a clean preparation. Tissue thus prepared can be stored for an indefinite period of time with occasional sterilization by autoclaving. The evaluation of this purification procedure has been presented in chapter 2.

#### (b) The experimental stage

The major piece of apparatus used in the experiment, along with the relative positions of the various components, is shown in figure 7.2. The stage was assembled from glass slides glued together with epoxy adhesive. The flexible glass rod, which served as a microforce transducer, was made by pulling a 5mm diameter solid glass rod over a bunsen burner flame until the desired diameter of 80 to 100um was obtained. Dow Corning high vacuum grease was applied between the movable glass slide and the stage to smooth out the manipulations during the experiment and to keep the extensions fixed at the desired point. The temperature control system was the same as the one described in chapter 5.

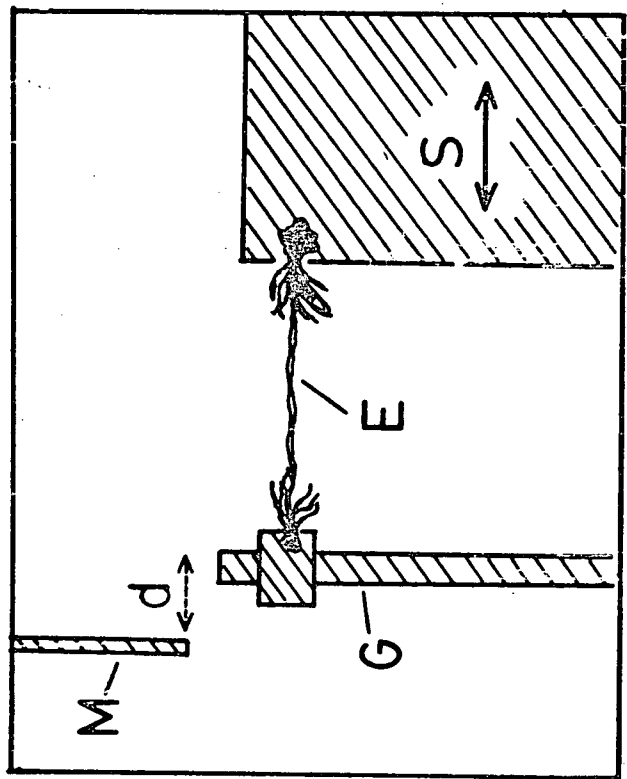
#### (c) Preparation of experimental specimen

A strip of dried purified elastin (approximately 2mm X 5mm in dimension) was mounted directly onto the experimental stage by anchoring one end to the flexible glass rod and the other end to the movable glass slide using rubber

Figure.7.2: The experimental stage.

Diagram of the experimental stage used for force, extension, and retardation measurements. The elastin fibre, E, was extended by manipulating the movable slide, S, and the extension was monitored by measuring the distance between two landmarks on the elastin fibre. The force experienced by the elastin fibre was calculated from the measurement of the deflection,  $d$ , of the glass rod, G, relative to a fixed marker, M.

Figure. 7.2.



cement. Distilled water was then added to the preparation, and the elastin fibres teased away, under a dissecting microscope with fine forceps, until a single connecting fibre was left intact between the glass rod and the movable slide (figure 7.2).

The preparation was then mounted between crossed polars, on a Wild M21 polarizing microscope, and the experiment was conducted by the manipulation of the mounted specimen at 300X magnification. The fibre was strained in a random steps, by shifting the movable glass slide, and the values for the extension, force, and retardation, were obtained as described below.

#### (d) Measurement of strain

Two distinguishing marks were noted in the unstrained state and the distance between them was calibrated using a Filar micrometer. The separating distance was evaluated at each extension step, and the elongation could then be represented as an absolute value, or as an extension ratio of the initial length.

#### (e) Measurement of force

The manipulation of the elastin fibre, which was done by moving the glass slide, exerted an extending force on the elastin fibre which could be quantitated by measuring the deflection of the flexible glass rod with reference to the fixed marker (figure 7.2), using a Filar micrometer. This

value could then be converted to an absolute force,  $F$ , by utilizing the equation for the bending of a beam:

$$F = d(3EI/l^3) \dots\dots 7.20$$

Where  $d$  is the deflection of the glass fibre,  $l$  is the length of the glass fibre (usually around 1.3 to 1.5 cm), and  $I$  is the second moment of area, which for a rod of circular cross-section of radius,  $r$ , takes the form:

$$I = \pi r^4/4 \dots\dots 7.21$$

The value of  $E$ , which is the Young's modulus of glass, was obtained by measuring the deflection of a macroscopic glass rod, when experiencing a bending force from several calibrated weights. Substituting these values for the deflection and force into equation 7.20 along with the dimension data, and solving for  $E$  gave a value of  $6.2 \times 10^{10} \text{Nm}^{-2}$  for the Young's modulus of glass.

The experimentally obtained force could then be represented as either the nominal stress (force/unit unstrained cross-sectional area) or the true stress (force/unit strained cross-sectional area). To insure against the presence of erroneous values resulting from the use of this method, one of the micro-force transducer glass rods was calibrated by hanging known weights on it's end and measuring the deflections. These deflections were always within 2% of the deflections predicted by use of equations 7.20 and 7.21.

#### (f) Calculation of cross-sectional area

The unstrained diameters were measured with the Filar

micrometer and the cross-sectional areas were calculated by assuming a circular cross-section. The cross-sectional areas for the strained fibres were calculated from the measured length change by assuming that the volume of the fibres remained constant with extension.

#### (g) Measurement of birefringence

The specimen on the polarizing microscope was orientated between crossed polars (polarizer at  $0^\circ$ , analyzer at  $90^\circ$ ) with its long axis at  $+45^\circ$  to the polarizer (positive angles being counter-clockwise). Illumination was by a 100watt quartz lamp, which along with an interference filter provided a green monochromatic light (546nm) source.

The retardations were measured, after each force-extension measurement, at the center of the fibre using a  $1/30$  wavelength Zeiss rotary compensator. This value of retardation was divided by the optical path length (taken to be the diameter at each extension step) to give the value for birefringence.

#### (h) Errors

Since it is hard to evaluate the errors involved in dealing with a system such as the one utilized in this study, a statistical approach was thought to be more feasible, and accordingly, the relevant statistical parameters are presented with the results. In general, the excellent reproducibility of the data and the minimum scatter, is taken to be a good

indicator of the systems reliability.

#### D. Physical Properties of Single Elastin Fibres

##### (a) General characteristics

The mechanical behaviour of single elastin fibres was observed to be completely elastic with no observable hysteresis or change with repetitive cycling of the strain. Typically, the fibres could be elongated to 100%-200% of their initial length ( $\lambda = 2$  to 3) before breaking. The cause of the failure could not be determined with certainty. It can only be stated that there was no observable plastic flow before failure. The failure itself occurred either as a result of a breakage of the strained portion under observation, or a breaking away of the fibre from the residual bundles of elastin which were used for anchoring the preparation. The tensile strength is probably in the range of  $10^6 \text{Nm}^{-2}$ .

##### (b) Mechanical properties and the derivation of $M_c$

Equation 7.6 indicates that if the data obtained for the mechanical properties of single elastin fibres is plotted as a graph of nominal stress versus  $(\lambda - \lambda^{-2})$ , it should yield a straight line of zero intercept and a slope equal to  $Gv_2^{1/3}$ . Figure 7.3,a, shows the mechanical data for eight single elastin fibres in distilled water at 24°C. It is evident that the relationship obeys the prediction of a straight line upto  $\lambda = 2$  (an extension of 100%). Beyond this extension, however,

the experimental points deviate from the straight line, seen as an upturn in the graph. This deviation is the result of the non-Gaussian properties of the network, which will be analyzed in detail later. For the moment, the analysis will be restricted to the linear portion of the stress-strain relationship.

The elastic modulus,  $G$ , obtained from the treatment of the data according to equation 7.8, has a value of  $4.1 \times 10^5 \text{ Nm}^{-2}$ . This was calculated from the slope of the linear portion of the plot (figure 7.3,a), using a value of  $\nu_2 = 0.65$  (Gosline 1978). Similarly, the value of  $M_c$ , which is the molecular weight of the chain between cross-links, was evaluated from equation 7.10, the value of the elastic modulus, and  $\rho = 1.33$ . This gave a value of 7,100 for the molecular weight of the chain between cross-links.

This use of equation 7.10 for the calculation of  $M_c$  assumes ideal tetra-functional cross-links. This is obviously an oversimplification since, in reality, imperfections such as loose ends etc. will be present in the network. It is possible to correct for these imperfections, assuming randomly distributed cross-linking, by utilizing a modification of equation 7.10, according to (Treloar 1975):

$$G = \rho RT(1 - 2M_c/M) / M_c \dots \dots 7.22$$

Where  $M$  is the molecular weight of the polymer before cross-linking. This relationship cannot, in the strictest sense, be applied to elastin since the cross-linking sites on the precursor protein, tropoelastin, are not randomly distributed

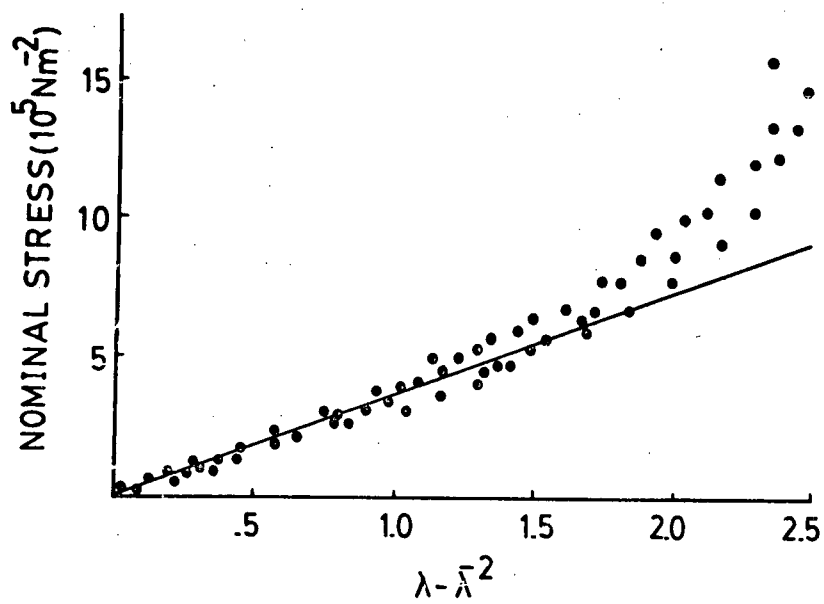
Figure.7.3: Physical properties of single elastin fibres.

(A) Graph of the force extension data for single elastin fibres plotted according to equation 7.6. The linear regression, through the first 30 points, has a correlation coefficient  $r=0.91$ .

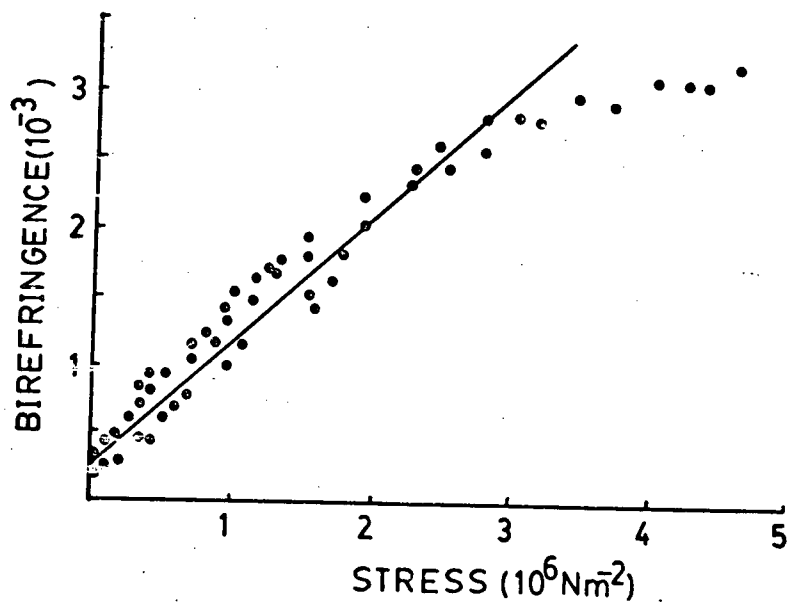
(B) Graph of the Birefringence-stress data for single elastin fibres plotted according to equation 7.12. The linear regression, through the first 30 points, has a correlation coefficient  $r=0.88$ .

Figure. 7. 3.

A



B



but, rather, occur in distinct locations on the tropoelastin molecule (Sandberg et.al. 1972). Nevertheless, the use of equation 7.22 should give an estimate of the lower limit of  $M_c$ . Utilizing the value obtained above, of 7100 for  $M_c$ , and equation 7.22, along with a value of 72,000 for the molecular weight of the precursor tropoelastin (Sandberg 1976), gives a corrected molecular weight of 6000 for the chain between crosslinks. Hence the data is consistent with a  $M_c$  value in the range of 7100 to 6000 g/mole. This result is in good agreement with the expected values calculated from the known biochemical composition and the cross-linking profiles of insoluble elastin (Gray et.al. 1973).

### (c) Photoelasticity

According to equation 7.12, a plot of birefringence versus stress, should give a straight line of slope  $C'$ . Figure 7.3,b, represents the data for eight single elastic fibres. As with the stress-strain relationship, the theoretical relationship is followed to a certain point, after which it deviates towards the stress axis, with the birefringence approaching its ultimate value. This departure from the theory can again be explained in terms of the non-Gaussian properties of the elastin network: the finite length of the chain between cross-links is responsible for this non-Gaussian shift, with the asymptotic limit representing the state of 's' links in full alignment. The existence of this common causal element, is supported by the observation that both the

Table.7.1: Kinetic theory parameters for elastin.KINETIC THEORY PARAMETERS FOR ELASTIN.

volume fraction	$V_2$	0.65
elastic modulus	$G$	$4.1 \times 10^5 \text{ Nm}^{-2}$
number of chains	$N$	$1.0 \times 10^{26} \text{ m}^{-3}$
average molecular weight of the chain between cross-links	$M_c$	6,000 to 7,100g/mole
stress-optical coefficient	$C'$	$1.0 \times 10^{-9} \text{ m}^2 \text{ N}^{-1}$
polarizability of the random link	$(\alpha_1 - \alpha_2)$	$2.8 \times 10^{-30} \text{ m}^3$

stress-strain graph (figure 7.3,a) and the stress-birefringence graph (figure 7.3,b) enter the non-Gaussian region at the same level of extension ( $\lambda=2$ ).

Concentrating on the linear portion of this graph (figure 7.3,b), the slope of this relationship yields a value for  $C'$  of  $1.0 \times 10^{-9} \text{m}^2 \text{N}^{-1}$ . Utilizing this value of  $C'$  and a value of  $\bar{n}=1.55$ , it is possible to solve for the polarizability of the random link ( $\alpha_1 - \alpha_2$ ). Doing this one obtains a value of  $2.84 \times 10^{-30} \text{m}^3$  for the polarizability of the random link at  $24^\circ\text{C}$ . The value calculated for the stress-optical coefficient,  $C'$ , is comparable to the results obtained by Weis-Fogh (1961b) for the invertebrate elastomer, resilin ( $1.0 \times 10^{-9} \text{m}^2 \text{N}^{-1}$  for elastin as compared to  $1.1 \times 10^{-9} \text{m}^2 \text{N}^{-1}$  for resilin). This is not surprising since they are both protein elastomers and would, therefore, be expected to have similar values for the average refractive index and the polarizability of the random link. The kinetic theory parameters derived for elastin are summarized in figure 7.1.

It should be mentioned that the data for elastin birefringence extrapolate to a positive birefringence at zero stress. This is consistent with the results obtained for unstrained single elastin fibres, which appear to have a small residual birefringence of about  $2.4 \times 10^{-4}$ . This residual birefringence has been shown to arise from the refractive index difference at the water/fibre interface. The "true" birefringence of the unstressed fibre is indistinguishable from zero (Aaron and Gosline 1980).

(d) Temperature dependence of the optical anisotropy

Equation 7.12 also states that the stress-optical coefficient,  $C'$ , should be inversely proportional to the absolute temperature,  $T$ , assuming that the mean refractive index and the polarizability of the random link remain unchanged. Figure 7.4,a, shows the experimentally obtained results for the temperature dependence of  $C'$ . It seems that the predictions of the kinetic theory (figure 7.4,a, dashed line) are followed qualitatively but the decrease with temperature is larger than that which would be predicted by equation 7.12.

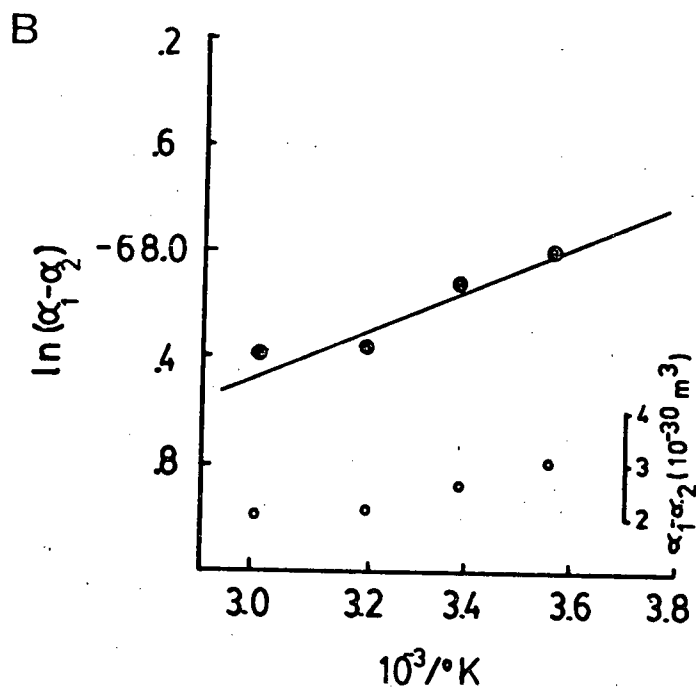
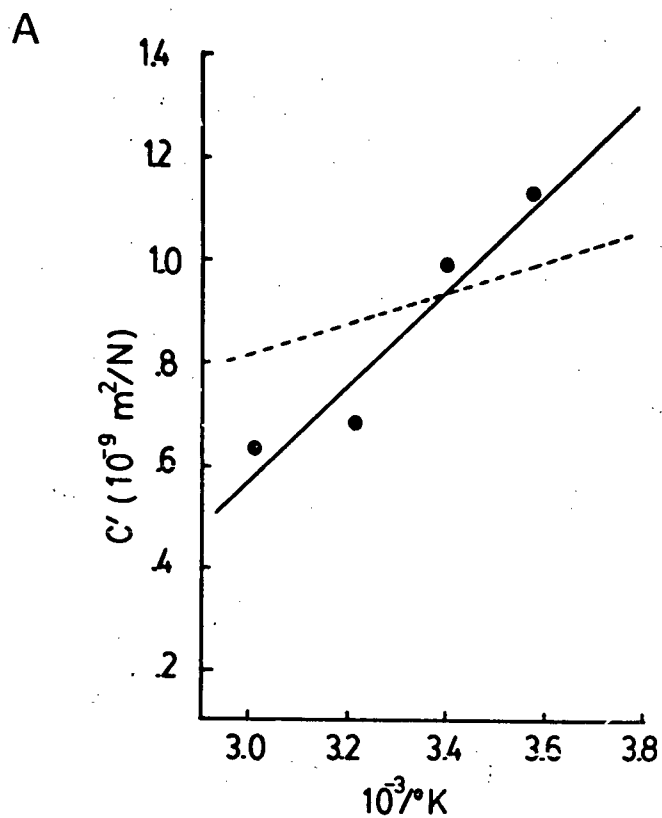
There are two possible sources for this deviation. First, since elastin decreases its volume with increasing temperature (Gosline 1978), the mean refractive index is expected to increase with temperature. However, the extent of this increase is small, and in any case increasing the refractive index should increase the value of the stress-optical coefficient. Second, it is possible that the polarizability of the random link ( $\alpha_1 - \alpha_2$ ) changes with temperature, which could account for the large decrease in  $C'$ . Figure 7.4,b (open circles), shows the value for the polarizability of the random link assuming that  $n$  remains unchanged with temperature. It is evident that the polarizability of the random link decreases by approximately 30% over the temperature range studied. The implication of this change is discussed below.

Figure.7.4: Temperature dependence of photcelasticity.

(A) Graph of the stress-optical coefficient,  $C'$ , versus  $1/T$ . (filled circles): experimental points. The linear regression has a correlation coefficient of  $r=0.92$ . (dashed line): expected relationship for the temperature dependence of  $C'$  calculated from equation 7.12.

(B) (open circles): dependence of the random link anisotropy on temperature. (filled circles): the same data plotted as an Arrhenius relationship according to equation 7.23. The activation energy calculated from the slope of the linear regression ( $r=0.94$ ) has a value of 1.6 kcal/mole.

Figure. 7.4.



As pointed out before, when dealing with real polymer chains, the presence of energy barriers to bond rotation implies that a number of chemical bonds are required to exhibit the properties of a random link. This also implies that as these energy barriers are overcome with an increase in temperature, the number of bonds needed to give a random link should decrease. Hence the length of this 'functional' link and consequently the polymer chain dimensions are expected to be temperature dependent. Studies on the temperature dependence of the optical properties of polymers other than elastin, have shown that the optical anisotropy of the random link usually decreases with increasing temperature (Saunders 1957), and this decrease is thought to reflect a reduction in the conformational restrictions on the molecules in the network, as discussed above. It has been shown that the variation of the link anisotropy with temperature is consistent with an Arrhenius type relationship of the form (Morgan and Treloar 1972):

$$(\alpha_1 - \alpha_2) = A \exp(E_a/RT) \dots \dots 7.23$$

Where  $E_a$  is an activation energy. Hence it is possible to obtain the value of  $E$  from a plot of  $\ln(\alpha_1 - \alpha_2)$  versus  $1/T$ . The value of the activation energy should reflect the magnitude of the energy barriers of the restrictions on the polymer chains.

A plot of the elastin data for the link anisotropy as a function of temperature is shown in figure 7.4,b (filled circles). From the slope of the graph one obtains a value of

1.6 kcal/mole for the activation energy. This value is comparable to the value obtained from nuclear magnetic resonance data for elastin peptides (Urry et.al. 1978d). The magnitude of this activation energy is too small to represent the melting or the formation of stable secondary structures, since the activation energies for these systems would be expected to have values in the range of 15 to 20 kcal/mole (Fraser and McCrae 1973). It is more plausible that this value, of 1.6 kcal/mole, is representative of the torsional energy barriers about the  $C^\alpha$ --CO and  $C^\alpha$ --N bonds of the polypeptide backbone. This explanation is consistent with the theoretical analysis of random polypeptides presented by Brant and Flory (1965 a and b).

(e) Non-Gaussian properties of the elastin network

The non-Gaussian properties of the elastin network were analyzed graphically by comparing the experimental results to the curves generated according to equations 7.13 to 7.15 for various values of  $s$ , which is the number of random links between cross-links. Figure 7.5,a and 7.5,b, presents this evaluation for the non-Gaussian mechanical and photoelastic properties of polymer networks. In each case the solid lines represent the experimental data obtained for single elastin fibres, reduced to the unswollen form according to equations 7.16 to 7.19. These lines were obtained by a least squares fit of the elastin data to regressions upto a tenth degree polynomial. The mechanical and photoelastic data were found to

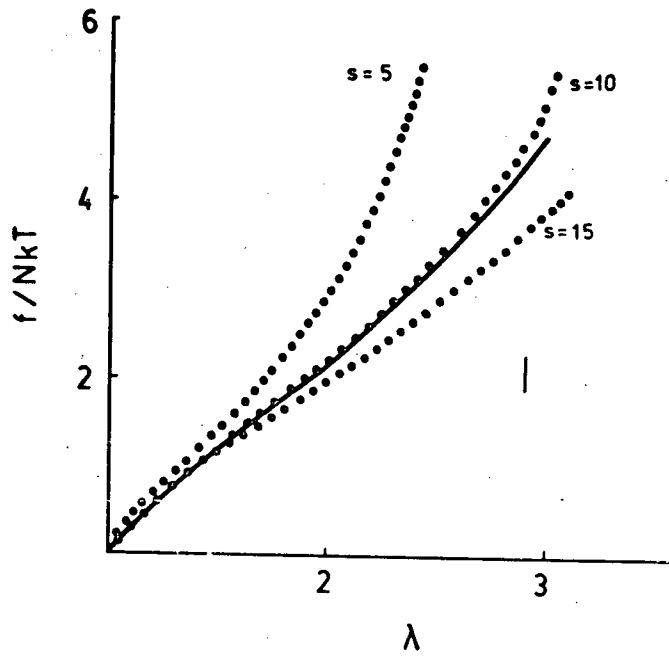
Figure.7.5: Non-Gaussian properties of the elastin network.

(A) Analysis of the non-Gaussian mechanical properties. The theoretical curves (open circles) were generated by evaluating equation 7.13 for various values of  $s$ . The filled circles represent the elastin data fit to a seventh degree polynomial:  
 $y = -0.15 \times 10^9 + 0.62 \times 10^9 x - 0.11 \times 10^{10} x^2 + 0.11 \times 10^{10} x^3 - 0.65 \times 10^9 x^4 + 0.22 \times 10^9 x^5 - 0.41 \times 10^8 x^6 + 0.32 \times 10^7 x^7$ . The solid vertical bar represents  $\pm$  standard deviation.

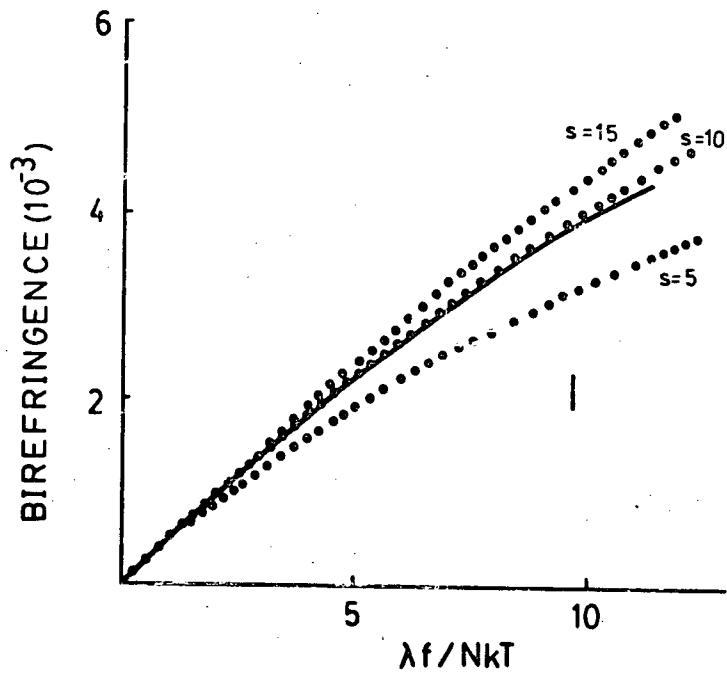
(B) Analysis of the non-Gaussian photoelastic properties. The theoretical curves (open circles) were generated by evaluating equations 7.14 and 7.15 for various values of  $s$ , using  $N = 1.0 \times 10^{28}$  chains/m<sup>3</sup> and  $(\alpha_1, -\alpha_2) = 2.84 \times 10^{-30}$  m<sup>3</sup>. The filled circles represent the elastin data fit to a fourth degree polynomial:  
 $y = 0.33 \times 10^{-3} + 0.82 \times 10^{-9} x + 0.36 \times 10^{-15} x^2 - 0.2 \times 10^{-21} x^3 + 0.26 \times 10^{-28} x^4$ . The solid vertical bar represents  $\pm$  standard deviation.

Figure 7.5.

A



B



have the best fit to seventh and fourth degree polynomials respectively (see legend for figure 7.5). The graphical evaluation in both cases yields a value of approximately 10, for the number of random links,  $s$ , between cross-links.

As indicated above, the value of the elastic modulus,  $G$ , is consistent with a molecular weight between cross-links of 6,000 to 7,100 g/mole. Since the average residue weight for elastin is about 84.5 g/mole (Sandberg 1976), this amounts to 71 to 84 amino acid residues between cross-links. Furthermore, since the analysis of the non-Gaussian behaviour indicated that 10 random links were present between cross-links, dividing the number of amino acid residues between cross-links by 10 gives a value of 7.1 to 8.4 amino acids per random link. That is, it takes about 7 to 8 amino acid residues to exhibit the properties of the statistical, freely rotating links which form the basis of the kinetic theory relationships. The validity of these numbers obtained from the properties of the elastin network will be evaluated in the next chapter.

### E. Conclusions

This chapter has presented convincing evidence that the properties of the elastin network are best described in terms of the kinetic theory relationships derived for entropy elastomers. Furthermore, since these theories of rubber elasticity are based on an assumption of a random network conformation, it is reasonable to state that the protein chains which make up the elastin fibres are themselves devoid

of any stable secondary structures. This conclusion is in agreement with the results of birefringence (Aaron and Gosline 1980) and nuclear magnetic resonance studies (Fleming et.al. 1980, Aaron et.al. 1980) of the elastin network. The evaluation of the activation energy for the network 'restrictions' indicates that, under normal conditions, the  $C^\alpha$ --CO and the  $C^\alpha$ --N torsional angles are the major determinants of protein random-coil dimensions, as proposed previously (Schimmel and Flory 1968, Miller and Goebel 1968).

## Chapter.VIII. A PREDICTIVE TEST FOR ELASTIN CONFORMATION

### A. Introduction

Having obtained some 'concrete' numbers from the analysis of the physical properties of elastin, according to the kinetic theory of rubber elasticity, it is tempting to extrapolate from the characteristics of the elastin protein to other proteins in the random coil conformation. In order to do so one must first define the 'characteristic variable' which is to be predicted using the experimentally obtained values (and manipulations of these values), and ideally one must then stumble across some literature that has 'observed values' for the same variable, preferably attained through a different technique of experimental analysis. The results of this comparison should allow one to evaluate the assumption of a random conformation for elastin.

### B. Characterization of Random Proteins

#### (a) The measurable dimension

If a person is given an object and asked to describe it's physical shape, he will usually respond with the appropriate adjective such as round, square, oblong, weird! etc. If asked to be specific, this person might then proceed to describe their dimensions in the usual terms like length, width, radius, axial ratio, but he probably will not make any progress with that 'weird' object. Random coiled polymers

would be classified by this frustrated person as belonging to the 'weird' category. In practice however, there is a dimension that can be utilized to describe a random coiled polymer. This dimension, as you know, is referred to as the root-mean-square (r.m.s.) distance,  $\langle r^2 \rangle^{1/2}$ . But what does this r.m.s. value represent in terms of a measurable dimension?

Consider an ideal gas molecule located at the origin at time  $t=0$ . Suppose that the movement of the molecule can occur in any direction (randomly) in discrete steps of length,  $l$ . If the molecule moves  $a$  steps per second, then after  $b$  seconds it will have moved  $s$  number of steps. Where  $s=ab$ . Re-evaluation of the molecules position after  $s$  steps will show that it has been displaced away from the origin by a distance characterized by the linear vector between the origin and this new position. This vector represents the end-to-end distance,  $\langle r \rangle$  (figure 8.1a). In transforming this analogy to real polymers one has to simply replace the spaces between two successive positions of the gas molecules by an 'ideal' link, made up of a number of chemical bonds, of length,  $l$ . This allows it's characterization by the measurable dimension  $\langle r \rangle$ , which now represents the distance between the two ends of the molecule (figure 8.1b).

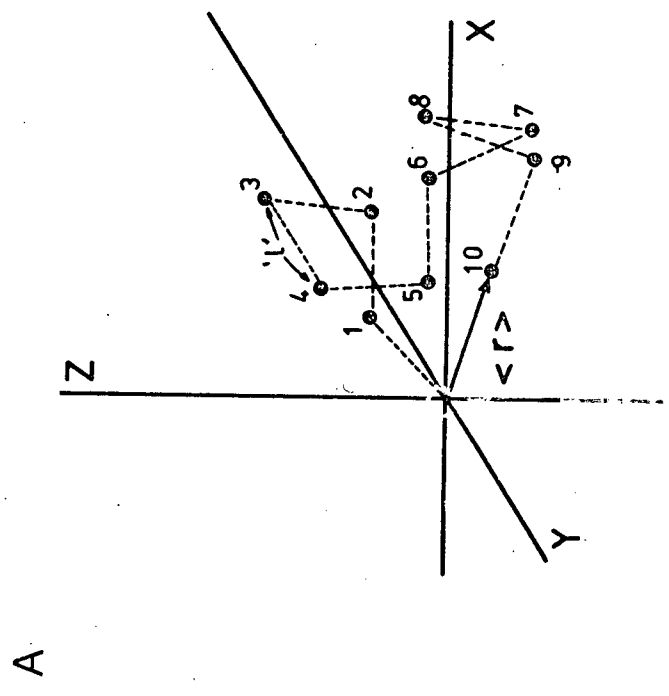
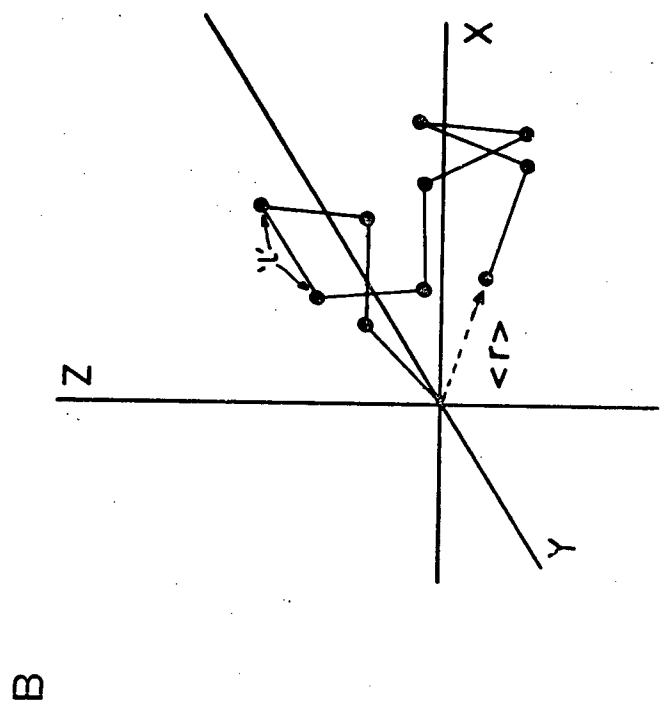
The clue, as to the conceptual framework that forms the analysis of 'random walk' systems, can be found in the definition of the adjective 'random'. The Merriam-Webster dictionary describes the word random in two ways. One is to

Figure.8.1: The random walk.

(A) A 10 step random walk for a gas molecule starting at the origin and moving in distinct steps of length  $l$ .  $\langle r \rangle$  is the end-to-end distance.

(B) Replacing the distance between two successive positions by an 'ideal' link of length  $l$ , allows the extension of the Gaussian derivations for random walks to real polymers.

Figure.8.1.



think of random as being haphazard. The other is to think of it in terms of chance. It is this second definition of random that describes it in terms of a 'probability of observing an occurrence', which allows a practical method for describing the random walk. Evaluation of the problem through Gaussian statistics yields a fairly simple result which characterizes the end-to-end distance,  $\langle r^2 \rangle^{1/2}$ , in terms of the number of links,  $s$ , and the length of the link,  $l$ , as (Flory 1953):

$$\langle r^2 \rangle = sl^2 \dots \dots 8.1$$

(b) Accounting for the non-ideality

The above derivations for random coils assumes an ideal system. This obviously does not occur in real polymers, which because of their finite volume, will display an 'excluded volume effect'. This essentially states that no two real molecules can occupy the same volume element. The result of this effect is to expand the domain of the random coil by a factor  $\alpha$ , which accounts for the non-ideality of the system (i.e. polymer-polymer interactions, and polymer-solvent interactions):

$$\langle r^2 \rangle^{1/2} = \alpha \langle r_0^2 \rangle^{1/2} \dots \dots 8.2$$

where  $r_0$  and  $r$  are the unperturbed and actual dimensions of the molecule respectively. In the case of a theta solvent, where the non-ideality of the polymer-solvent interactions balances out the non-ideality of the polymer-polymer interactions,  $\alpha$  is equal to unity, and the above equation

reduces to equation 8.1.

### C. R.M.S. Values From Viscosity

#### (a) Viscosity of random coils

There are present in the literature a vast number of papers that deal with the viscosity of random hydrocarbon polymers (Flory 1949, Fox et.al. 1951, Kurata et.al. 1960, Kurata and Stockmayer 1963, Stockmayer and Fixman 1963). These studies have developed theoretical relationships and have obtained experimental parameters for the prediction of random-coil dimensions. Only recently have there been any attempts made to extend these viscosity relationships to the study of random protein polymers (Brant and Flory 1965, a and b, Tanford et.al. 1966, 1967, Reisner and Rowe 1969), and the results indicate the applicability of this type of approach to proteins.

Tanford et.al. (1966) have published studies on the viscosity of proteins in 6M GuHCl, where these polymers behave as random coils. Applying the appropriate relationships, these authors have evaluated the r.m.s. distances for a number of proteins. This is fortunate since, as mentioned before, it will allow a comparison for the predicted values obtained from the properties of the elastin protein. However, in order to ensure that this comparison takes place between equivalent variables, a number of corrections must be made to the published values.

(b) Correction of viscosity values

The equation that describes the molecular weight dependence of the intrinsic viscosity for linear polymers takes the form (Yang 1961):

$$[\eta]_0 = KM^\lambda \dots\dots 8.3$$

Where  $[\eta]_0$  is the intrinsic viscosity,  $K$  is an empirical constant for a given polymer-solvent system,  $M$  is the molecular weight of the polymer (or the number of residues in a protein), and  $\lambda$  is the exponent that describes the polymer conformation, having a value of 0.5 for random polymers in a theta solvent, and a value greater than 1 for rod-like proteins (Tanford 1961). In the case of proteins, it is convenient to deal with them in terms of the number of residues as opposed to the actual molecular weight, since different proteins have different average residue weights. Doing this, Tanford et.al. (1966, 1967) assigned a values of 0.684 and 0.67 for  $K$  and  $\lambda$  respectively. The value of 0.67 obtained for  $\lambda$  indicates that guanidine hydrochloride is a good solvent for proteins. This should result in the expansion of the random-coil domain and, hence, it is necessary that the expansion coefficient,  $\alpha$ , be evaluated and corrected for before making the comparison to the predictions from the elastin network.

I have chosen to do this by manipulating the viscosity data by an alternate analysis. The intrinsic viscosity of random-coils can be described by (Kurata and Stockmayer 1963):

$$[\eta] = KM^{1/2} \alpha^3 \dots \dots \dots 8.4$$

In this formulation  $\chi$  is taken to be equal to 0.5, and any deviations due to solvent effects is accounted for in the expansion coefficient  $\alpha$ . This forms the basis for the evaluation of  $\alpha$  according to:

$$\alpha^3 = [\eta] / [\eta]_0 \dots \dots \dots 8.5$$

Hence if one can evaluate  $K$ , it is possible to obtain a theoretical value for  $[\eta]_0$  by assuming  $\alpha = 1$ . One can then utilize the actual value measured for the intrinsic viscosity,  $[\eta]$ , the calculated value for  $[\eta]_0$ , and equation 8.5, to get a value for  $\alpha$ .

The evaluation of  $K$  for the Tanford data was done by the method of Stockmayer and Fixman (1963), which gave a value of 1.3 cc/gm for this parameter (see appendix 3). The results of the subsequent calculations are presented in table 8.1, along with the corrected values for the end-to-end distance obtained by Tanford et.al. (1966, 1967). It should be mentioned that the high values obtained for the expansion coefficient,  $\alpha$ , are consistent with 6molar  $\text{GuHCl}$  being a good solvent. Furthermore, the molecular weight dependence of  $\alpha$  is also consistent with the results expected from the theoretical treatment for random polymers (Flory 1953).

#### D. Predictions From The Elastin Network

##### (a) Calculation of $s$

Equation 8.1 states that if the number of random links,

Table.8.1: Predictions for random-coil proteins.

PREDICTIONS FOR THE DIMENSIONS OF RANDOM-COIL PROTEINS.

number of residues	observed values <sup>a</sup>			predicted $\langle r^2 \rangle^{1/2}_A^0$		ratio		
	$\langle r^2 \rangle^{1/2}_A^0$	expansion coefficient: $\alpha$	corrected $\langle r^2 \rangle^{1/2}_A^0$	b	c	$\frac{\langle r^2 \rangle^{1/2}_b}{\langle r^2 \rangle^{1/2}_c}$	$\frac{\langle r^2 \rangle^{1/2}_b}{\langle r^2 \rangle^{1/2}_{obs.}}$	
insulin	26	44	0.97	45	38	41	.84	.92
ribonuclease	124	101	1.03	98	83	90	.85	.92
hemoglobin	144	112	1.07	106	89	97	.84	.92
myoglobin	153	120	1.09	110	92	100	.84	.91
$\beta$ -lactoglobulin	162	126	1.11	113	95	103	.84	.91
chymotrypsinogen	242	148	1.10	134	116	126	.87	.94
aldolase	365	189	1.12	168	142	154	.85	.92
serum albumin	627	258	1.17	220	166	202	.85	.92
thyroglobulin	1500	401	1.18	341	288	313	.85	.92
myosin	1790	443	1.19	372	314	342	.84	.92

<sup>a</sup>data from Tanford et.al 1966, 1967.

<sup>b</sup>for 7aa/random link.

<sup>c</sup>for 8aa/random link.

and the length of the link is known, then, it is possible to predict a value for the end-to-end distance,  $\langle r^2 \rangle^{1/2}$ . The analysis of the properties of the elastin network indicated that between 7 and 8 amino acid residues are required to give a 'functional' random link. Hence, it is possible to obtain a value of  $s$  for any given protein by dividing the the number of residues in the protein by the number of amino acid residues per link ( i.e. 7 to 8). In trying to evaluate a value for the length of the link,  $l$ , I have chosen a qualitative approach which is based on the theoretical derivations for the dimensions of random proteins.

#### (b) Calculation of $l$

Flory and his co-workers have dealt with the theoretical evaluation of random proteins and have evaluated the energetics of random protein dimensions, which usually resulted in energy minima for bond angles at  $\psi=270$ ,  $\phi=120$  (Schimmel and Flory 1968, Miller et.al. 1967, Miller and Goebel 1968). Although the actual bond angles present in random polymers will be distributed over a range of values, the value at the energetic minimum should reflect an 'average' for the distribution. I have therefore used this value ( $\psi=270$ ,  $\phi=120$ ) to calculate the displacement along the random link using the relationships provided by Schellman and Schellman (1963). Doing this I obtained values of  $19.8\text{\AA}$  and  $23.4\text{\AA}$  for the length,  $l$ , of a random link made up of 7 and 8 amino acids respectively, which allowed me to predict values

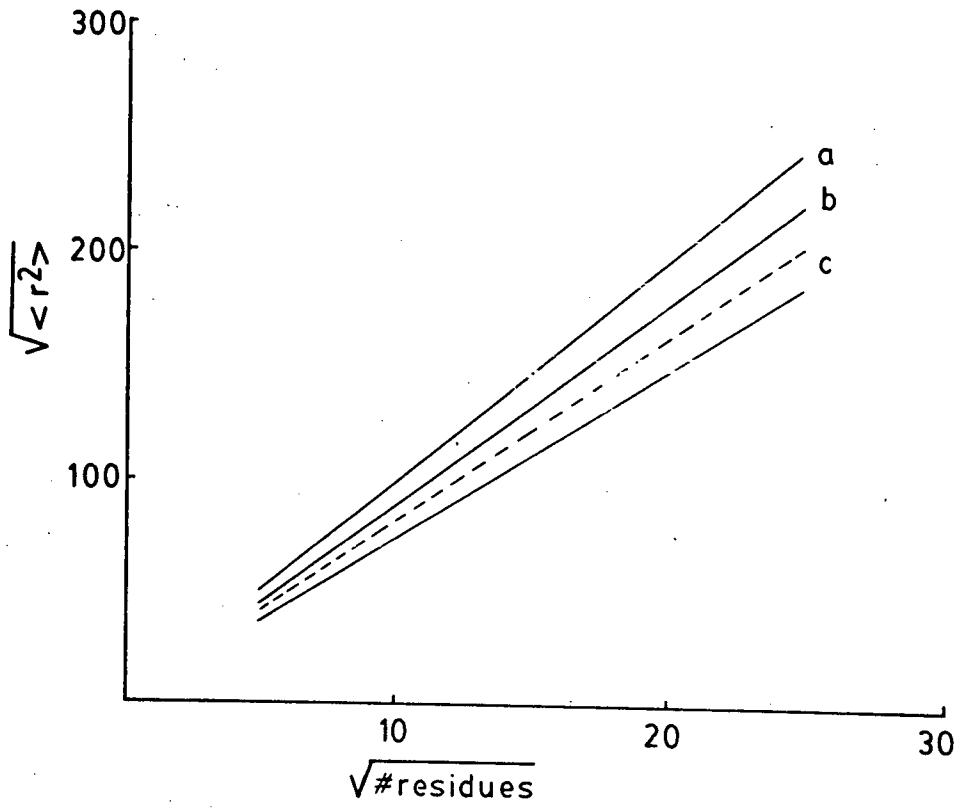
of r.m.s. distances for various proteins using equation 8.1 and a value of 1 for  $\alpha$ . This should permit a valid comparison to the observed values (Tanford et.al. 1966, 1967) since they have been corrected for the expansion coefficient as described above.

### E. Discussion and Conclusions

The results, which are summarized in table 8.1 and figure 8.3, indicate that the predictions obtained from the properties of the elastin network are in excellent agreement, within limits of the uncertainties inherent in their calculation, with both the theoretical expectations from the statistical mechanical treatment of peptide conformation (Miller and Goebel 1968) (figure 8.3,a) and the experimental observations (figure 8.3,b) on random coiled proteins. The fact that the predictions from the elastin data are lower than the expected values can be reasonably attributed to the high glycine content of this protein. Glycine makes up almost a third of the amino acid content of elastin (Sandberg 1976), and one would expect this to result in a reduction of the restrictions on the protein chain mobilities in the network. This would lower the number of amino acid residues required to give a random link, as compared to most proteins which contain lesser amounts of glycine. It is reasonable to expect that more than 8 amino acid residues would be required to give a random link for proteins which do not exhibit such extremes in amino acid composition as elastin. This would have the effect

Figure.8.2: Predictions for the dimensions of random-coil protein.

Root-mean-square distance for various proteins as a function of the number of amino acid residues. (a) Theoretical predictions from Miller and Goebel 1968. (b) Experimentally obtained values from Tanford et.al. 1966 and 1967, corrected for non-ideality (see Table 8.1). (c) Predictions from the elastin system according to equation 8.1: (solid line) for 7aa/random link, (broken line) for 8aa/random link.

Figure. 8.2.

of increasing the value of  $l$ , which is the length of the random link, resulting in even closer agreement between the predicted and observed values.

Chapter. IX. CONCLUSIONS.

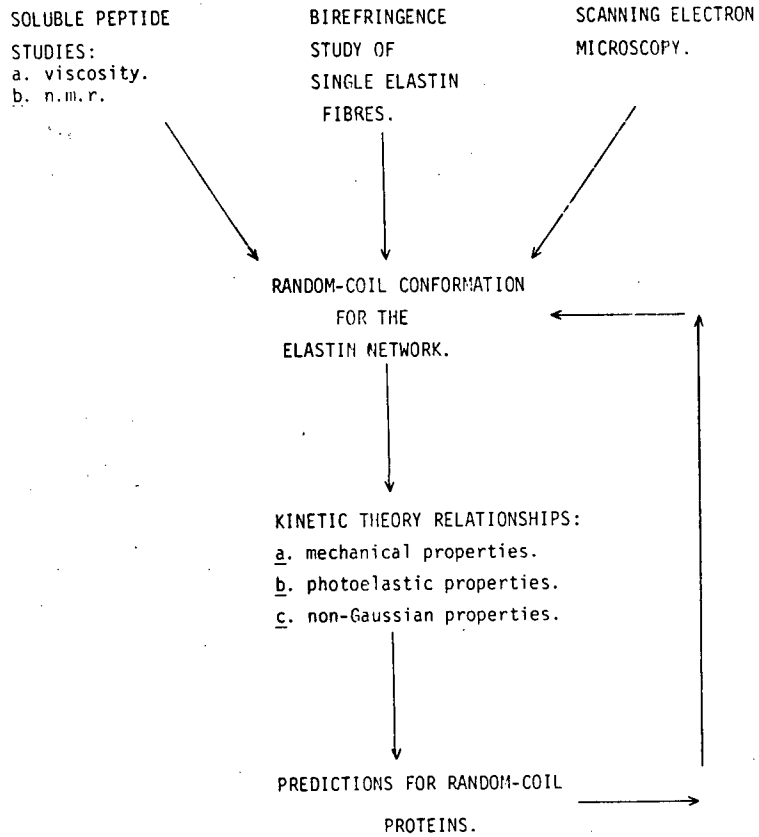
Unlike most of the biopolymers known to us, there are a number of proteins that fulfill their biological roles by being random. The elastomers Resilin, Abductin and as shown in this thesis, Elastin, belong to this group of biomolecules. The biological function performed by these elastic proteins is to antagonize the movements of muscles. Muscles can only contract, and because of this there is a need for an opposing mechanism that can restore the muscle to its functional state after each contraction cycle. This antagonism can be provided by other muscles as in skeletal movements, hydrostatic systems as in many marine organisms, and passive elastic elements. The elastin proteins probably evolved in response to this last need. Furthermore, muscles are restricted in their performance by their metabolic needs, and are generally characterized by high turnover. On the other hand, elastomers being passive mechanical components, are not restricted by metabolic needs, and due to their low turnover the only metabolic cost to the organism is that of synthesizing it in the first place. Hence, it seems plausible that the advantages of passive elasticity are realized in the metabolic savings to the animal. This describes their function. But as stated in the introduction to this thesis, simply stating that proteins like elastin are rubber-like does not tell us about the functioning mechanism. Over the years, several theories of elasticity have been proposed in an attempt to characterize the the elastic mechanism but only one theory, The Kinetic Theory of Rubber

Elasticity, has been able to account for and, in most cases predict, the macroscopic properties of elastomeric materials.

Like most theoretical frameworks that are based on mathematical derivations the kinetic theory makes some very convenient and crucial assumptions, the most important of which is that of a random conformation. It is this assumption which has prevented its general acceptance by protein chemists. The current thought in biochemistry and biopolymer research is summarized by the statement---"if it has a primary sequence it must have a tertiary structure". Although this statement might be valid for proteins in general, it does not account for the exceptional class of protein elastomers. On the basis of this statement a number of people have stated that the approach adopted by the kinetic theory is unacceptable since, in their minds it invokes the concept of 'phantom' chains and 'ideal' links. This bitter pill of random conformation might be easier to swallow if the phantom chains are restated in terms of real polymers to whom all conformations ARE EQUALLY ACCESSIBLE (WHICH IS THE SAME AS SAYING THAT THERE IS NO ONE STABLE conformation). This allows the mathematics of random walks to be applied to real polymer networks that are devoid of stable secondary structures.

In using the kinetic theory relationships to explain the macroscopic properties of single elastin fibres, I have also had to assume a random network conformation for elastin. This assumption was tested using different methods of investigation (see summary figure, 9.1). Viscosity experiments were used to

Figure.9.1: Summary figure for the thesis.

Figure.9.1.SUMMARY.

evaluate the shape of the soluble elastin. These studies did not support the presence of any rod-like structures. Polarized microscopy was used to test for molecular organization. The results indicated a random conformation. Nuclear magnetic resonance studies were used to investigate the mobility of the elastin network. The analysis showed that the elastin network is characterized by rapid motions. Assimilating these results, one should be able to state quite confidently that the assumption of a random network for elastin is justified. The fact that elastin can serve as a model for random-coil proteins offers further support in favour of this assumption. In conclusion it seems that the kinetic theory of rubber elasticity provides a valid theoretical framework for the analysis of the entropic elastomeric properties of the rubber-like proteins which, in general are characterized by random conformations.

APPENDIX.I: Thermoelasticity(A) Thermodynamic Relationships

Since an elastic system, in its functional state, is involved in the storage and dissipation of mechanical energy, it is possible to evaluate the basis of this mechanism by using thermodynamic relationships.

According to the first law of thermodynamics, energy,  $E$ , can be converted from one form to another, but it cannot be created or destroyed. Hence when considering an elastic sample and its surroundings, for a given deformation,  $dE$  is equal to zero. If, however, one considers only the sample, for a reversible process one can write:

$$dE=dq+dw.....A.1.1$$

where  $q$  represents the heat evolved by the process, and  $w$  represents the work. Both  $dq$  and  $dw$  are considered to be positive when heat flows from the sample to the surroundings and work is done by the sample on the surroundings, respectively.

For a reversible process, the second law of thermodynamics defines the change in entropy,  $S$ , in terms of the heat and the absolute temperature,  $T$ , according to:

$$dS=dq/T.....A.1.2$$

Solving for  $dq$ , and substituting into equation A.1.1, one gets:

$$dE=TdS+dw.....A.1.3$$

Using these equations it is possible to define a state function,

referred to as the Helmholtz free energy,  $F$ , as:

$$F = E - TS \dots\dots\dots A.1.4$$

At constant temperature, pressure, and volume, this equation takes the form:

$$dF = dE - TdS \dots\dots\dots A.1.5$$

Substituting equation A.1.3 into the above gives:

$$dF = dw \dots\dots\dots A.1.6$$

Utilizing equations A.1.2 and A.1.6 one can write equation A.1.5 as:

$$dw = dE - dq \dots\dots\dots A.1.7$$

This equation forms the basis of the thermodynamic analysis of reversible systems, and it is possible, by means of thermodynamic book-keeping, to evaluate the various components of a given process. In the particular case of a materials mechanical response, it allows one to determine the magnitudes of the contribution to the total retractive force,  $f$ , from the energy,  $f_e$ , and the entropy,  $f_s$ , components:

$$f = f_e + f_s \dots\dots\dots A.1.8$$

### (B) The Thermodynamic Experiment

The thermodynamic experiment can be carried out in two ways:

1. The sample can be immersed in a diluent, and keeping it at a fixed extension, one can follow the change in the retractive force,  $f$ , as a function of temperature. The data can then be evaluated according to:

$$f = f_e + T \left( \frac{df}{dT} \right) \dots \dots \dots A.1.9$$

2. The sample, in a diluent, is extended at a constant temperature, and the heat released, along with the work ( i.e. the area under the force extension graph) is monitored. The energy component is then evaluated according to equation A.1.7.

For the sake of convenience, the two methods outlined above will be referred to as constant strain and constant temperature thermoelastic experiments, respectively.

### (C) Thermoelasticity of Kinetic Elastomers

With reference to the elasticity of materials, if the mechanism responsible for the retractive force consists of a system that involves the deformation of a rigid lattice (as in the case of metals, collagen, keratin, and silk), where most of the energy is stored in the alteration of bond lengths and orbitals, the restoring force arises from a change in the internal energy component as indicated by the magnitude of energy component,  $f_e$ , obtained from a thermodynamic experiment ( $f_e/f=1$ ).

In the case of natural rubbers, however, it has been shown that the strain energy is stored as a decrease in the conformational entropy of the system. These materials exhibit a  $f_s/f$  ratio of approximately one, with the  $f_e$  term being small. Materials of this type are thought to conform to the kinetic theory of rubber elasticity, which requires a random, kinetically agitated conformation at the molecular level

(Treloar 1975).

APPENDIX.II: PREPARATION OF SOLUBLE ELASTIN BY PHOTOLYSIS.A. Introduction

Recently there has been a lot of interest in the physical properties and the primary structure of the precursor protein, tropoelastin. This research has created a need for a convenient method to isolate the tropoelastin molecule which, upto now, has been isolated from lathyritic animals. The use of a biological source carries with it the usual problems of high expense and low productivity. A paper by Foster et.al. (1975), where they used 2000 chicks to get 55gms of wet tissue which in turn yielded 35mg of tropoelastin, illustrates this point quite clearly. Hence it seemed valuable to develop a procedure to isolate the precursor protein, from the freely available, insoluble elastin by chemical means.

This chapter deals with a method that utilizes the absorption characteristics of the elastin cross-links to induce their lysis and the subsequent release of the soluble peptides. Since this procedure is a reversal of the biological pathway that results in formation of the insoluble elastin in the first place (by the linking of tropoelastin into an insoluble network), it should hopefully yield a monomeric peptide that represents the precursor protein.

B. Methodology(a) Rationale

The rationale for the use of photolysis to cleave the cross-links of elastin is based on a paper by Joussot-Dubien and Houdard (1968) who studied the cleavage of pyridinium rings by ultra-violet radiation. The relevance to the elastin cross-links lies in the fact that the (iso)desmosines are tetra-substituted pyridinium rings, as demonstrated by Thomas *et.al.* (1963). This aspect of elastin chemistry led Baurain *et.al.* (1976, 1977) to attempt the use of photolysis for the purpose of solubilizing fibrous elastin. These authors were able to demonstrate a cleavage of the (iso)desmosine cross-links, but they could not isolate any soluble peptides from their preparations. The methodology presented in this chapter utilizes an additional step which results in the release of soluble peptides from the photolysed elastin.

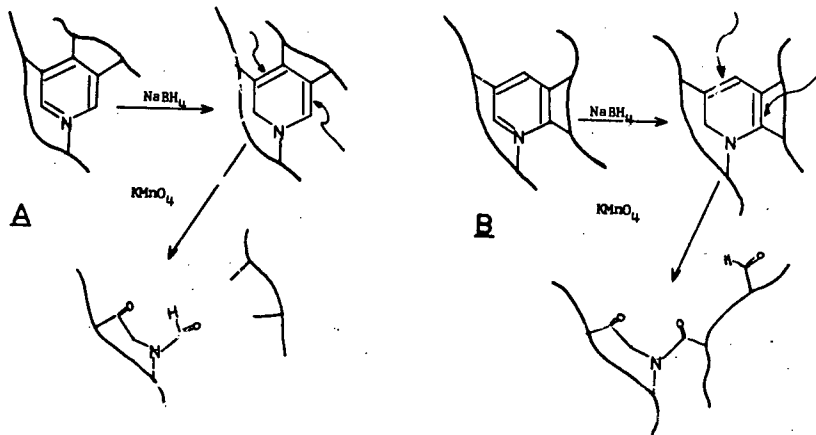
The hypothetical reaction pathway for this method is shown in figure A.2.1 (as based on the the work of Joussot-Dubien 1968 and Baurain 1976). The irradiation of the cross-links with ultra-violet light (275-285nm) results in the cleavage of the single bond between the nitrogen and carbon<sup>6</sup> (figure A.2.1). This product is unstable at low pH and/or high temperature and can be broken down (figure A.2.1). The next step involves the cleavage of the unsaturated carbon bonds, using standard oxidative techniques, to give soluble peptides. This pathway is essentially the same for both the desmosine and iso-desmosine as outlined in figure A.2.1.

The obvious question to ask at this time is: why not just oxidize the unsaturated cross-links without having to bother

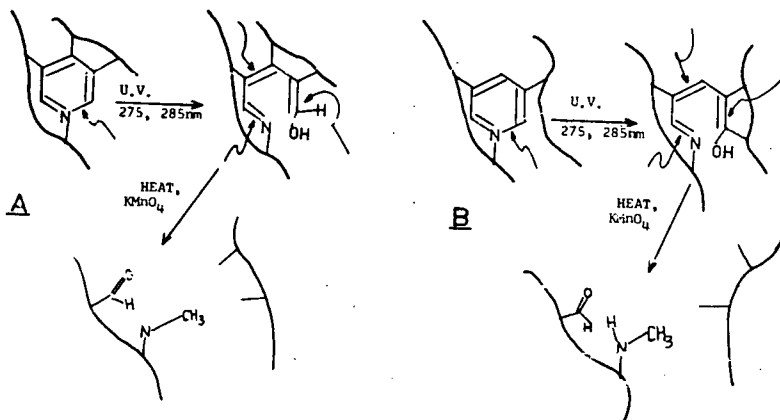
Figure.A.2.1: Photolysis of elastin.  
(I) oxidation pathway for elastin.  
(II) photolysis of elastin followed by oxidation.  
(A: pathway for desmosines, E: pathway for isodesmosines.)

Figure A. 2. 1.

I



II



with the photolysis? The reason for this is demonstrated by the pathway outlined in figure A.2.1. Reduction of the desmosine by dihydroborate followed by potassium permanganate oxidation results in the separation of the two cross-linked peptides (figure A.2.1). The same procedure, if utilized on the iso-desmosines, does not give satisfactory results, since the movement of the cross-linking position from carbon<sup>4</sup> to carbon<sup>6</sup> prevents the release of the two peptides. As the tropoelastin molecule is linked at about ten points along its length (Gray et.al. 1973), if any of these cross-links were to be an iso-desmosine, the peptides would be retained in the insoluble network. It is this problem which is circumvented by the photolysis, allowing the combination of the two procedures to give soluble peptides.

#### (b) Procedure

Elastin from ligament nuchae was purified by extraction with 0.1N NaOH at 100°C for 45 minutes (Lansing 1952). The resulting material was dried and ground to a fine powder and washed with copious quantities of boiling distilled water. 500mg of this powdered elastin was hydrated overnight in 200ml of distilled water that had been adjusted to pH4.4 with 2N HCl. This solution was photolysed using an immersion type ultraviolet lamp (Hanovia 450W, medium pressure, u.v. Model). A Corex filter was used to remove wavelengths below 270nm to prevent the photolysis of peptide bonds and, at the same time, provide adequate irradiation for the cleavage of the cross-

links which absorb at 275-285nm (Thomas et.al. 1963).

The samples were photolysed for 6 hours, at the end of which the solid elastin was collected by centrifugation. It was then stirred into a periodate-permanganate oxidation solution (Lemieux 1955) at 48°C for 24 hours. The mixture was centrifuged and the supernatant was carefully aspirated. The precipitate, which contained mostly insoluble elastin was discarded. The supernatant was dialyzed against running tap water for 24 hours, followed by dialysis against 4L of distilled water (1L X 24 hrs.) and lyophilized. The resulting peptides had a clean white appearance. A control consisting of the oxidation step without photolysis was also conducted.

### C. Results and Discussion

#### (a) Yield

The amount of peptide recovered after the last lyophilization step was about 40mg/gm of original dry weight. Although this is a substantial yield as compared to the biological sources (Sykes and Partridge 1974), it is probably not the optimum yield for this procedure. Examination of the oxidative step (in retrospect) reveals a very crucial blunder. Specifically, soluble elastin peptides such as tropoelastin and alpha-elastin, undergo an inverse temperature transition at 37°C, which upon standing for 12 or more hours forms an irreversible precipitate. As is clear from the methods section, the oxidative step was carried out at 45°C for 24

hours, and it is possible that a major part of the soluble elastins prepared in this manner precipitated out and were lost during the separation of the insoluble elastin from the supernatant, which contained the remainder of the soluble proteins. Oxidation of the photolysed elastin at a lower temperature for longer periods should result in better yields.

The oxidation of unphotolysed elastin gave no detectable results.

#### (b) Characterization of the soluble peptides

Molecular weight determination of the peptides was performed on a 15% polyacrylamide-SDS gel. The results are presented in figure A.2.2. Much to my surprise, and delight, there appeared to be only one protein band at 66,000 molecular weight. This could mean that (a) the procedure yields a homogeneous peptide or (b) that there are other peptides released in small quantities that could not be detected by the crude procedures used in this initial characterization. This aspect has not been investigated fully.

Although the amino acid analyses has not been done, it is possible to make some predictions based on the work of Davril et.al. (1977). It is expected that the soluble protein should have a higher lysine content as compared to insoluble elastin, due to the liberation of a free lysine after the photolysis of the cross-links. In addition to this, one would expect to have a lower content of tyrosine due to their destruction at the wavelength used for the photolysis, which is in the range of

the absorption peak for this amino acid. The rest of the amino acids are not expected to be altered.

The branching characteristics of this peptide have not been studied as yet, but this deserves some mention here. If the peptide turns out to be a branched polymer, either due to incomplete photolysis or oxidation, then this method is not useful for the production of peptides, that can be more easily attained by other methods. But if this peptide turns out to be an unbranched linear polymer it might be interesting to speculate on the implications.

First, it could be possible that this peptide represents the precursor component of the insoluble elastin protein. Second, since the molecular weight of tropoelastin is about 72,000 as compared to the value of 66,000 obtained for the peptide in this study, it implies a post-translational modification of the tropoelastin protein before its incorporation into the insoluble state. This is supported by studies which report that enzyme inhibitors are necessary in the biological isolation procedure to obtain a 72,000 weight tropoelastin molecule (Foster et.al. 1975). In the absence of these inhibitors the resultant product has a molecular weight of 66,000 (Sandberg 1969) and has been shown to be missing a N-terminal peptide.

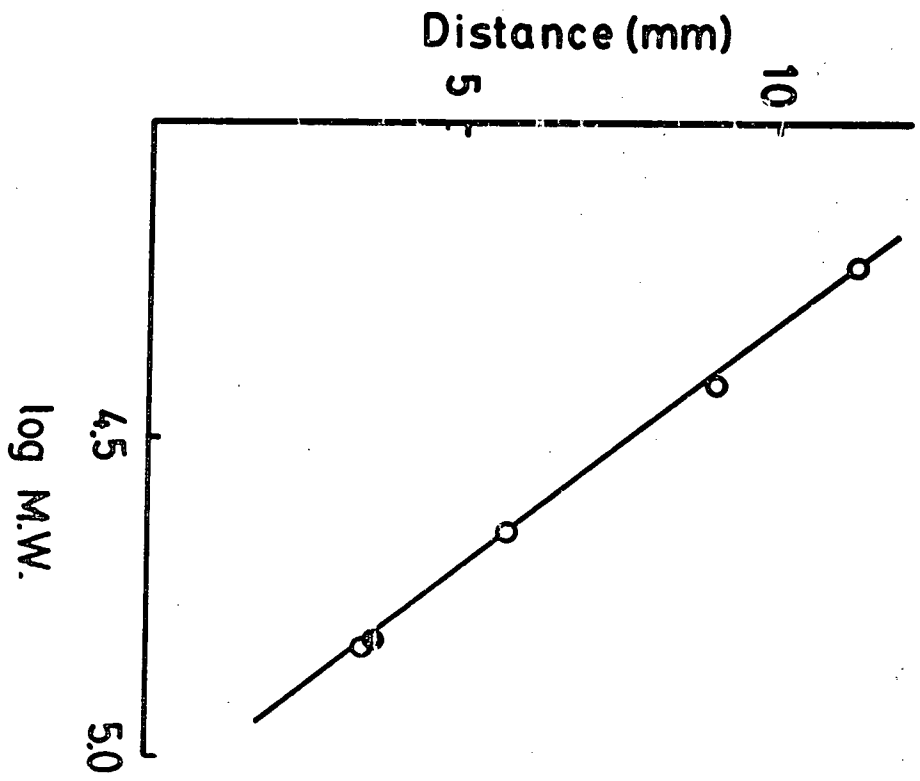
In conclusion, the high yield of soluble peptides and the possibility that they/it might turn out to be the precursor protein argues for the further development of this technique for the isolation of elastin fragments, to be followed up with

Figure.A.2.2: Molecular weight of photolysis peptides.

SDS-polyacrylimide gel electrophoresis results for the photolysis products:

- (o) molecular weight markers: Albumin (66,000), Ovalbumin (45,000), Trypsinogen (26,000), Beta-lactoglobulin (18,000), Lysozyme (14,000).  
(•) photolysis peptide.

Figure A.2.2.



further characterization of the soluble products.

Appendix.III: PREDICTIONS FOR TROPOLASTIN VISCOSITYA. The Relevant Equation

The molecular weight dependence for the intrinsic viscosity,  $[\eta]$ , of unbranched, random polymers, can be stated in terms of an empirical constant,  $K$ , and the number of residues,  $M$ , as (Stockmayer and Kurata 1963):

$$[\eta]_0 = KM^{1/2} \dots \dots \dots A.3.1$$

This equation applies to ideal polymers and polymers in theta-solvent systems. A more useful derivation of this equation provided by Stockmayer and Fixman (1963) allows the characterization of the viscosity in any solvent, and takes the form:

$$[\eta] = KM^{1/2} + 0.51\bar{\Phi}BM \dots \dots \dots A.3.2$$

where  $\bar{\Phi}$ , is a universal constant with a value of  $2.1 \times 10^{23}$  (c.g.s.) and  $B$  is defined according to:

$$B = \bar{v}^2 (1 - 2X) / VN \dots \dots \dots A.3.3$$

where  $\bar{v}$ , is the partial specific volume of the polymer,  $V$  is the molar volume of the solvent,  $N$  is Avogadro's number, and  $X$  is the Flory interaction parameter (Flory 1953).

B. Application to Tropoelastin

According to equation A.3.2, a plot of  $[\eta]/M^{1/2}$  versus  $M^{1/2}$ , should give a straight line with an intercept equal to  $K$ . This has been done for the data obtained for proteins (in a random coil conformation) by Tanford et.al. (1966, 1967) and was calculated to have a value of 1.3 cc/gm (figure A.3.1).

Figure.A.3.1: Viscosity of random-coil proteins.  
Plot of data from Tanford et.al. 1966, according to  
equation A.3.2.

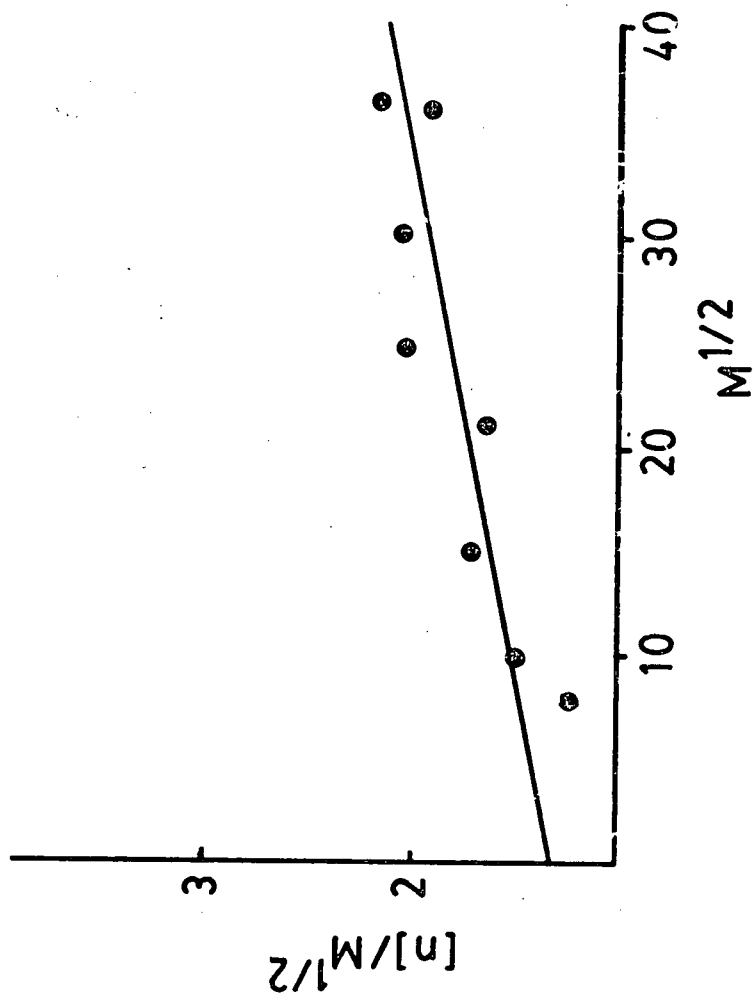
Figure.A.3.1.

Table.A.3.1: Prediction for tropoelastin viscosity.

## PREDICTIONS FOR TROPOELASTIN VISCOSITY.

$T^{\circ}\text{C}$	$\chi^*$	$B (10^{-26})$	$[\eta] \text{ cc/g}$
0	.699	-2.66	35.48
10	.786	-3.83	34.42
20	.875	-5.02	33.33
30	.943	-5.93	32.50
40	1.01	-6.80	31.71

\* from Cosline 1977.

What makes this manipulation useful is that it is possible to obtain  $X$  values for the elastin protein from studies of network swelling (Gosline 1978). Elastin decreases its volume with an increase in temperature and according to equation A.3.2 and A.3.3, this should lead to a decrease in  $B$  and a subsequent decrease in the intrinsic viscosity. These equations allow the prediction of the magnitude of this decrease in  $[\eta]$ . The results of the calculations for the intrinsic viscosity of tropoelastin in water, as a function of temperature, are presented in table A.3.1, using  $M$  equal to 850 (Sandberg 1976),  $X$  values taken from Gosline (1977) and  $\bar{v}$  equal to .725 (Partridge et.al. 1955). It should be interesting to compare the actual experimental results to these theoretical predictions in order to support a random coil conformation for the tropoelastin molecule.

Appendix.IV: EVALUATION OF PROTEIN CONFORMATION

In chapter 8 I have presented some values for the parameters that characterize random proteins. Being encouraged by their apparent generality, I have ventured to devise an empirical method for the evaluation of protein conformation.

Using the values of  $s$  and  $l$  (as presented in chapter 8) and equation 8.1 it should be possible to predict the end-to-end distance for any given protein made up of a given number of residues. From this value one can calculate the radius of gyration,  $R_g$  (figure A.4.1), for the random molecule according to (Tanford 1961):

$$R_g^2 = \langle r^2 \rangle / 6 \dots \dots \dots A.4.1$$

If the density of the protein is known, one can calculate the volume,  $v$ , of the single molecule:

$$v = (\text{molecular weight}) / (\text{density}) \cdot 6.02 \times 10^{23} \dots \dots \dots A.4.2$$

(although this analysis assumes that there is no hydration of the molecule, the hydrodynamic volume could be used in place of the volume given by equation A.4.2).

Using this value of volume one can calculate the dimensions and the radius of gyration for a number of shapes as follows. For rods of length  $l$ , the radius of gyration is given by (Tanford 1961):

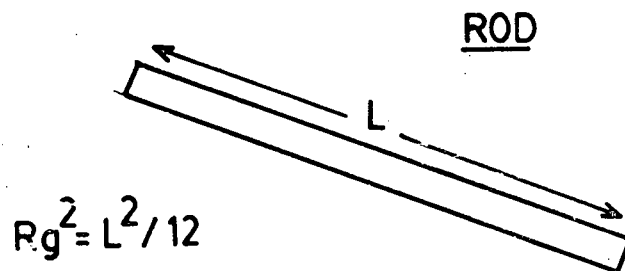
$$R_g^2 = l^2 / 12 \dots \dots \dots A.4.3$$

The length can be calculated from the volume for different diameter rods according to:

$$l = v / (\pi r^2) \dots \dots \dots A.4.4$$

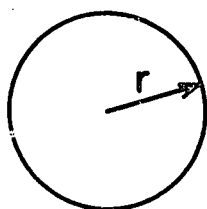
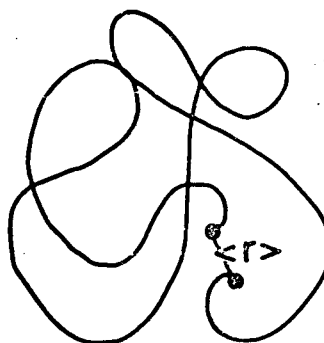
For spheres of radius,  $r$ , the radius of gyration is given

Figure.A.4.1: Radius of gyration for various shapes.  
Radius of gyration for rods, random-coils, and spheres, from Tanford 1961.

Figure. A.4.1.

RANDOM COIL

$$R_g^2 = \langle r^2 \rangle / 6$$

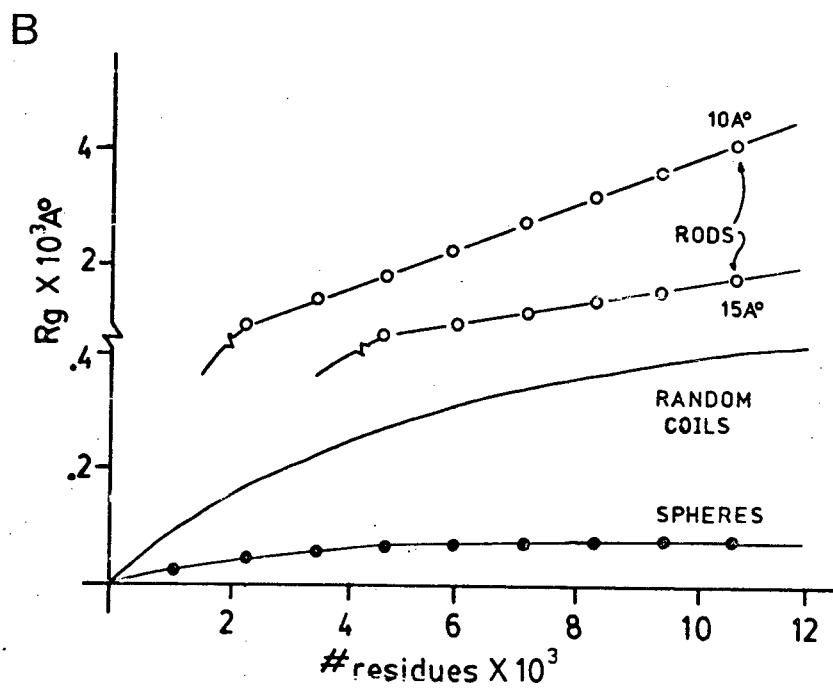
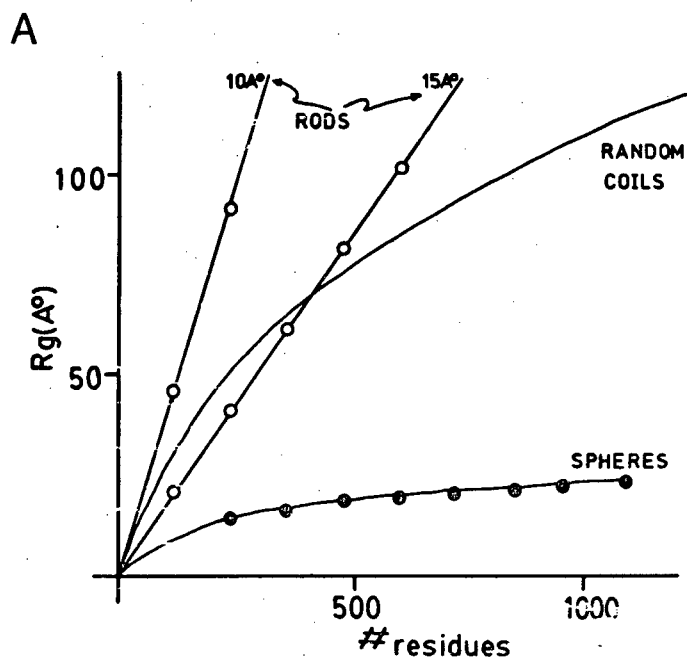


SPHERE

$$R_g^2 = r^2(3/5)$$

Figure.A.4.2: Evaluation of protein conformation.  
Plots of radius of gyration  $R_g$ , versus number of residues for different shapes:  
(A) low molecular weight range.  
(B) high molecular weight range.

Figure A.4.2.



by (Tanford 1961):

$$R_g^2 = (3/5)r^2 \dots \dots \dots A.4.5$$

and similarly  $r$  could be calculated from the volume and the following equation:

$$r^3 = (v) (3/4 \pi) \dots \dots \dots A.4.6$$

These above equations can be used to generate graphical relationships for the different shapes. This has been done in figure A.4.2a for the dependence of the radius of gyration on the number of residues.

Given a protein of known molecular weight and composition, a comparison of  $R_g$  values obtained from experiments such as light scattering (Timasheff and Townend 1970) to the standard curves should allow a rapid evaluation of the proteins conformational state. As is evident from figure A.4.2a, the uncertainties at the lower limit of molecular weight are high, but this type of analysis should provide reasonable answers for proteins of high molecular weight (figure A.4.2b).

Appendix.V: DETERMINATION OF SOLVENT EFFECTS ON RANDOM COILS

A similar approach as the one presented above, could be used to evaluate the effects of solvents on proteins that are known to be in the random coil conformation. One can predict  $R_g$  as a function of the number of residues from equation 8.1 and A.4.1, and generate standard curves for different values of the expansion factor,  $\alpha$  :

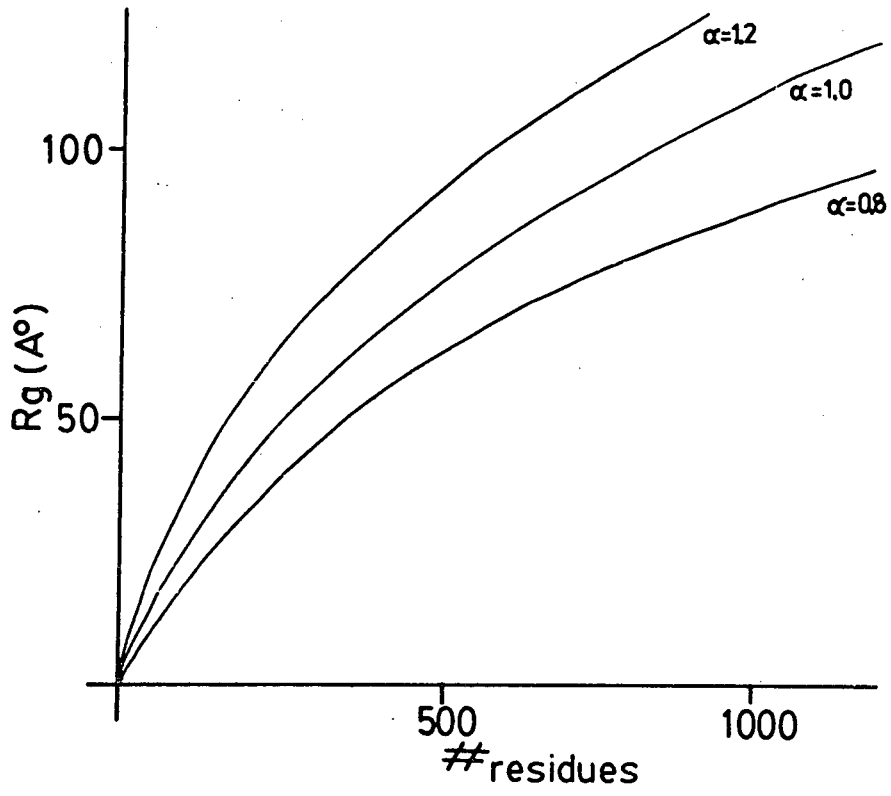
$$R_g^2 = \alpha^2 R_{g0}^2 \dots \dots \dots A.5.1$$

This has been done in figure A.5.1. Again, a comparison of  $R_g$  values obtained from other sources will allow a graphical evaluation of  $\alpha$ , for any given protein. It might also be feasible to incorporate the relationships provided Zimm and Stockmayer (1949), which would allow this method to be extended to the analysis of branched polymers.

As a final comment, it should be pointed out that the entire basis for the arguments presented in this, and the previous, appendix assumes that the absolute numbers obtained for the composition of a random link (8.4aa/link) and the length of the link,  $l$ , apply to proteins in general. This is probably an unreasonable assumption for proteins that show extremes in their amino acid composition. Also the comparison of Figures A.4.2a and A.5.1, indicates that it would be impossible to distinguish between rods and random coils at low molecular weights, where the interference effects, from the solvent interactions with the random coils, would tend to mask the shape anisotropy of the rods. This problem should be reduced at the higher molecular weights.

Figure.A.5.1: Evaluation of solvent effects on random coils.

Plots of radius of gyration  $R_g$ , versus number of residues for random-coils for different values of the expansion coefficient  $\alpha$  .

Figure.A.5.1.

Appendix.VI: AMINO ACID COMPOSITION AND ELASTIN EVOLUTION

In a recent publication Sage and Gray (1979) have presented data for the amino acid composition of elastin from a wide variety of sources. In their data there is a substantial amount of information for the elastin composition of the bony fishes, and I have attempted to use the 'likeness' of the elastin from the different sources to develop an evolutionary succession for the elastin of these fishes. The numerical analysis itself was carried out by the following expression (Matsumura et.al. 1979):

$$DI_{jk} = \sum_i^n |AA_{ij} - AA_{ik}| \dots\dots A.6.1$$

where  $AA_{ij}$  is the number of residues per thousand of the amino acid  $i$ , in a protein specified by  $j$ , and  $AA_{ik}$  is the number for the same amino acid in the protein specified by  $k$ . Similar expressions to this have been utilized by a number of workers to evaluate the relatedness between proteins and, then, to extrapolate to the relatedness of the source species (Fondy and Holonan 1971, Metzger et.al. 1968, Harris and Teller 1973). Equation A.6.1 was evaluated on a computer with a Fortran program, for 13 groups of fishes, and this allowed me to compile a difference index matrix for their elastin composition (table A.6.1). Based on this result an evolutionary scheme was derived as shown in figure A.6.1. No attempt was made to analyze the results beyond this point.

Table A.6.1: Difference index for elastin composition.

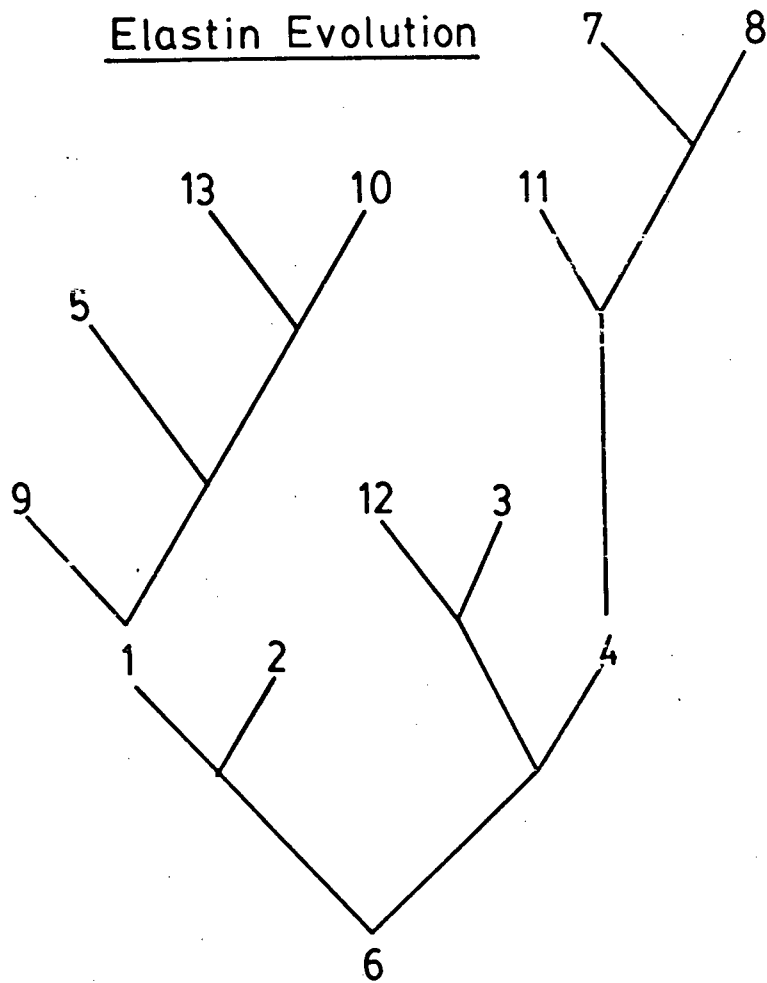
		DIFFERENCE INDEX FOR ELASTIN COMPOSITION.												
		1	2	3	4	5	6	7	8	9	10	11	12	13
1	---	---	69.9	87.4	96.8	107.9	82.7	157.6	164.8	82.0	174.8	289.1	213.9	298.2
2	---	---	---	79.7	116.3	143.4	81.0	199.1	200.9	116.3	212.3	290.6	192.2	345.9
3	---	---	---	---	71.4	117.3	80.9	156.2	160.0	89.4	228.4	226.1	143.1	345.2
4	---	---	---	---	---	129.7	62.5	98.2	112.6	111.8	232.6	195.9	179.3	341.0
5	---	---	---	---	---	---	136.8	161.1	169.7	146.3	181.3	293.4	231.2	297.7
6	---	---	---	---	---	---	---	139.9	140.1	107.1	222.7	237.2	176.6	323.1
7	---	---	---	---	---	---	---	---	100.4	157.0	215.8	189.5	243.9	310.6
8	---	---	---	---	---	---	---	---	---	142.4	174.8	221.9	210.1	284.8
9	---	---	---	---	---	---	---	---	---	---	184.0	243.1	180.1	305.4
10	---	---	---	---	---	---	---	---	---	---	---	331.3	247.1	238.4
11	---	---	---	---	---	---	---	---	---	---	---	---	186.4	424.3
12	---	---	---	---	---	---	---	---	---	---	---	---	---	339.7
13	---	---	---	---	---	---	---	---	---	---	---	---	---	---

1.	black grouper	5.	porcupine fish	9.	starry flounder
2.	black cod	6.	walleyed pike	10.	carp
3.	ling cod	7.	yellowfin tuna	11.	steelhead
4.	pacific yellowtail	8.	toadfish	12.	king salmon
				13.	tarpon

Figure.A.6.1: Elastin evolution.  
Evolutionary sequence for elastin of higher fishes  
based on table A.6.1.

Figure.A.6.1.



LITERATURE CITED

- Aaron, B.E., and Gosline, J.M. 1980. Optical properties of single elastin fibres indicate a random conformation. Nature in press.
- Aaron, B.E., and Gosline, J.M. 1980. Elastin as a random network elastomer: a mechanical and optical analysis of single elastin fibres. Submitted to Biopolymers.
- Aaron, B.E., Burns, P.D., Marshall, A.G., and Gosline, J.M. 1980. In preparation.
- Alexander, R. McN. 1966. Rubber-like properties of the inner hinge-ligament of Pectinidae. J. Exp. Biol. 44: pp. 119-130.
- Anderson, J.C. 1976. Glycoproteins of the connective tissue matrix. Int. Rev. Conn. Tiss. Res. 7: pp. 251-322.
- Anderson, S.O. 1971. Resilin. Comprehensive Biochemistry. 26C: pp. 633-657.
- Astbury, W.T. 1940. The molecular structure of the fibres of the collagen group. J. Int. Soc. Leather Trades' Chemists. 24: pp. 69-92.
- Ayer, J.P. 1964. Elastic tissue. Int. Rev. Conn. Tiss. Res. 2: pp. 33-100.
- Bairati, A., and Gotte, L. 1977. Caratteri della birefrangenza delle fibre elastiche. XXXIV Congresso Nazionale della Societa Italiana di Anatomia. Riassunti delle relazioni e delle comunicazioni. Trieste, Italy.
- Banga, I., and Balo, J. 1960. The elasticity increasing property of elastomuco proteinase. Biochim. Biophys. Acta. 40: pp. 367-368.
- Bashaw, J., and Smith, K.J. 1968. Thermoelasticity of networks in swelling equilibrium. J. Polymer Sci. 6: pp. 1041-1050.
- Baurain, R., LaRoche, J.F., and Lamy, F. 1976. Photolysis of desmosine and isodesmosine by u.v. Light. Eur. J. Biochem. 67: pp. 155-164.
- Bear, R.S., Schmitt, F.C., and Young, J.A. 1937. The ultrastructure of nerve axoplasm. Proc. Roy. Soc. Lon. Ser. B. 123: pp. 505-515
- Bear, R.S. 1942. The long X-ray diffraction spacings of collagen. J. Am. Chem. Soc. 64: pg. 727.
- Bear, R.S. 1944. X-ray diffraction studies on protein fibres.

I: the large fibre-axis period of collagen. J. Am. Chem. Soc. 66: pp 1297-1305.

Bedford, G.R., and Katritzky, A.R. 1963. Proton magnetic resonance spectra of degradation products from elastin. Nature 200: pg. 652.

Bennett, H.S. 1950. The microscopical investigation of biological materials with polarized light, in "McLung's handbook of microscopical technique". Third edition. Ruth M.J. Ed. Paul B. Hoeber, Inc. New York. pp. 591-677.

Boucek, R.J., Noble, N.C., and Woessner, J.F. 1959. Properties of fibroblasts, in "Connective tissue, thrombosis, and atherosclerosis". Page, I.H. Ed. Academic Press. New York. Pp. 193-211.

Bowen, I.J. 1953. Physical studies on a soluble protein obtained by the degradation of elastin with urea. Biochem. J. 55: pp. 766-768.

Bradbury, E.M., and Rattle, H.W.E., 1972. Simple computer-aided approach for the analyses of the nuclear magnetic resonance spectra of histones. Eur. J. Biochem. 27: pp. 270-281.

Brant, D.A., and Flory, P.J. 1965a. The configuration of random polypeptide chains. I: experimental results. J. Am. Chem. Soc. 87: pp. 2788-2791.

Brant, D.A., and Flory, P.J. 1965b. The configuration of random polypeptide chains. II: theory. J. Am. Chem. Soc. 87: pp. 2791-2800.

Bugenberg de Jong, H.G. 1949. Crystallization-coacervation-flocculation, in "Colloid science" volume 2. Kruyt, H.R. Ed. Elsevier Publishing Co. Amsterdam. Pp. 232-258.

Carnes, W.H., Hart, M.L., and Hodgkin, N.M. 1977. Conformation of aortic elastin revealed by scanning electron microscopy of dissected surfaces. Advances in Exp. Med. And Biol. 79: pp. 61-70.

Carton, R.W., Dainauskas, J., and Clark, J.W. 1962. The isolation and physical properties of single elastic fibres. Federation Proc. 19: pg. 383.

Carton, R.W., Dainauskas, J., and Clark, J.W. 1962. Elastic properties of single elastic fibres. J. Appl. Physiology. 17: pp. 547-551.

Ceccorulli, G., Scandola, M., and Pezzin, G. 1977. Calorimetric investigation of some elastin-solvent systems. Biopolymers. 16: pp. 1505-1512.

- Charm, S.E., and Kurland, G.S. 1974. "Blood flow and Microcirculation". John-Wiley and Sons Ltd. New York. 312 pp.
- Chrambach, A., and Rodbard, D. 1971. Polyacrylimide gel electrophoresis. Science. 172: pp 440-451.
- Clark, G., Coalson, R.E., and Nordquist, R.E. 1973. Methods for connective tissue, in "Staining procedures". Clark, G. Ed. Williams and Wilkins Co. Baltimore. Pp. 215-217.
- Cleary, E.G., and Cliff, W.J. 1978. The substructure of elastin. Exp. And Molec. Path. 28: pp. 227-246.
- Cohn, E.S., and Edsall, J.T. 1943. Density and apparent specific volume of proteins, in "Proteins, amino acids, and peptides". Cohn, E.J., and Edsall, J.T. Eds. Hafner Publishing Co. New York. Pp. 370-396.
- Cotta-Pereira, G. Rodrigo, F.G., and David-Ferreira, J.F. 1977. The elastin system fibres. Advances in Exp. Med. And Biol. 79: pp. 19-30.
- Cox, R.C., and Little, K. 1962. An electron microscope study of elastic tissue. Proc. Roy. Soc. Ser.B. 155: pp. 232-242.
- Cox, B., Starcher, B., and Urry, D. 1973. Coacervation of alpha-elastin results in fibre formation. Biochim. Biophys. Acta. 317: pp. 209-213.
- Cox, B., Starcher, B., and Urry, D. 1974. Coacervation of tropoelastin results in fibre formation. J. Biol. Chem. 249: 997-998.
- Cozzone, P., Toniolo, C., and Jardetzky, O. 1980. Nmr study of the main components of clupienes and their possible interaction with nucleic acids. Febs. Letters. 110: pp. 21-24.
- Davril, M., Han, K., Guay, M., and Lamy, F. 1979. Photolysis of crosslinked peptides from elastin of porcine aorta. Febs. Letters. 98: pp. 128-134.
- Dayhoff, M. 1976. Atlas of protein sequence and structure. Vol. 5, supp. 2. National Biomedical Res. Foundation. Washington D.C. Pg.267.
- Dempsey, E.W. 1952. The chemical characterization and the submicroscopic structure of elastic tissue. Science. 116: pg. 520.
- Diehl, J.M., and Iterson, G. 1935. Die doppelbrechung von chitinsehn. Kolloid. Z. 73: pp. 142-146.
- Dorrington, K., Grut, W., and McCrum, N.G. 1975. Mechanical

state of elastin. Nature. 255: pp. 476-478.

Dorrington, K.L., and McCrum, N.G. 1977. Elastin as a rubber. Biopolymers 16: pp. 1201-1222.

Dwek, R.A. 1973. "Nuclear magnetic resonance in biochemistry." Oxford University Press. Oxford. 629 pp.

Egmond, M.R., Rees, D., Welsh, J., and Williams, R.J.P. 1979.  $^1\text{H}$ -nmr studies on glycophorin and it's carbohydrate-containing tryptic peptides. Eur. J. Biochem. 97: pp. 73-83.

Ellis, G.E., and Packer, K.J. 1976. Nuclear spin-relaxation studies of hydrated elastin. Biopolymers. 15: pp. 813-832.

Field, J.M., Rodger, G.W., Hunter, J.C., Serafini-Fracassini, A., and Spina, M. 1978. Isolation of elastin from the bovine auricular cartilage. Arch. Biochem. Biophys. 191: pp. 705-713.

Finlay, J.B., and Stevens, F.S. 1973. The fibrous component of the bovine ligamentum nuchae observed in the scanning electron microscope. J. Microscopy. 99: pp. 57-63.

Fisher, J. 1979. Ultrastructure of elastic fibres. Acta. Histochemica. 65: pp. 87-98.

Fleming, W.W., Sullivan, C.E., and Torchia, D.A. 1980. Characterization of the molecular motions in  $^{13}\text{C}$ -labelled aortic elastin by  $^{13}\text{C}$ - $^1\text{H}$  double magnetic resonance. Biopolymers. 19: pp. 597-617.

Flory, P.J. 1949. The configuration of real polymer chains. J. Chem. Phys. 17: pp. 303-310.

Flory, P.J. 1953. "Principles of polymer chemistry." Cornell University Press. London. 672 pp.

Fondy, T.P., and Holonan, P.D. 1971. Structural similarities within groups of pyridine nucleotide-linked dehydrogenases. J. Theor. Biol. 31: pp. 229-244.

Foster, J.A., Bruenger, E., Gray, W.R., and Sandberg, L.B. 1973. Isolation and amino acid sequences of tropoelastin peptides. J. Biol. Chem. 248: pp. 2876-2879.

Foster, J.A., Shapiro, R., Voynon, F., Crombie, G., Faris, B., and Franzblau, C. 1975. Isolation of soluble elastin from lathyrctic chicks. Comparison to tropoelastin from copper defficient pigs. Biochemistry. 14: pp. 5343-5347.

Foster, J.A., Mecham, R.P., and Franzblau, C. 1976. A high molecular weight species of soluble elastin. Biochem. Biophys. Res. Ccmmun. 72: pp. 1399-1406.

Foster, J.A., Mecham, R., Imberman, M., Faris, B., and Franzblau, C. 1970. A high molecular weight species of soluble elastin. Advances in Exp. Med. And Biol. 79: pp. 351-369.

Fox, T.G., Fox, J.C., and Flory, P.J. 1951. The effect of rate of shear on the viscosity of dilute solutions of polyisobutylene. J. Am. Chem. Soc. 73: pp. 1901-1904.

Franzblau, C. 1971. Elastin. Comprehensive Biochemistry. 26C: 659-712.

Fraser, R.B.D., and McCrae, T.P. 1973. "Conformation in fibrous proteins." Academic Press Inc. New York. 628 pp.

Frey-Wyssling, A. 1953. "Submicroscopic morphology of proctoplasm." Elsevier, Amsterdam. 237 pp.

Gosline, J.M., Weis-Fogh, T., and Yew, F.F. 1975. Reversible structural changes in a hydrophobic protein, elastin, as indicated by fluorescence probe analysis. Biopolymers. 14: pp. 1811-1826.

Gosline, J.M. 1977. The role of hydrophobic interactions in the swelling of elastin. Advances in Exp. Med. And Biol. 79: pp. 415-421.

Gosline, J.M. 1978. The temperature-dependent swelling of elastin. Biopolymers. 17: pp. 697-707.

Gosline, J.M., and French, C.J. 1979. Dynamic mechanical properties of elastin. Biopolymers. 18: pp. 2091-2103.

Gotte, L., Meneghelli, V., and Castellani, A. 1965. Electron microscope observations and chemical analyses of human elastin, in "Structure and function of connective and skeletal tissue." Jackson, S.F., Harkness, R.D., Partridge, S.M., and Tristram, G.R. Eds. Butterworths. London. Pp. 93-100.

Gotte, L., Pezzin, G., and Stella, G.D. 1966. Mechanical properties of elastin, dry and swollen in different solvents, in "Biochimie et physiologie du tissu conjonctif." Comte, P. Ed. Ormeco. Lyon. Pp. 145-154.

Gotte, L., Giro, M.G., Volpin, D., and Horne, R.W. 1974. The ultrastructural organization of elastin. J. Ultrastructure Res. 46: pp. 23-33.

Gotte, L., Volpin, D., Horne, R.W., and Mammi, M. 1976. Electron microscopy and optical diffraction of elastin. Micron. 7: pp. 95-102.

Grant, M.E., Steven, F.S., Jackson, D.S., and Sandberg, L.B. 1971. Carbohydrate content of insoluble elastins prepared from adult bovine and calf ligamentum nuchae and tropoelastin

- isolated from copper-deficient porcine aorta. Biochem. J. 121: pp. 197-203.
- Gray, W.R., Sandberg, L.B., and Foster, J.A. 1973. Molecular model for elastin structure and function. Nature. 246: pp. 461-466.
- Gross, J. 1949. The structure of elastic tissue as studied with the electron microscope. J. Exp. Med. 89: pp. 699-708.
- Grut, W., and McCrum, N.G. 1974. Liquid drop model of elastin. Nature. 251: pg. 165.
- Guth, E., James, H.M., and Mark, H. 1946. The kinetic theory of rubber elasticity, in "Advances in colloid science". II. Interscience. New York. Pp. 253-281.
- Hall, D.A., and Czerkawski, J.W. 1961. The reaction between elastase and elastic tissue, 4. Soluble elastins. Biochem. J. 80: pp. 121-127.
- HALL, D.A. 1976. The preparation of soluble elastins, in "The methodology of connective tissue research." Hall, D.A. Ed. Joyson-Bruvvers Ltd. Oxford. Pp. 105-108.
- Harkness, M.L.R., Harkness, R.D., and McDonald, D.A. 1957. The collagen and elastin content of the arterial wall in the dog. Proc. Roy. Soc. Ser. B. 146: pp. 541-551.
- HARRIS, G.E., and Teller, D.S. 1973. Estimation of the primary sequence homology from amino acid composition of evolutionarily related proteins. J. Theor. Biol. 38: pp. 347-362.
- Hart, M.L., Beydler, S.A., and Carnes, W.H. 1978. The fibrillar structure of aortic elastin. Scanning electron microscopy. Vol. II. S.E.M. Inc. AMF O'Hare, Illinois. Pp. 21-25.
- Hass, G.M. 1939. Elastic tissue. Arch. Pathology. 27: pp. 334-365.
- Henderson, L.E., Orsollan, S., and Konigsberg, W. 1979. A micromethod for the complete removal of dodecyl sulphate from proteins by ion-pair extraction. Anal. Biochem. 93: pp. 153-157.
- Hoeve, C.A.J., and Flory, P.J. 1958. The elastic properties of elastin. J. Am. Chem. Soc. 80: pp. 6523-6525.
- Hoeve, C.A., and Flory, P.J. 1974. The elastic properties of elastin. Biopolymers. 13: pp. 677-686.
- Huggins, M.L. 1942. The viscosity of dilute solutions of long-

chain molecules. IV: Dependence on concentration. J. Am. Chem. Soc. 64: pp. 2716-2718

Jamieson, A.M., Downs, C.E., and Walton, A.G. 1972. Studies of elastin coacervation by quasielastic light scattering. Biochim. Biophys. Acta. 271: 34-47.

Jamieson, A.M., Simil-Glovaski, E., Tansey, K., and Walton, A.G. 1976. Studies of elastin coacervation by quasielastic light scattering. Faraday Disc. Chem. Soc. 61: pp. 194-204.

Joussot-Dubien, J., and Houdard-Pereyre, J. 1969. Photolyse de la pyridine en solution aqueuse. Bull. Soc. Chim. France. 8: pp. 2619-2623.

Kadar, A. 1977. Scanning electron microscopy of purified elastin with and without enzymatic digestion. Advances in Exp. Med. And Biol. 79: pp. 45-53.

Kakivaya, S.R., and Hoeve, C.A.J. 1975. The glass point of elastin. Proc. Natl. Acad. Sci. 72: pp. 3505-3507.

Karrer, H.E., and Cox, J. 1961. An electron microscope study of the aorta in young and ageing mice. J. Ultrastructure Res. 5: pp. 1-13.

Keith, D.A., Paz, M.A., and Gallop, P.M. 1979. Differences in valyl-proline sequence content in elastin from various bovine tissues. Biochim. Biophys. Res. Commun. 87: pp. 1214-1217.

Kelly, R.E., and Rice, R.V. 1967. Abductin: A rubber-like protein from the internal triangular hinge ligament of Pecten. Science. 155: pp. 208-210.

Khaled, Md. A., Renugopalakrishnan, V., and Urry, D.W. 1976. Pmr and conformational energy calculations of repeat peptides of tropoelastin: The tetrapeptide. J. Am. Chem. Soc. 98: 7547-7553.

Kirk, J.E. 1959. Mucopolysaccharides of arterial tissue, in "The arterial wall". Lansing, A.S. Ed. Williams and Wilkins. Baltimore. Pp. 161-191.

Kolpak, H. 1935. Rontgenstrukturuntersuchungen uber elastisches gewebe unter besonderer berucksichtigung der dehnung und entquellung. Kolloid Z. 73: pp. 129-142.

Kornfeld-Poullain, N., and Robert, L. 1968. Effet de differents solvants organiques sur la degradation alkaline de l'elastine. Bull. Soc. Chim. Biol. 50: pp. 759-771.

Kurata, M., Stockmayer, W.H., and Roig, A. 1960. Excluded volume effect of linear polymer molecules. J. Chem. Phys. 33: pp. 151-155.

Kurata, M., and Stockmayer, W.H. 1962. Rept. On Progr. In Polymer Phys. Japan. 5: pp. 23-26.

Lansing, A.L., Rosenthal, T., Alex, M., and Dempsey, E. 1952. The structure and chemical characterization of elastic fibres as revealed by elastase and by electron microscopy. Anat. Rec. 114: pp. 555-576.

Lemieux, R.U., and von Rudloff, E. 1955. Periodate-permanganate oxidations. I. Oxidations of olefins. Can. J. Chem. 33: pp. 1701-1709.

Lent, R.W., Smith, B., Salledo, B., Farris, G., and Franzblau, C. 1969. Studies on the reduction of elastin. II. Evidence for the presence of alpha-amino adipic acid -semialdehyde and its aldol condensation product. Biochemistry. 8: pp. 2837-2845.

Lo, S., Russell, J.C., and Taylor, A.W. 1970. Determination of glycogen in small tissue samples. J. Appl. Physiology. 28: pp. 234-236.

Long, M.M. 1980. Personal communication.

Lyerla, J.R., and Torchia, D.A. 1975. Molecular mobility and structure of elastin deduced from the solvent and temperature dependence of  $^{13}\text{C}$ -magnetic resonance relaxation data. Biochemistry. 14: pp. 5175-5183.

Mammi, M., Gotte, L., and Pezzin, G. 1970. Comparison of soluble and native elastin conformations by far u.v. Circular dichroism. Nature. 225: pp. 380-381.

Mark, J.E. 1976. The dependence of the swelling of elastin on elongation and its importance in fluorescence probe analysis. Biopolymers. 15: pp. 1853-1856.

Marshall, A.G. 1979. Spectroscopic dispersion versus absorption. A new method for distinguishing a distribution in peak position from a distribution in line width. J. Phys. Chem. 83: pp. 521-524.

Maruyama, K., Natori, R., and Nonomura, Y. 1976. A new elastic protein from muscle. Nature. 262: pp. 58-60.

Matsumura, T., Hasegawa, M., and Shigei, M. 1979. Collagen biochemistry and the phylogeny of echinoderms. Comp. Biochem. Physiol. E. 62: pp. 101-105.

Metcalf, J.C. 1970. Nuclear magnetic resonance spectroscopy, in "Physical principles and techniques of protein chemistry". Part B. Sydney, J.L. Ed. Academic Press. New York. Pp. 275-363.

Metzger, H., Shapirc, M.B., Mosimann, J.E., and Vinton, J.E. 1968. Assessment of compositional relatedness between proteins. Nature. 219: pp. 1166-1168.

Meyer, K.H., and Ferri, C. 1936. Die elastischen eigenschaften der elastischen und der kollagenen fasern und ihre molekulare deutung. Pflugler's Arch. Ges. Physiol. 238: pp. 78-90.

Meyer, K., Davidson, E., Linker, A., and Hoffman, P. 1956. The acid mucopolysaccharide of connective-tissue. Biochim. Biophys. Acta. 21: pp. 506-518.

Miller, W.G., Brant, D.A., and Flory, P.J. 1967. Random-coil configurations of polypeptide co-polymers. J. Mol. Biol. 23: pp. 67-80.

Miller, W.G., and Goebel. 1968. Dimensions of protein random coils. Biochemistry. 7: pp. 3925-3935.

Minns, J.R., and Steven, S.F. 1974. Scanning electron microscopy of stretched elastic fibres. Micron. 5: pp. 127-133.

Mistrali, L., Volpin, D., Garibaldo, G.B., and Cifferri, A. 1971. Thermodynamics of elasticity in open systems. J. Phys. Chem. 75: pp. 142-149.

Moczar, M., Moczar, E., and Robert, L. 1979. Peptides obtained from elastin by hydrolysis with aqueous ethanolic potassium hydroxide. Conn. Tiss. Res. 6: pp. 207-213.

Morgan, R.J., and Treolar, L.R.G. 1972. Photoelastic studies of polymers and co-polymers in the rubbery state. J. Polym. Sci. A2. 10: pp. 51-69.

Mukherjee, D.P., Kagan, H.M., Robert, E.J., and Franzblau, C. 1976. Effects of hydrophobic elastin ligands on the stress-strain properties of elastin fibres. Conn. Tiss. Res. 4: pp. 177-179.

Narayanan, A.S., and Page, R.C. 1976. Demonstration of a precursor-product relationship between soluble and cross-linked elastin, and the biosynthesis of the desmosines in vitro. J. Biol. Chem. 251: pp. 1125-1130.

Oplatka, A., Michaeli, I., and Katchalsky, A. 1960. Thermoelasticity of open systems. J. Polym. Sci. 46: pp. 365-371.

Partridge, S.M., Davis, H.F., and Adair, G.S. 1955. Soluble proteins derived from partial hydrolysates of elastin. Biochem. J. 61: pp. 11-21.

Partridge, S.M. 1962. Elastin, in "Advances in protein

chemistry." 17: pp. 227- 302.

Partridge, S.M., Thomas, J. Elsdon, D.F. 1965. The nature of the cross-linkages in elastin, in "Structure and function of connective and skeletal tissue". Jackson, S.F., Harkness, R.D., Partridge, S.M., and Tristram, G.R. Eds. Butterworths. London. Pp. 88-92.

Partridge, S.M. 1967a. Diffusion of solutes in elastin fibres. Biochim. Biophys. Acta. 140: pp. 132-135.

Partridge, S.M. 1967b. Gel filtration using a column packed with elastin fibres. Nature. 213: pg.1123.

Partridge, S.M. 1968. Elastin structure and biosynthesis, in "Symposium on fibrous proteins". Crewther, W.G. Ed. Plenum Press. New York. Pp. 246-264.

Partridge, S.M., and Whiting, A.H. 1979. Molecular weights and stokes radii of soluble elastins. Biochim. Biophys. Acta. 576: pp. 71-80.

Pasquali-Ronchetti, I., Forinieri, C., Baccarini-Contri, M., and Volpin, D. 1979. The ultrastructure of elastin revealed by freeze-fracture electron microscopy. Micron. 10: pp. 88-99.

Pathrapankel, A.A., Hart, M.L., Winge, A.R., and Carnes, W.H. 1977. The biosynthesis of elastin by an aortic medial cell culture. Advances in Exp. Med. And Biol. 79: pp. 397-412.

Pfeiffer, H.H. 1943. Polarisationsmikroskopische messugen an kollagenfibrillen in vitro. Arch. Exper. Zellforsch. Besonders Gewebeluecht. 25: pp. 92-104.

Quintarelli, G., Belloci, M., and Zito, R. 1973. Structural features of Insoluble elastin. Histochemie. 37: pp. 49-60.

Ramachandran, G.N., and Santhanam, M.S. 1957. Structure of elastin. Proc. Ind. Acad. Sci. A. 45: pp. 124-132.

Ramachandran, G.N. 1963. "Aspects of protein structure." Academic Press. London. Pg. 39.

Rapaka, R.S., and Urry, D.W. 1978. Coacervation of sequential polypeptide models of tropoelastin. Int. J. Pep. Prot. Res. 11: pp. 97-108.

Reisner, A.H., and Rowe, J. 1969. Intrinsic viscosity of randomly coiled polypeptide of 30,000 daltons and it's effect on the solution of the Mark-Houwink equation. Nature. 222: pp. 558-559.

Robert, B., Szigeti, M., Derouette, J.C., and Robert, L. 1971. Studies on the nature of the microfibrillar component of

elastic fibres. Eur. J. Biochem. 21: pp. 507-516.

Robert, L., and Hornebeck, W. 1976. Preparation of insoluble and soluble elastins, in "The methodology of connective tissue research". Hall, D.A. Ed. Joyscn-Bruvvers Ltd. Oxford. Pp. 81-103.

Robert, L., 1977. Elastic chemistry. Advances in Exp. Med. And Biol. 79: pp. 139-144.

Romhanyi, G. 1958. Submicroscopic structure of elastic fibres as observed in the polarization microscope. Nature. 182: pp. 929-930.

Rhodin, J., and Dalhamn, T. 1955. Electron microscopy of collagen and elastin in the lamina propria of the tracheal mucosa of rat. Exp. Cell. Res. 9: pp. 371-375.

Ross, R., and Bornstein, P. 1969. The elastic fibre. I. The separation and partial characterization of its macromolecular components. J. Cell Biol. 40: pp. 366-379.

Ross, R., Fialkow, P.J., and Altman, L. 1977. The morphogenesis of elastic fibres. Advances in Exp. Med. And Biol. 79: pp. 7-17.

Rosenbloom, J., Harsch, M., and Cywinski, A. 1980. Evidence that tropoelastin is the primary precursor in elastin biosynthesis. J. Biol. Chem. 255: pp. 100-106.

Sage, H., and Gray, W.R. 1979. Studies on the evolution of elastin. I. Phylogenetic distribution. Comp. Biochem. Physiol. B. 64: pp. 313-327.

Sandberg, L.B., Weissman, N., and Smith, D.W. 1969. The purification and partial characterization of a soluble elastin-like protein from copper deficient porcine aorta. Biochemistry. 8: pp. 2940-2945.

Sandberg, L.B., Weissman, N., and Gray, W.R. 1971. Structural features of tropoelastin related to the sites of cross-links in aortic elastin. Biochemistry. 10: pp. 52-56.

Sandberg, L.B., Gray, W.R., and Bruenger, E. 1972. Structural studies of alanine and lysine rich regions of porcine aortic tropoelastin. Biochim. Biophys. Acta. 285: pp. 453-458.

Sandberg, L.B. 1976. Elastin structure in health and disease. Int. Rev. Conn. Tiss. Res. 7: pp. 160-210.

Sandberg, L.B., Gray, W.R., Foster, J.A., Torres, A.R., and Alvarez, V.L. 1977. Advances in Exp. Med. And Biol. 79: pp. 277-284.

- Saunders, D.W. 1957. The photoelastic properties of cross-linked amorphous polymers. III. Interpretation of results on polythene, polymethylene, natural rubber, and gutta-percha. Trans. Faraday Soc. 53: pp. 860-870.
- Schein, J., Carpousis, A., and Rosenbloom, J. 1966. Evidence that tropoelastin exists as a random-coil. Advances in Exp. Med. And Biol. 79: pp. 727-740.
- Schellman, J.A., Schellman, C. 1963. The conformation of polypeptide chains in proteins, in "The proteins". Neurath, H. Ed. Academic Press. New York. Pp. 1-37.
- Schimmel, P.R., and Flory, P.J. 1968. Conformational energies and configurational statistics of co-polypeptides containing l-proline. J. Mol. Biol. 34: pp. 105-120.
- Schmidt, W.J. 1939. Einige unterrichtsversuche zur doppelbrechung der elastinfasern. Kolloid Z. 89: pp. 233-237.
- Serafini-Fracassini, A., and Tristam, G.R. 1966. Electron microscope study and amino acid analysis on human aortic elastin. Proc. Roy. Soc. Edinburgh. B. 69: pp. 334-337.
- Serafini-Fracassini, A., Field, J.M., and Spina, M. 1976. The macromolecular organization of the elastin fibril. J. Mol. Biol. 100: pp. 73-84.
- Serafini-Fracassini, A., Field, J.M., Smith, J.W., Stephens, W.G.S. 1977. The ultrastructure and mechanics of elastic ligaments. J. Ultrastruct. Res. 58: pp. 244-251.
- Serafini-Fracassini, A., Field, J.M., and Hinnie, J. 1978. The primary filament of bovine elastin. J. Ultrastruct. Res. 65: pp. 190-193.
- Shadwick, R. 1980. A protein elastomer from Octopus arteries. In preparation.
- Simha, R. 1940. The influence of Brownian movements on the viscosity of solutions. J. Phys. Chem. 44: pp. 25-34.
- Smith, D.W., Abraham, P.A., and Carnes, W.H. 1975. Cross-linkage of salt-soluble elastin in vitro. Biochem. Biophys. Res. Commun. 66: pp. 893-899.
- Starcher, B.C., Saccomuni, G., and Urry, D.W. 1973. Coacervation and ion-binding studies on aortic elastin. Biochim. Biophys. Acta. 310: pp. 481-486.
- Stockmayer, W.H., and Fixman, M.J. 1963. On the estimation of unperturbed dimensions from intrinsic viscosities. J. Polym. Sci. C. 1: pp. 137-141.

Stokes, A.R. 1963. "The theory of the optical properties of inhomogeneous materials". E. And F.N. Spon Ltd. London. 172 pp.

Stothers, J.B. 1972. Carbon-13 nmr spectroscopy. Academic Press. New York. 253 pp.

Sykes, B.C., and Partridge, S.M. 1972. Isolation of a soluble elastin from lathyrctic chicks. Biochem. J. 130: pp. 1171-1172.

Tamburro, A.M., Guantieri, V., Daga-Gordini, D., and Abatangelo, G. 1977. Conformational transitions of alpha-elastin. Bicchim. Biophys. Acta. 492: pp. 370-376.

Tanford, C. 1961. "Physical chemistry of macromolecules". Wiley. New York. 710 pp.

Tanford, C., Kawahara, K., and Lapanje, S. 1966. Demonstration of random-coil behavior. J. Biol. Chem. 241: pp. 1921-1923.

Tanford, C., Kawahara, K., and Lapanje, S. 1967. Proteins as random coils. I. Intrinsic viscosities and sedimentation coefficients in concentrated guanidine hydrochloride. J. Am. Chem. Soc. 89: pp. 729-736.

Tanford, C. 1973. "The hydrophobic effect." John Wiley and Sons. New York. 200 pp.

Thomas, J., Elsdon, D., and Partridge, S. 1963. Partial structure of two major degradation products from cross-linkages in elastin. Nature. 200: pp.651-652.

Timasheff, S.N., Susi, H., Townend, R., Stevens, L., Gorbunoff, M.J., and Kymosinski, T.F. 1967. Application of C.D. And I.R. Spectroscopy to the conformation of proteins in solution, in "Conformation of biopolymers." Ramachandran, G.N. Ed. Academic Press. London. Pp. 173-196.

Torchia, D.A., and Piez, K.A. 1973. Mobility of elastin chains as determined by <sup>13</sup>C-nmr. J. Mol. Biol. 76: pp. 419-423.

Treloar, L.R.G. 1975. "The physics of rubber elasticity." Clarendon Press. Oxford. 310 pp.

Urry, D.W., and Ohnishi, T. 1974. Recurrence of turns in repeat peptides of elastin: the hexapeptide ala-pro-gly-val-gly-val sequences and derivatives, in "Peptides, polypeptides, and proteins". Blout, E.R., Bovey, F.A., Goodman, M., and Lotan, N. Eds. John Wiley and Sons. New York.

Urry, D.W., Long, M.M. 1976a. Conformations of the repeat peptides of elastin in solution. C.F.C. Crit. Rev. Biochem. 4: pp. 1-45.

Urry, D.W., Okamoto, K., Harris, R.D., Hendrix, C.F., and Long, M.M. 1976b. Synthetic cross-linked polypeptide of tropoelastin: an anisotropic fibrillar elastomer. Biochemistry. 15: pp. 4083-4089.

Urry, D.W., Khaled, M.A., Rapaka, R.S., and Okamoto, K. 1977a. Nuclear overhauser enhancement evidence for inverse temperature dependence of hydrophobic side chain proximity in the polytetrapeptide of tropoelastin. Biochem. Biophys. Res. Commun. 79: pp. 700-705.

Urry, D.W., and Long, M.M. 1977b. Advances in Exp. Med. And Biol. 79: pp. 685-714.

Urry, D.W., Khaled, M.A., Renugopalakrishnan, V., and Rapaka, R.S. 1978a. Proton magnetic resonance and conformational energy calculations of the repeat peptides of tropoelastin. The hexapeptide. J. Am. Chem. Soc. 100: pp. 696-705.

Urry, D.W., Long, M.M., and Sugano, H. 1978b. Cyclic analog of elastin hexapeptide exhibits an inverse temperature transition leading to crystallization. J. Biol. Chem. 253: pp. 6301-6302.

Urry, D.W. 1978c. Molecular perspectives of vascular wall structure and disease: the elastic component, in "Perspectives in biology and medicine". 21: pp. 265-295.

Urry, D.W., Trapane, T.L., and Abu Khaled, M. 1978d. Temperature dependence of rotational correlation times for an inverse temperature transition. A fundamental characterization. J. Am. Chem. Soc. 100: pp. 7744-7746.

Volpin, D., and Cifferri, A. 1970. Thermoelasticity of elastin. Nature. 225: pg. 382.

Volpin, D., Pasquali-Ronchetti, I., Urry, D.W., and Gotte, L. 1976a. Banded fibres in high temperature coacervates of elastin peptides. J. Biol. Chem. 251: pp. 6871-6873.

Volpin, D., Urry, D.W., Cox, B.A., and Gotte, L. 1976b. Optical diffraction of tropoelastin and alpha-elastin coacervates. Biochim. Biophys. Acta. 439: pp. 253-258.

Volpin, D., Urry, D.W., Pasquali-Ronchetti, I., and Gotte, L. 1976c. Studies by electron microscopy on the structure of coacervates of synthetic polypeptides of tropoelastin. Micron. 7: pp. 193-198.

Walton, A.G., and Blackwell, J. 1973. "Biopolymers". Academic Press Inc. New York. 604 pp.

Weber, K., and Osborn, M. 1969. The reliability of molecular weight determination by dodecyl sulphate-polyacrylimide gel

electrophoresis. J. Biol. Chem. 244: pp. 4406-4412.

Weis-Fogh, T. 1961a. Thermodynamic properties of Resilin, a rubber-like protein. J. Mol. Biol. 3: pp. 520-531.

Weis-Fogh, T. 1961b. Molecular interpretation of the elasticity of resilin. J. Mol. Biol. 3: pp. 648-667.

Weis-Fogh, T., and Anderson, S.O. 1970. New molecular model for the long-range elasticity of elastin. Nature. 277: pp. 718-721.

Wilkes, G.L. 1971. The measurement of molecular orientation in polymeric solids. Advances in Polym. Sci. 8: pp. 91-136.

Wohlisch, E., Wetnauer, E., Gruning, W.D., and Rohrbach, R. 1943. Thermodynamische analyse der dehnung des elastischen gewebes vom standpunkt der statistisch-kinetischen theorie der kautschuke-lastizitat. Kolloid Z. 104: pp. 14-24.

Wolinski, H., and Glagov, S. 1964. Structural basis for the static mechanical properties of the aortic media. Circ. Res. 14: pp. 400-413.

Wood, G.C. 1958. Biochem J. 69: pp. 538-546.

Yang, J.T. 1961. The viscosity of macromolecules in relation to molecular conformation. Advances in protein chemistry. 16: pp. 323-400.

Zimm, B.H., and Stockmayer, W.H. 1949. The dimensions of chain molecules containing branches and rings. J. Phys. Chem. 17: pp. 1301-1314.